Spring 2023 – Epigenetics and Systems Biology
Discussion Session (Environmental Epigenetics)
Michael K. Skinner – Biol 476/576
Week 12 (March 30)

Environmental Epigenetics

Primary Papers

1. Ben Maamar, et al. (2018) Environmental Epigenetics 26;4(2):dvy010, 1-19. (PMID: 29732173)
2. Ben Maamar, et al. (2019) Developmental Biology 445: 280-293. (PMID: 30500333)
3. Cao N, et al. (2022) Circulation. 2022 Oct 4;146(14):1082-1095. (PMID: 36004643)

Discussion

Student 28 – Ref #1 above

- What is the experimental design?
- What epigenetic technologies and alterations were investigated?
- What is the primary conclusion of the study?

Student 29 – Ref #2 above

- What is the experimental design?
- What were the developmental origins of the sperm epimutations?
- What conclusions on the development of the sperm epimutations are made?

Student 30 – Ref #3 above

- What exposure was used?
- What transgenerational disease was observed?
- What treatment inhibited the transgenerational effect?

Environmental Epigenetics, 2018, 1–19

doi: 10.1093/eep/dvy010
Research article

RESEARCH ARTICLE

Alterations in sperm DNA methylation, non-coding RNA expression, and histone retention mediate vinclozolin-induced epigenetic transgenerational inheritance of disease

Millissia Ben Maamar[1], Ingrid Sadler-Riggleman[1], Daniel Beck[1], Margaux McBirney[1], Eric Nilsson[1], Rachel Klukovich[2], Yeming Xie[2], Chong Tang[2], Wei Yan[2,‡] and Michael K. Skinner[1,*,‡]

[1]Center for Reproductive Biology, School of Biological Sciences, Washington State University, Pullman, WA 99164-4236, USA and [2]Department of Physiology and Cell Biology, University of Nevada, Reno School of Medicine, 1664 North Virginia Street, MS557, Reno, NV 89557, USA

*Correspondence address. Center for Reproductive Biology, School of Biological Sciences, Washington State University, Pullman, WA 99164-4236, USA. Tel: +1-509-335-1524; Fax: +1-509-335-2176; E-mail: skinner@wsu.edu

‡Both authors contributed equally to this study.

Managing Editor: Christopher Faulk

Downloaded from https://academic.oup.com/eep/article/4/2/dvy010/4987173 by guest on 30 November 2022

Abstract

Epigenetic transgenerational inheritance of disease and phenotypic variation can be induced by several toxicants, such as vinclozolin. This phenomenon can involve DNA methylation, non-coding RNA (ncRNA) and histone retention, and/or modification in the germline (e.g. sperm). These different epigenetic marks are called epimutations and can transmit in part the transgenerational phenotypes. This study was designed to investigate the vinclozolin-induced concurrent alterations of a number of different epigenetic factors, including DNA methylation, ncRNA, and histone retention in rat sperm. Gestating females (F0 generation) were exposed transiently to vinclozolin during fetal gonadal development. The directly exposed F1 generation fetus, the directly exposed germline within the fetus that will generate the F2 generation, and the transgenerational F3 generation sperm were studied. DNA methylation and ncRNA were altered in each generation rat sperm with the direct exposure F1 and F2 generations being distinct from the F3 generation epimutations. Interestingly, an increased number of differential histone retention sites were found in the F3 generation vinclozolin sperm, but not in the F1 or F2 generations. All three different epimutation types were affected in the vinclozolin lineage transgenerational sperm (F3 generation). The direct exposure generations (F1 and F2) epigenetic alterations were distinct from the transgenerational sperm epimutations. The genomic features and gene pathways associated with the epimutations were investigated to help elucidate the integration of these different epigenetic processes. Our results show that the three different types of epimutations are involved and integrated in the mediation of the epigenetic transgenerational inheritance phenomenon.

Received 30 January 2018; **revised** 20 March 2018; **accepted** 22 March 2018

© The Author(s) 2018. Published by Oxford University Press.
This is an Open Access article distributed under the terms of the Creative Commons Attribution Non-Commercial License (http://creativecommons.org/licenses/by-nc/4.0/), which permits non-commercial re-use, distribution, and reproduction in any medium, provided the original work is properly cited. For commercial re-use, please contact journals.permissions@oup.com

Key words: epigenetics; sperm; spermatogenesis; transgenerational; inheritance; DNA methylation

Introduction

Environmentally induced epigenetic transgenerational inheritance is defined as "germline (sperm or egg) transmission of epigenetic information between generations in the absence of any continued exposure or genetic manipulation." In 1987 the word epimutation was introduced to describe heritable changes in genes which were not due to changes in DNA sequence [1]. A number of different epigenetic factors have been described and are critical in regulating gene expression including chromatin structure and non-coding RNA (ncRNA) methylation which have become an intensively active field of research. The modification of histones, particularly acetylation and methylation, play a crucial role in regulating genome activity [2]. DNA methylation can provide a primary switch where methylation triggers the changes that lead to a closed (not allowing gene transcription) or opened chromatin configuration (allowing gene transcription) [3]. The role of ncRNA in epigenetic events has become increasingly important [4–6]. All these epigenetic processes can be altered by numerous environmental exposures [7]. These environmental exposures can alter the early development of various organ systems that result in later life adult individuals with greater susceptibilities to develop disease when they encounter a second disease-promoting stimulus [8].

Epigenetic alterations in the germline mediate the heritable molecular relationship between the environment and gene expression [9, 10]. Studies have observed epigenetic transgenerational inheritance effects in different species, including plants [11], flies [12], worms [13], fish [14], birds [15] rodents [16–18], pigs [19], and humans [20]. This phenomenon has been observed in a large number of organisms showing that epigenetic transgenerational mechanisms are conserved and induced by environmental factors [21]. Many studies on environmental toxicants have been conducted, such as 2, 3, 7, 8-tetrachlorodibenzo [p]dioxin [22], permethrin and *N*, *N*-diethyl-meta-toluamide mixture [23], jet fuel JP-8 [24], plastics mixture [bisphenol-A, bis (2-ethylhexyl)phthalate, dibutyl phthalate] [25], dichlorodiphenyltrichloroethane (DDT) [26], methoxychlor [27], and atrazine [28]. For each exposure, alterations in DNA methylation have been observed in F3 generation rat sperm.

The first compound showing a transgenerational effect was vinclozolin. Vinclozolin [3-(3, 5-dichlorophenyl)-5methyl-5-vinyl-1, 3-oxazolidine-2, 4-dione] is a fungicide used on fruits and vegetables crops. This chemical was found to exert significant antiandrogenic effects [29, 30]. Vinclozolin administration to pregnant female mice during the gestation period of embryonic days E13–E17 (which corresponds to fetal gonadal sex determination) was found to affect the offspring [16, 31]. This chemical also demonstrated transgenerational (F1 through F4 generations) effects on male fertility and altered the DNA methylation patterns in the F2 and F3 generation sperm [16]. This suggested that environment can induce epigenetic changes in the germline and be inherited to contribute to disease. Other exposures since then have been shown to promote epigenetic transgenerational phenotypes [21]. One of the proposed mechanisms is that "epimutations" induced in the germline become "imprinted-like" and therefore escape the post-fertilization DNA methylation erasure. The altered epigenome leads to modified transcriptomes in somatic cells resulting in adult-onset disease susceptibility [27, 32, 33]. Anway and collaborators revealed that following transient gestational exposure to F0 generation females between E8 and E15 (corresponding to the epigenetic reprogramming of germ cells and gonadal sex determination) the F1, F2, F3, and F4 generation adult males showed increased spermatogenic apoptosis and a decreased sperm number and motility [16]. Altered DNA methylation patterns in F2 and F3 generation vinclozolin lineages were also observed [34]. Prostate abnormalities were noted in F1–F4 generation males [35], severe anemia during pregnancy in F1–F3 generation females [36] and also sexually dimorphic changes in anxiety behaviors [37]. The mRNA expression of 196 genes was found to be consistently different in testis among the F1–F3 generation vinclozolin animals compared to the F1–F3 generation controls [35]. Transcription alterations in prostate from F3 males [35], hippocampus and amygdala in F3 males and females [37], and Sertoli cells [38] were also reported. These studies demonstrate the effects of vinclozolin transgenerationally on somatic gene expression.

The involvement of sperm small non-coding RNA (sncRNA) in the impact of traumatic stress in early life across generations was also investigated. Sperm RNAs from traumatized males were injected into fertilized wild-type oocytes which reproduced the behavioral and metabolic alterations in their offspring [39]. This suggests that sncRNAs are sensitive to environmental factors in early life which can be passed to the next generation and contribute to the inheritance of trauma-induced phenotypes [39]. Subsequently vinclozolin has also been shown to alter transgenerationally the sncRNA in sperm [40]. Previous studies have revealed that ncRNA can modulate gene expressions and many of them have been identified to participate in the epigenetic control by affecting DNA methylation [41, 42] or by interacting with various types of proteins involved in histone modification or chromatin remodeling [43–46]. Therefore, long ncRNA (lncRNA) is an ideal mediator to regulate local and sequence-specific DNA methylation or demethylation which may also trigger epigenetic disorders and transgenerational effects [43].

The lncRNAs have been hypothesized to maintain epigenetic memory and a recent study has correlated lncRNA differential expression to DDT-induced epigenetic transgenerational inheritance [7]. The sncRNAs were also implicated when the effects of starvation were found to induce the production of sncRNAs that persisted for multiple generations and resulted in a longer lifespan for the F3 generation [47]. Total estimates for both lncRNA and sncRNA in a single spermatozoa have exceeded 20 000 [48, 49]. As such, there are various different kinds of small RNAs found in spermatozoa including: micro-RNA (miRNAs) and siRNAs involved in regulating spermatogenesis via translation; piwi-interacting RNAs (piRNAs) believed to regulate transcript stability in the germline; and many smaller classes of sncRNA such as tRNA-derived sncRNAs and mitosRNAs have also been discovered in spermatozoa [50, 51]. The expression of ncRNAs throughout spermatogenesis has been shown to be differential [51], suggesting an environmentally induced disruption of ncRNA expression in spermatogenic cells can have lasting effects for generations. Both DNA methylation and ncRNA transgenerational alterations have been reported to be altered in the epigenetic transgenerational inheritance phenomenon, but to the best of our knowledge no studies have examined histone modifications until recently [52]. Several studies have

Downloaded from https://academic.oup.com/eep/article/4/2/dvy010/4987173 by guest on 30 November 2022

observed conserved genes associated with histone retention sites and modifications [53] indicating modifications of histones may have an impact transgenerationally.

This study was designed to investigate concomitantly the epigenetic modifications of DNA methylation, ncRNA, and histones retention in sperm. The transgenerational model used for this study involves epigenetic transgenerational inheritance of sperm epigenetic alterations and disease triggered by vinclozolin exposure. This study will use this vinclozolin-induced epigenetic transgenerational inheritance of disease in rats to investigate the epigenetic changes in the F1, F2, and F3 generation sperm. This information combined with associated genes will be useful in the elucidation of the molecular processes implicated in the epigenetic transgenerational inheritance phenomenon. Observations demonstrate all three epigenetic processes are potentially involved and reflect transgenerational epimutations, including a novel role of new induced transgenerational differential histone retention sites (DHRs), and distinct transgenerational DNA methylation and ncRNA epimutations.

Results

The experimental design (Fig. 1A) involved a daily transient exposure of gestating female F0 generation rats during embryonic days E8–E14 to 100 mg/kg per day of vinclozolin in dimethylsulfoxide (DMSO) using intraperitoneal injection as previously described [16]. A separate control generation lineage was exposed during Days E8–E14 of gestation to vehicle DMSO alone. Six different gestating females from different litters for each control and vinclozolin lineage were used. The F1 generation offspring were obtained and aged to 90-day postnatal age and selected males and females bred within the control or vinclozolin lineage. The F2 generation offspring were obtained and aged to 90 days and selected males and females from different litters bred to generate the F3 generation. No sibling or cousin breeding was used to avoid any inbreeding artifacts. All the males were sacrificed at 120 days of age for epididymal sperm collection. In previous studies, onset of disease was primarily observed between 6 and 12 months of age [54], hence the postnatal 120-day (P120) males were used to avoid any disease artifacts. The only disease detectable at P120 is testis spermatogenic cell apoptosis [16]. Selected male testis at each generation for both the control and vinclozolin lineages was used for spermatogenic cell apoptosis analysis. A significant level of apoptosis was observed in the F3 generation vinclozolin lineage (Fig. 1B) supporting the transgenerational phenotype of the vinclozolin model used. The sperm collected was then used for epigenetic analysis.

Sperm DNA Methylation Alterations

Methylated DNA immunoprecipitation (MeDIP) followed by DNA next-generation sequencing (NGS) for a MeDIP-Seq analysis was used to identify the differential DNA-methylated regions (DMRs) between the control versus vinclozolin lineage male sperm. Initially the sperm DNA was sonicated to produce DNA fragments of 200–500 bp. A methylcytosine antibody was used to immunoprecipitate the methylated DNA fragments. Libraries were generated for sequencing 50-bp paired-end reads to assess differential levels (read depths) of DNA methylation. The DMRs for the F1, F2, and F3 generation sperm were determined and different threshold p values are shown in Fig. 2. A *P*-value of $P < 1e\text{-}06$ was chosen for comparison of all single 100-bp windows, as well as DMRs with multiple (≥ 2) adjacent windows. The direct exposure F1 generation sperm had the lowest number of DMRs (Fig. 2A), the F2 generation an increased number of DMRs (Fig. 2B), and the F3 generation the highest number of DMRs (Fig. 2C). The DMR lists are presented in the Supplementary Tables S1–S3. A comparison of the DMRs at $P < 1e\text{-}06$ demonstrated minimal overlap with a higher level of overlap between the F2 and F3 generations (Fig. 2D). The majority of the alterations in sperm DNA methylation was unique between the generations. A small set of 44 overlapping DMRs between the F2 and F3 generation sperm are presented in the Supplementary Table S4.

The chromosomal locations of the DMRs for each generation are shown in Fig. 3. Nearly all the chromosomes display DMRs as indicated by the red arrowheads and some present clusters of DMRs indicated by black boxes. These different generation DMR clusters are also primarily distinct between the generations with little overlap (Fig. 3D). The CpG density of the DMRs for the F1, F2, and F3 generation sperm is shown in Fig. 4A–C. The CpG density of the DMRs at $P < 1e\text{-}06$ is shown and reveals that the predominant density is one CpG per 100 bp with a range between 1 and 4 CpG. The lengths of the DMRs are presented in Fig. 4D–F and shows that their predominant length is 1 kb and a range of 1–5 kb for each generation DMRs. Thus, the DMRs are associated with CpG deserts with 10–20 CpG within 1 kb [55]. The lists of DMRs with their chromosomal locations, size, and CpG density are presented in the Supplementary Tables S1–S3 for the F1, F2, and F3 generation DMRs, respectively.

Sperm ncRNA Alterations

The differential ncRNA present in sperm between the control versus vinclozolin lineages was determined with NGS using RNA-Seq analysis previously described [40]. The sperm total ncRNA was collected and then sncRNA and lncRNA prepared with appropriate ncRNA extraction and sequencing library procedures described in the Methods section. The read depths of differential ncRNA levels were determined for the F1, F2, and F3 generation sperm with a comparison of the control versus vinclozolin lineage sperm. The lncRNA for each generation with different *P*-value thresholds is compiled in Fig. 5A. The *P*-value used for subsequent analysis selected was $P < 1e\text{-}04$. The sncRNA for each generation with several *P*-value thresholds is shown in Fig. 5B. The *P*-value used for sncRNA analysis selected was $P < 1e\text{-}04$. The lncRNA is higher in number than the sncRNA. For the lncRNA, the F1 generation has a higher number than the F3 generation, and the F3 generation has a lower number than the F2 generation (Fig. 5C). The sncRNA was divided into categories with the piRNA, the miRNA, and the small tRNA being present, as well as a mixture of uncategorized sncRNA (other) (Fig. 5D). Therefore, each generation had differential ncRNA present and they were different between each generation.

The chromosomal locations of the differential ncRNA are presented for lncRNA in Fig. 6. The red arrowheads identify individual lncRNA and regional clusters of lncRNA are shown in black boxes. The F1, F2, and F3 generation lncRNAs are present on all chromosomes (Fig. 6A–C). The analysis of the lncRNA overlap between the generations indicated that the vast majority of differential lncRNA was distinct for each generation (Fig. 6D). The chromosomal locations of the differential ncRNA are shown for sncRNA in Fig. 7A–C. The overlap analysis between the three generations is shown in Fig. 7D. It reveals that the majority of differential sncRNA was unique for each generation. Both the long and small differential ncRNAs were predominantly distinct from the transgenerational F3

Downloaded from https://academic.oup.com/eep/article/4/2/dvy010/4987173 by guest on 30 November 2022

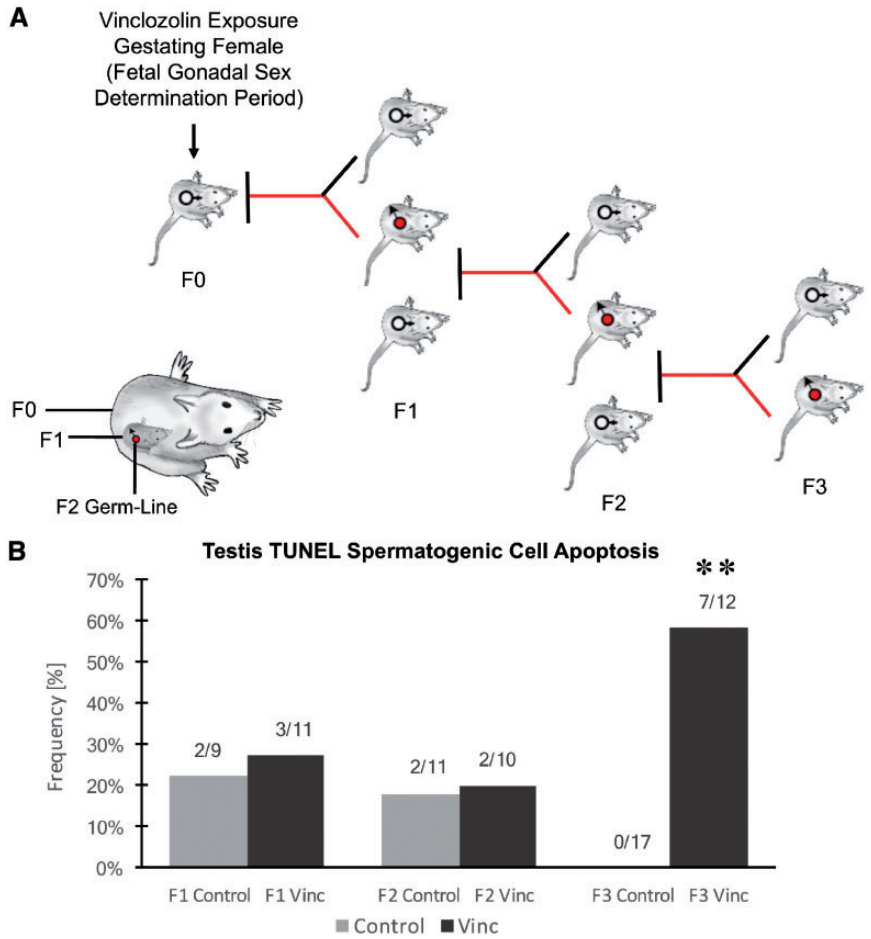

Figure 1: animal breeding scheme and disease. **(A)** Experimental design of F0 generation gestating female exposure then F1, F2, and F3 generations being generated for sperm collection. The direct exposure of the F0 generation female, F1 generation fetus, and F2 generation germline is also shown. **(B)** Testis spermatogenic cell apoptosis as determined with TUNEL analysis of testis histology sections with frequency (%) of apoptosis for each generation and lineage shown. The (**) indicates statistical significance with control with a $P < 0.01$ with a Fishers exact *T*-test

generation ncRNA. The lists of differential ncRNA separated by category for identification, chromosomal location, size, statistics and gene associations are presented in the Supplementary Tables S5–S7 for lncRNA and Supplementary Tables S8–S10 for sncRNA for the F1, F2, and F3 generations, respectively.

Sperm Histones Alterations

A core of histone retention sites have been previously shown in control and vinclozolin lineage rat sperm that are not altered following exposure, but the F3 generation vinclozolin lineage sperm had an increase in the number of histone retention sites [52]. This study examined the sites (DHRs for the F1, F2, and F3 generation control versus vinclozolin lineage sperm with a procedure similar to the DMR analysis. Interestingly, the F1 and F2 generations had negligible DHRs showing no major difference between control and vinclozolin lineages (Fig. 8A and B). However, the F3 generation comparison of the control versus vinclozolin lineage sperm identified an increased number of DHRs (Fig. 8C). The chromosomal locations of these DHRs are represented in Fig. 8D. An overlap analysis of these DHRs between F1, F2, and F3 revealed that each of them was unique (Fig. 8E). DHRs were induced in the F3 generation lineage sperm thus displaying a transgenerational effect whereas a direct exposure did not trigger major alterations. The DHRs are listed with identification, location, size and associated genes in the Supplementary Tables S11–S13 for the F1, F2, and F3 generations, respectively.

Epimutation Gene Associations

The Supplementary Tables S1–S9 provide the lists of DMRs, ncRNAs, and DHRs for all the epigenetic alterations (i.e. epimutations) identified. The known gene associations for these epimutations were determined using genomic location and are also listed. All the associated genes were classified by relevant functions and the functional categories are presented for each generation in Fig. 9A. For this analysis, sncRNA and lncRNA were combined. The top ten gene categories containing multiple genes for F1, F2, and F3 generations are presented for DMRs, ncRNA, and DHRs separately. Epimutations were found predominantly in the metabolism, signaling, and transcription categories. The predominant gene categories for the F1 generation were mostly found with the lncRNA (Fig. 9A). The predominant gene categories for the F3 generation were similar as the F1 generation but found in the DMRs. The ratio of epimutations between the generations was highest for DMRs in the F3 generation, highest for ncRNA in the F1 generation, and negligible DHRs are present in the F1 and F2 generations, but present in the F3 generation (Fig. 10A).

Downloaded from https://academic.oup.com/eep/article/4/2/dvy010/4987173 by guest on 30 November 2022

A Control versus vinclozolin F1 generation lineage DMRs

p-value	All Window	Multiple Window
0.001	21869	2434
1e-04	3815	285
1e-05	736	47
1e-06	**170**	**20**
1e-07	52	12

Number of significant windows	1	2	3	4	5	10
Number of DMR	150	15	2	1	1	1

B Control versus vinclozolin F2 generation lineage DMRs

p-value	All Window	Multiple Window
0.001	31185	4239
1e-04	5965	551
1e-05	1270	125
1e-06	**327**	**42**
1e-07	126	24

Number of significant windows	1	2	3	4	6	8
Number of DMR	285	33	5	1	2	1

C Control versus vinclozolin F3 generation lineage DMRs

p-value	All Window	Multiple Window
0.001	46835	11604
1e-04	12240	2534
1e-05	3560	724
1e-06	**1203**	**274**
1e-07	457	123

Number of significant windows	1	2	3	4	5	6	7	8	9	≥10
Number of DMR	929	173	52	20	8	4	5	2	1	9

D Overlap of DMRs

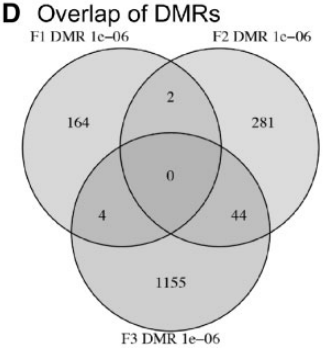

Figure 2: DMR analysis. **(A)** F1 generation control versus vinclozolin lineage DMRs. **(B)** F2 generation control versus vinclozolin lineage DMRs. **(C)** F3 generation control versus vinclozolin lineage DMRs. The number of DMRs found using different *P*-value cutoff thresholds is presented. The All Window column shows all DMRs. The Multiple Window column shows the number of DMRs containing at least two adjacent significant windows. **(D)** The DMR overlap ($P \leq$ 1e-06) for the F1, F2, and F3 generation sperm

The integration of the different epigenetic alterations is suggested in Fig. 9A and B with epimutation-associated genes in specific pathways and gene categories. The majority of the gene categories and pathways observed in the F1 generation was associated with the lncRNAs. The same phenomenon was found in the F3 generation but associated with the DMRs (Fig. 9A and B). Two pathways, axon guidance and pathways in cancer, were selected to investigate the potential overlap with genes involving the lncRNA- and DMR-associated genes (Supplementary Figs. S1 and S2). For the F1 and F3 generation lncRNA and DMRs the pathways were represented by both types of epimutations at independent genes, and few had the same gene involving a lncRNA in the F1 generation and DMR in the F3 generation. In both generations the pathways were affected, but with different types of epimutations.

The Venn diagrams of DMRs, DHRs, and ncRNA suggest negligible overlap between the different types of epimutations within the same generation comparison (Fig. 9C). So, the different epigenetic alterations have different genomic locations and minimal overlap between each other in the same generation. The total list of associated genes with the DMRs, ncRNAs, and DHRs are presented in the Supplementary Tables S1–S13.

Discussion

This study was designed to help understand how three different epigenetic processes in sperm are correlated with vinclozolin-induced epigenetic transgenerational inheritance of disease. A number of transgenerational diseases including testis disease, ovarian disease, kidney pathology, prostate abnormalities, and

Downloaded from https://academic.oup.com/eep/article/4/2/dvy010/4987173 by guest on 30 November 2022

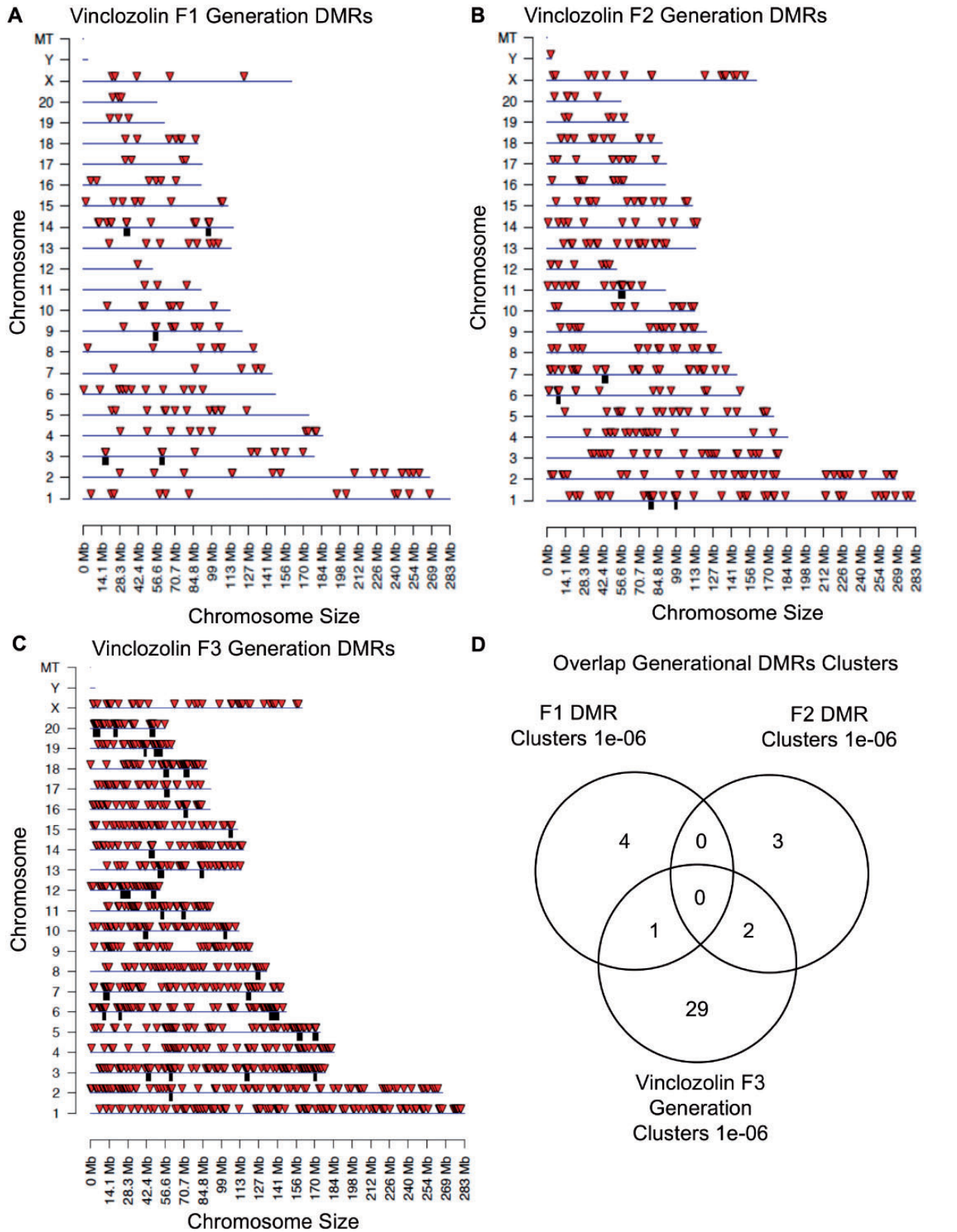

Figure 3: chromosomal locations and overlaps of DMRs. **(A)** Vinclozolin F1 generation DMRs. **(B)** Vinclozolin F2 generation DMRs. **(C)** Vinclozolin F3 generation DMRs. The DMR locations on the individual chromosomes are shown with red arrowheads and clusters of DMRs with black boxes. All window DMRs at a *P*-value threshold of 1e-06 are shown. **(D)** Overlap of the different generations DMR clusters

Downloaded from https://academic.oup.com/eep/article/4/2/dvy010/4987173 by guest on 30 November 2022

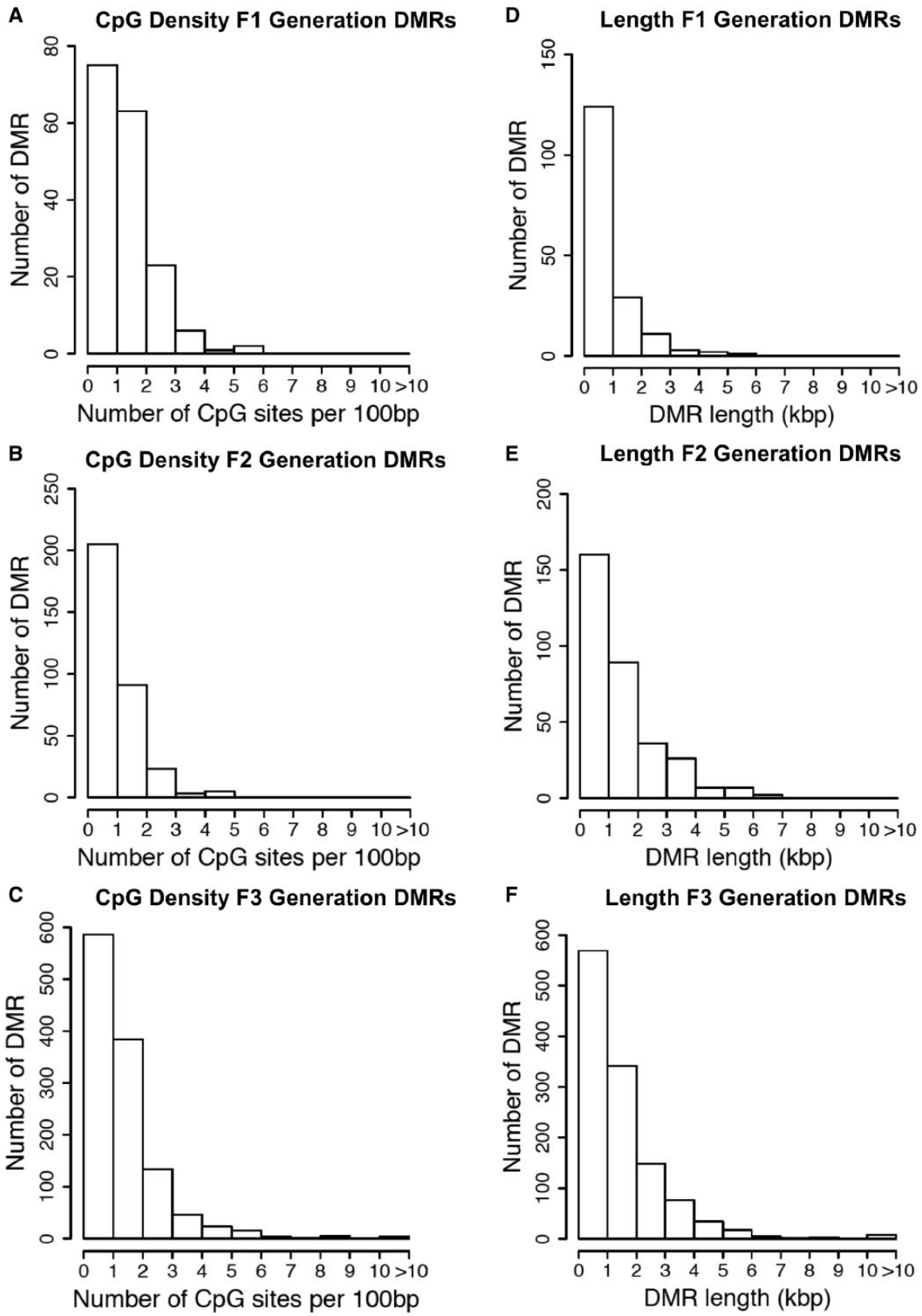

Figure 4: DMR CpG density. **(A)** F1 generation, **(B)** F2 generation, and **(C)** F3 generation. Histograms of the number of DMRs at different CpG densities (CpG/100 bp). All DMRs at a *P*-value threshold of 1e-06 are shown. DMR length (kb) for **(D)** F1 generation, **(E)** F2 generation, and **(F)** F3 generation. Histograms of the number of DMR at different length (kb) are shown

Downloaded from https://academic.oup.com/eep/article/4/2/dvy010/4987173 by guest on 30 November 2022

A **Control versus Vinclozolin Lineage Long ncRNA**

P-value	F1	F2	F3
0.001	2031	2255	601
1e-04	**947**	**542**	**400**
1e-05	0	0	0
1e-06	0	0	0
1e-07	0	0	0

B **Control versus Vinclozolin Lineage Small ncRNA**

P-value	F1	F2	F3
0.001	57	23	69
1e-04	**32**	**8**	**34**
1e-05	14	3	16
1e-06	6	0	8
1e-07	4	0	3

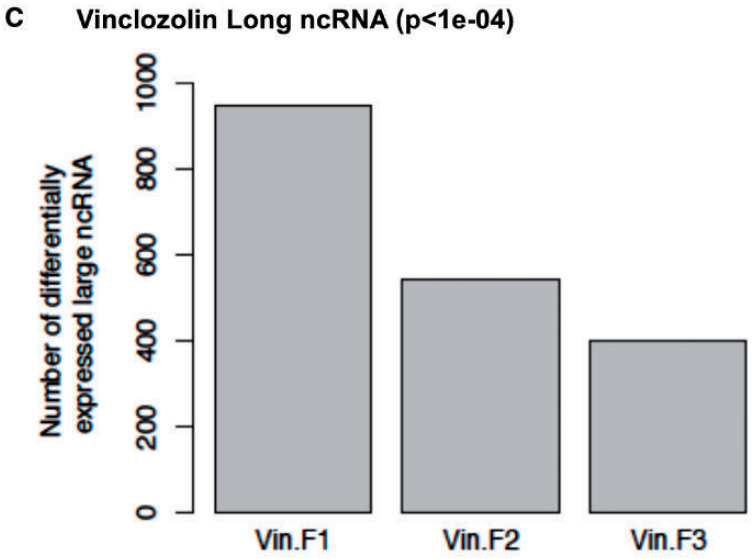

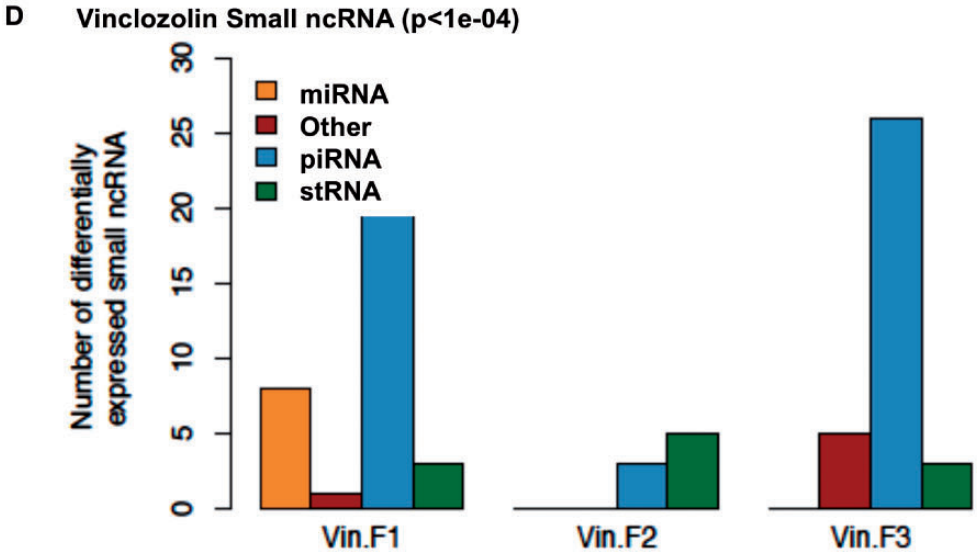

Figure 5: ncRNA differentially regulated in control versus vinclozolin lineage F1, F2, and F3 generation sperm. **(A)** lncRNA and **(B)** sncRNA numbers at different P-value thresholds. **(C)** The number of lncRNA ($P < 1e\text{-}04$) for the F1, F2, and F3 generation correlated to the number of differential lncRNA. **(D)** The number of sncRNA ($P < 1e\text{-}04$) for the F1, F2, and F3 generation correlated to the number of miRNA, piRNA, stRNA, and other sncRNA

anxiety behaviors have been shown to be induced by vinclozolin [37, 56]. Analyzing in parallel DNA methylation, ncRNA content, and histone retention in the same sperm samples from F1, F2, and F3 generation control versus vinclozolin lineage rats provides a broader comprehensive analysis of epigenetic alterations linked with environmentally induced germline epimutations. Classic toxicology studies for risk assessment investigate the direct exposure of the individual only, disregarding the impacts on future generations. However, transgenerational studies on environmental toxicants have shown that even if a

Downloaded from https://academic.oup.com/eep/article/4/2/dvy010/4987173 by guest on 30 November 2022

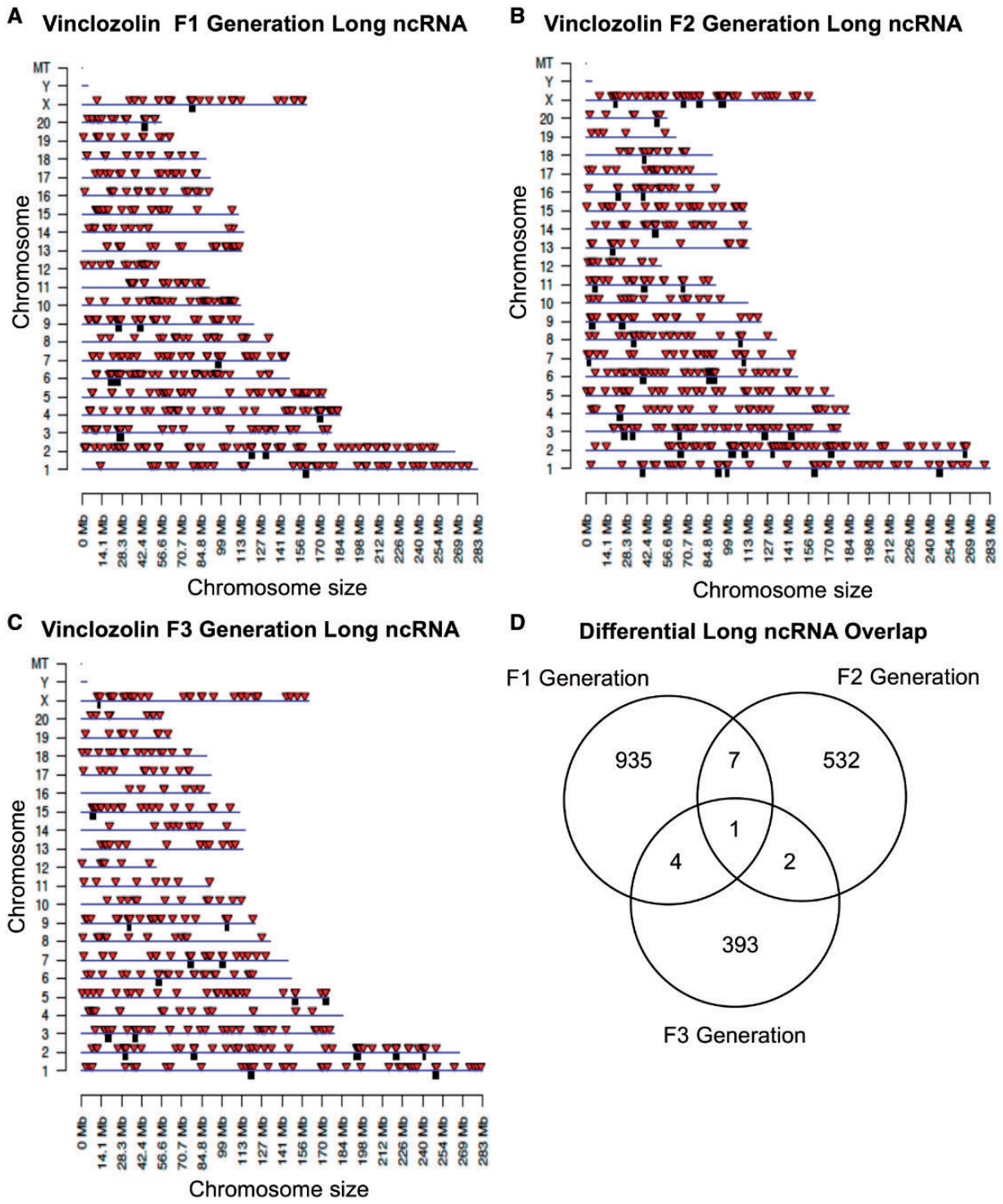

Figure 6: chromosomal locations of lncRNA. **(A)** F1 generation, **(B)** F2 generation, and **(C)** F3 generation sperm. The lncRNA locations on the individual chromosomes are indicated with red arrowheads and clusters with black boxes. The lncRNA at a *P*-value threshold of 10^{-4} is shown. **(D)** The overlap between the lncRNA ($P < 1e\text{-}04$) in the three vinclozolin generations. Overlaps were determined based on common ncRNA names

compound seems safe or has negligible risk from direct exposure mechanisms, it can affect the offspring of future generations [28]. Treatment of a gestating F0 generation female exposes the F1 generation fetus and the germline that will generate the F2 generation (Fig. 1A). Thus, the F1 generation represents a direct exposure, the F2 generation is a mix of direct and generational exposure, and the F3 generation and subsequent generations are considered purely transgenerational. This study investigates and compares the sperm epimutations in each of these generations.

Alterations in DNA methylation patterns were the first epigenetic process shown in F3 generation sperm [16, 57].

Downloaded from https://academic.oup.com/eep/article/4/2/dvy010/4987173 by guest on 30 November 2022

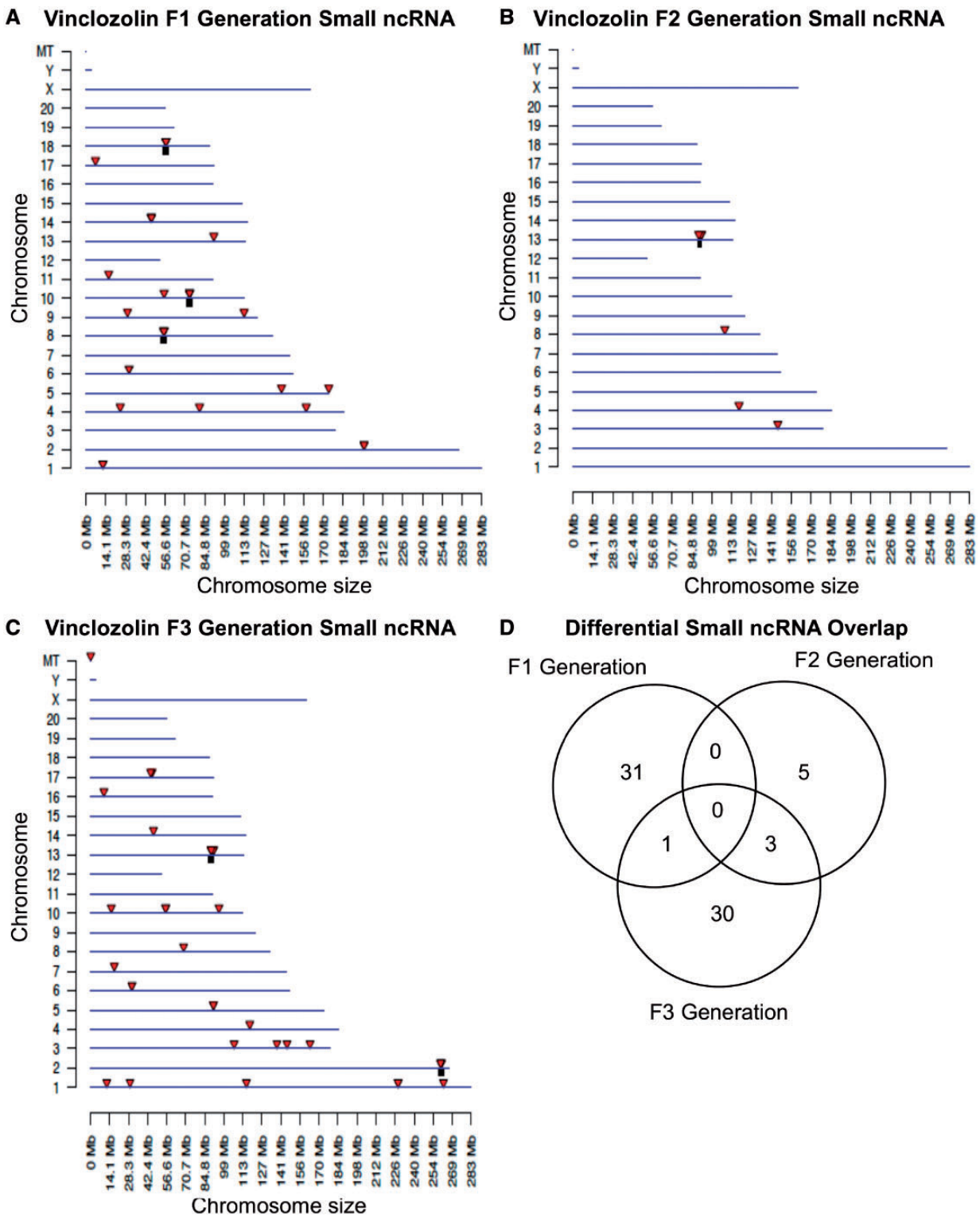

Figure 7: chromosomal locations of small ncRNA. **(A)** F1 generation, **(B)** F2 generation, and **(C)** F3 generation. The sncRNA locations on the individual chromosomes are indicated with red arrowheads and clusters with black boxes. The sncRNA at an FDR-adjusted *P*-value threshold of $P < 1e\text{-}04$ is shown. **(D)** The overlap between the sncRNAs ($P < 1e\text{-}04$) in the three vinclozolin generations. Overlaps were determined based on common RNA names

Therefore, many studies have focused on DNA methylation alterations in the germline and since then numerous chemicals, nutrition or stress exposures have been shown to induced transgenerational phenotypes [21]. A previous study identified a distinct set of DMRs in vinclozolin lineage rat sperm DNA methylation between the F1 and the F3 generation [58]. Most DMRs identified in this study are unique between the F1, F2, and F3 generations. This shows that the direct exposure F1 generation sperm and transgenerational F3 generation sperm DMRs are specific to each generation. Interestingly, we observed

Downloaded from https://academic.oup.com/eep/article/4/2/dvy010/4987173 by guest on 30 November 2022

A Vinclozolin F1 Generation DHRs

P-value	All Window	Multiple Window
1e-04	161	3
1e-05	22	2
1e-06	**5**	**0**
1e-07	0	0
1e-08	0	0
Number of significant windows	1	
Number of DHRs	5	

B Vinclozolin F2 Generation DHRs

P-value	All Window	Multiple Window
1e-04	122	3
1e-05	21	1
1e-06	**3**	**0**
1e-07	0	0
1e-08	0	0
Number of significant windows	1	
Number of DHRs	3	

C Vinclozolin F3 Generation DHRs

P-value	All Window	Multiple Window
1e-04	3542	169
1e-05	627	23
1e-06	**99**	**2**
1e-07	19	0
1e-08	5	0
Number of significant windows	1	2
Number of DHRs	97	2

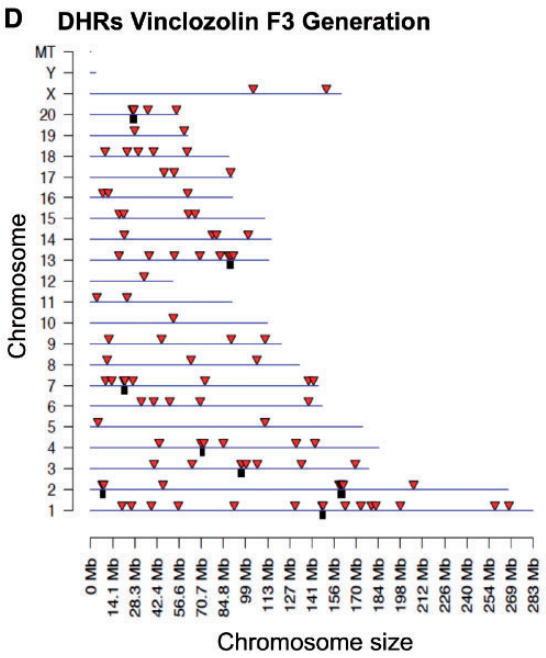

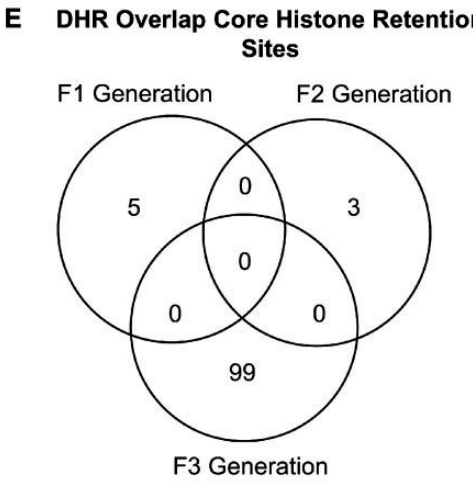

Figure 8: vinclozolin DHRs. **(A)** F1 generation, **(B)** F2 generation, and **(C)** F3 generation. The number of DHRs found using different *P*-value cutoff thresholds. The All Window column shows all DHRs. The Multiple Window column shows the number of DHRs containing at least two significant windows. **(D)** Chromosomal locations of the DHRs in the F3 generation on individual chromosomes are indicated by red arrowheads and DHR clusters with black boxes. All DHRs at a *P*-value threshold of 1e-06 are shown. **(E)** The DHR overlap ($P < 1e\text{-}06$) for the F1, F2, and F3 generation sperm

that the F2 generation seems to have fewer epimutations and has minimal overlap with the F1 and F3 generations. A small set of overlapping DMRs between the F2 and F3 generation sperm are presented in the Supplementary Fig. S4. These represent the potential transgenerational DMR that appear first in the F2 generation. In addition, no known imprinted genes correlated to the DMRs identified. As classic imprinted genes are resistant to environmental alterations in regards to DNA methylation [59], they do not appear in the differential DNA methylation regions observed.

Environmental conditions such as traumatic stress in early life in mice altered miRNA expression and behavioral and metabolic responses in the progeny. Several miRNAs were affected in the serum and brain of the traumatized animals and their progeny when adult. Sperm of traumatized males was also affected. Injection of sperm ncRNAs from these males into fertilized wild-type oocytes reproduced the behavioral and metabolic changes in the resulting offspring. These results suggest that sncRNAs are sensitive to environmental factors in early life and contribute to the inheritance of trauma-induced phenotypes across generations [39]. Vinclozolin-induced epigenetic transgenerational inheritance of disease has also been shown to involve alterations in sperm sncRNA [40]. Transgenerational lncRNA and sncRNA have been proposed to have diverse functions [5]. The sncRNA often targets specific genes through alterations in mRNA metabolism or binding protein [60], whereas the lncRNA regulates the transcriptional machinery and targets multiple distal genes. In this study, the number of lncRNA was much higher than the number of sncRNA. The overlap between each generation was very low or nonexistent. The piRNA was the most common class of sncRNA for the F1 and F3 generations, stRNAs (small tRNA fragments) were the most common for the F2 generation (Fig. 5D). Our results show that concurrent DNA methylation and ncRNA alterations in sperm may be

Downloaded from https://academic.oup.com/eep/article/4/2/dvy010/4987173 by guest on 30 November 2022

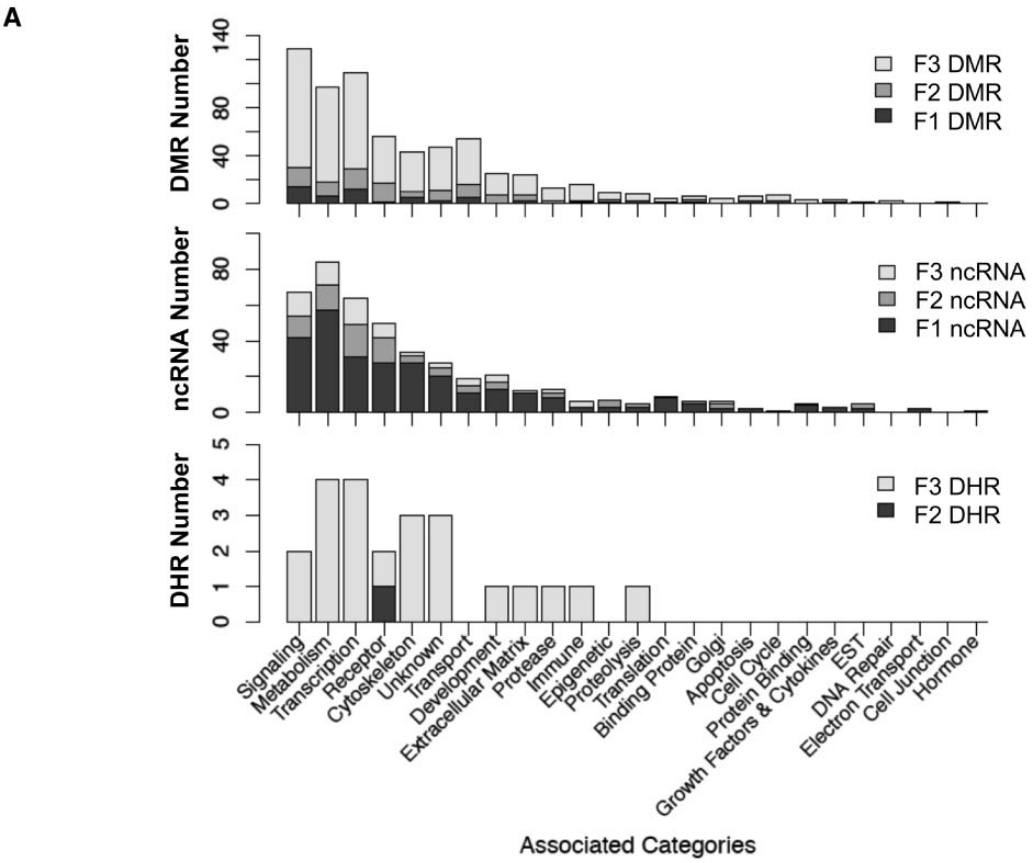

B

Generations	F1				F2				F3			
Epimutations	DMRs	lncRNA	sncRNA	DHRs	DMRs	lncRNA	sncRNA	DHRs	DMRs	lncRNA	sncRNA	DHRs
Axon Guidance	5	3			1				10			
Metabolic Pathways		35			4	5			41			
cGMP-PKG Signaling Pathway		6							14			
Human Papillomavirus Infection		6						3	10	3		
Olfactory Transduction		4			5	3			13	5		
Pathways in Cancer		10				3			13	3		
Neuroactive Ligand-Receptor Interaction		3			4				7			
Wnt Signaling Pathway		7							4	3		

C

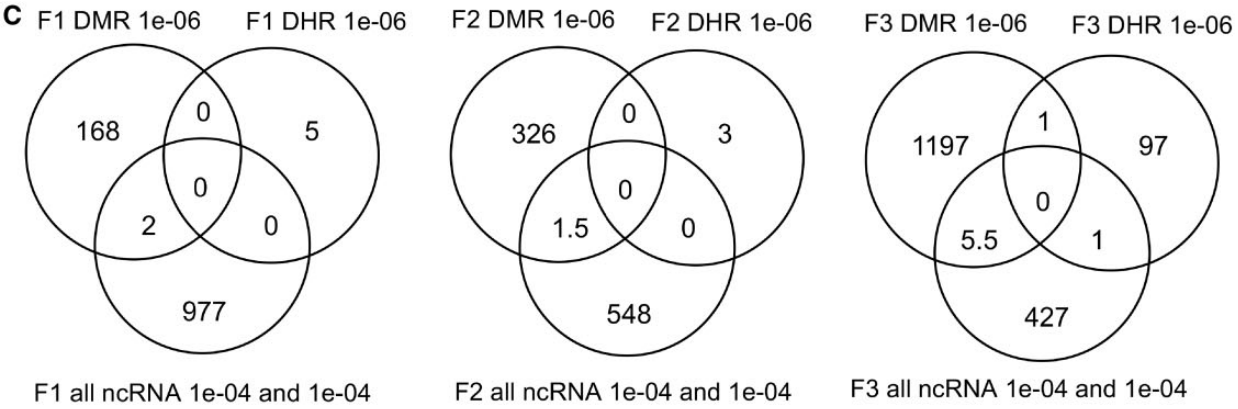

Figure 9: epimutation overlaps and gene associations. **(A)** The number of DMR, ncRNA, and DHR epimutation-associated genes in each gene category for the F1, F2, and F3 generations. **(B)** Gene pathways with epimutation-associated genes for the DMRs, DHRs and ncRNAs in the F1, F2 and F3 generations. The pathways with greater than three associated genes for each epimutation type are listed that were in general common between generations. **(C)** Overlaps of the F1, F2, and F3 generation epimutations between the DMRs, DHRs, and ncRNAs

Downloaded from https://academic.oup.com/eep/article/4/2/dvy010/4987173 by guest on 30 November 2022

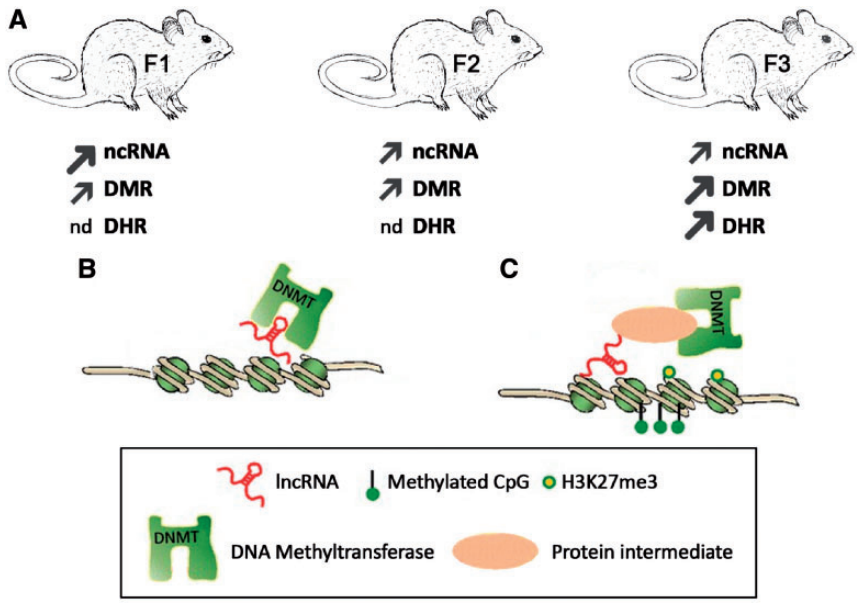

Figure 10: The regulatory mechanisms of DNA methylation by lncRNAs. **(A)** Summary of the different epimutations in the F1, F2, and F3 generation exposed rat sperm with larger/thicker arrows reflecting larger numbers of epimutations than thinner arrows and nd (negligible detected). **(B)** lncRNA/DNMT interaction prevents locus-specific DNA methylation locally *in cis*. **(C)** lncRNA interacts with DNMT1 (methyltransferase 1) indirectly through a protein intermediate. Figure modified from [43]

associated with the epigenetic transgenerational inheritance phenomenon.

Sperm chromatin not only has a unique structure to condense and protect the paternal DNA, but it also provides epigenetic information supporting early embryonic development. The histones and other chromatin proteins remaining are located in structurally and transcriptionally relevant positions in the genome and carry diverse posttranslational modifications relevant to the control of embryonic gene expression. In *Caenorhabditis elegans* and *Drosophila*, inheritance of phenotypes has been associated with histone modifications [13, 61] which has not been reported in mammals. Histone modifications and retentions have been shown to be implicated in male fertility [53, 62]. However, until recently the role of histone retention has not been implicated in transgenerational inheritance studies [52]. At the end of spermatogenesis the histones are removed in many species and the DNA is condensed by protamines forming highly dense nucleoprotamine complexes [63]. Generally, 5–10% of histones are retained and are thought to play a role in the zygotic and early embryonic gene expression [53, 64–67]. In this study, the hypothesis that vinclozolin could alter histone retentions in a transgenerational manner was investigated. In a previous study, control sperm rats were shown to have a highly reproducible core set of histones [52]. This core set of histones generally remained the same in the control animals and the animals exposed to vinclozolin between the F1, F2, and F3 generations. Because of its high reproducibility and consistency between each generation, and despite the treatment with DDT or vinclozolin, these core histone sites are highly conserved and speculated to be critical for early development [52]. The analysis of DHRs revealed that the F1 and the F2 generation control versus vinclozolin lineage sperm had negligible DHRs (Fig. 8). This observation suggests that the direct vinclozolin exposure does not alter histone retention or trigger any changes. However, the F3 generation control versus vinclozolin lineage sperm DHRs increased considerably in comparison to the F1 and F2 generation DHRs. In addition to the DMRs and ncRNAs, alterations in histone retention sites are also associated with the vinclozolin-induced transgenerational F3 generation sperm. Unlike the ncRNAs and DMRs, the F1 and F2 generation histone retention sites were not affected in the exposed animals. The DHR epimutations are all present in the transgenerational F3 generation sperm and therefore might also play a role in mediating the epigenetic transgenerational inheritance phenomenon.

In order to investigate the integration of DMRs, ncRNA, and DHR, the overlap of the different genomic sites between the different epimutations was analyzed. The chromosomal locations of the DMR, ncRNA, and DHR epimutations were distinct with a low number of overlaps. These transgenerational epimutations have chromosomal localizations that are distinct between each other, but generally they are present in regions with similar genomic features (e.g. CpG desert and size). The genome evolving over time develops regions that have very low cytocine (C) levels due to the ability of DNA methylation of the CpG site to promote susceptibility for a C to T conversion point mutation. Over 90% of the known point mutations in the genome are C to T conversions. Therefore, if a cluster of CpG sites with DNA methylation are conserved evolutionarily in these deserts of CpG, they likely are functionally important [55].

The gene associations of the transgenerational epimutations identified two similar categories of genes for the ncRNA and the DMRs involving metabolism, signaling, and transcription. The analysis comparing the F1, F2, and F3 generation epimutation-associated genes showed minimal overlap between the different types of epimutations (Fig. 9C). Each one of them (DMRs, ncRNA, DHRs) appears to associate with different pathways and may be integrated on a functional level. Although the epimutations in sperm can have associated genes, the sperm are transcriptionally silenced due to the compaction of DNA with protamines and complete loss of transcriptional machinery. The epimutations observed will primarily function in the early embryo to impact gene expression and epigenetic programming to alter the embryonic stem cell epigenome and transcriptome. Therefore all somatic cells derived from this stem cell population will have altered epigenomes and transcriptomes, and those sensitive to that will have a susceptibility to develop

Downloaded from https://academic.oup.com/eep/article/4/2/dvy010/4987173 by guest on 30 November 2022

disease later in life. Therefore, the epimutation gene associations may be important for later somatic cell development and differentiation, but not relevant to sperm function.

Interestingly, the comparisons in the F1, F2, and F3 generations provide insights into the direct exposure effects to vinclozolin and transgenerational impacts of the exposure. The F1 and F2 generations are exposed directly to vinclozolin (Fig. 1B), whereas the F3 generation is the first transgenerational generation. The effects observed in the F1 and F2 generations were different from the ones observed in the F3 generation. Predominantly, ncRNAs were altered by the direct exposure to vinclozolin in the F1 generation whereas the DNA methylation and histone retention sites were more predominant in the F3 generation. Histone retention did not seem to be affected by a direct exposure of vinclozolin. Therefore, the number of ncRNA was dramatically altered in the F1 generation, but to a lesser extent in the F2 and F3 generations. The altered ncRNA was also distinct between each generation (Fig. 9B). The transgenerational F3 generation alterations in DNA methylation, ncRNAs, and histone retention are distinct from the direct exposure in the F1 and F2 generations.

The analysis of the different epimutations associated gene pathways revealed that the F1 generation ncRNA seemed to be targeted by the direct vinclozolin exposure. However, these ncRNA epimutations (predominantly lncRNA) associated gene pathways disappeared in the F3 generation and similar associated gene pathways were found within the DMRs. The hypothesis is that the ncRNA could be more sensitive to the direct exposure to vinclozolin, then mediate the formation of the other epimutations in the next generation with DNA methylation and histone retention becoming permanent and mediating the epigenetic transgenerational inheritance in the future generations. An emerging hypothesis is the capacity of ncRNAs to modulate gene expression and many of them have been identified to participate in epigenetic control by interacting with various types of proteins involved in histone modification or chromatin remodeling [43]. Although these ncRNA regulations have not been observed in transgenerational animals, lncRNAs appear to be able to modulate DNA and/or histone methylation [43, 68]. Therefore, ncRNA may be the epimutation that helps mediate the formation and actions of the other types of epimutations. Based on Zhao *et al.*, two hypotheses are proposed to explain how lncRNA can interact directly or indirectly with diverse DNMT members (Fig. 10B) [43]. Through recruitment or eviction the lncRNA can either promote or repress DNA methylation *in cis* or *in trans*. The dynamic of the lncRNA repertoire and the ncRNA plasticity to interact with DNA, ncRNA, and protein makes lncRNA a potential mediator to regulate local and sequence-specific DNA methylation or demethylation. Although lncRNA are not as well annotated or functionally linked as sncRNA, as seen in Supplementary Tables S5–S7 nearly a third of those observed have associated genes. These modifications can result in global changes in DNA methylation profile, thus changing how cells can respond to diverse stimuli (Fig. 10). Even though it has not been shown yet, an interplay between lncRNA and histones is likely. Clearly an integration and interplay between the different epigenetic processes will be critical in the epigenetic transgenerational phenomenon and regulation of genome activity.

Studies are in progress to explore the integration of these transgenerational epimutations. One of the possibilities is that the transgenerational epimutations developed in the F1 and F2 generations alter the developmental epigenetic programming of the primordial germ cells (PGCs) which are the stem cells for the germline. This epigenetic alteration in the PGCs development and become permanently established and is transmitted through the germline to the next generation. This germline reprogramming will promote the epigenetic transgenerational inheritance phenomenon. Epigenetic alterations in the transgenerational PGCs have already been observed [32, 69], but further studies are required to better understand the PGCs' transgenerational mechanisms. This study provides new insights into the distinct epigenetic alterations between a direct exposure phenomenon and the transgenerational impact of the exposure. Additional support that vinclozolin is concurrently altering these different types of epimutations comes from similar observations of concurrent alterations following DDT exposure [7].

Further investigation is needed to better understand the integrated mechanisms of the unique transgenerational F3 generation germline epigenetic alterations. It appears that the phenomenon is more complex than just a direct exposure triggering the formation of epimutations that are then simply maintained in the subsequent generations. This study finds concurrent alterations of DNA methylation, ncRNA, and histone retention in the sperm. Observations indicate that all three types of epimutations are involved in the epigenetic transgenerational inheritance phenomenon. The ncRNA have already been shown to act on DNA methylation or histone methylation [43, 68]; so it is not surprising to discover that DNA methylation, ncRNA, and histone retention appear to be integrated to facilitate the epigenetic transgenerational inheritance. The potential impact of these epimutations on disease etiology and other areas in biology requires further investigation and clarification of the mechanisms involved.

Methods

Animal Studies and Breeding

Female and male rats of an outbred strain Hsd: Sprague Dawley SD®™ (Harlan) at about 70 and 100 days of age were fed *ad lib* with a standard rat diet and received *ad lib* tap water for drinking. To obtain time-pregnant females, the female rats in proestrus were pair-mated with male rats. The sperm-positive (Day 0) rats were monitored for diestrus and body weight. On Days 8 through 14 of gestation [36], the females received daily intraperitoneal injections of vinclozolin (100 mg/kg BW/day) or DMSO. The vinclozolin was obtained from Chem Service Inc. (West Chester, PA) and was injected in a 20-µl DMSO vehicle as previously described [70]. Treatment lineages are designated "control" or "vinclozolin" lineages. The treated gestating female rats were designated as the F0 generation. The offspring of the F0 generation rats were the F1 generation. Non-littermate females and males aged 70–90 days from the F1 generation of control or vinclozolin lineages were bred to obtain F2 generation offspring. The F2 generation rats were bred to obtain F3 generation offspring. Individuals were maintained for 12 months and euthanized for sperm collection. The F1–F3 generation offspring were not themselves treated directly with vinclozolin. The control and vinclozolin lineages were housed in the same room and racks with lighting, food, and water as previously described [54, 70, 71]. All experimental protocols for the procedures with rats were pre-approved by the Washington State University Animal Care and Use Committee (IACUC approval # 02568-49).

Testis sections from the males were obtained, fixed for histology, and examined by Terminal Deoxynucleotidyl Transferase-mediated dUTP Nick End Labeling (TUNEL) assay (*in situ* cell death

Downloaded from https://academic.oup.com/eep/article/4/2/dvy010/4987173 by guest on 30 November 2022

detection kit, Fluorescein, Sigma, St. Louis, MO) to assess spermatogenic cell apoptosis.

Epididymal Sperm Collection and DNA

The epididymis was dissected free of connective tissue, a small cut made to the cauda and tissue placed in 5 ml of 1× PBS solution for up to 24 h at 4°C. The epididymal tissue was minced and the released sperm was centrifuged at 6000 g, then the supernant removed, and the pellet resuspended in NIM buffer, to be stored at −80°C until further use. One hundred microliters of sperm suspension was sonicated to destroy somatic cells and tissue, spun down at 6000 g, the sperm pellet washed with 1× PBS once, and then combined with 820 µl DNA extraction buffer and 80 µl 0.1 M DTT. The sample was incubated at 65°C for 15 min. Following this incubation 80 µl proteinase K (20 mg/ml) was added and the sample incubated at 55°C for at least 2 h under constant rotation. Then 300 µl of protein precipitation solution (Promega, A7953) was added, the sample mixed thoroughly and incubated for 15 min on ice. The sample was centrifuged at 12 500 g for 30 min at 4°C. One milliliter of the supernatant was transferred to a 2-ml tube and 2 µl of glycoblue and 1 ml of cold 100% isopropanol were added. The sample was mixed well by inverting the tube several times, then left in −20°C freezer for at least 1 h. After precipitation the sample was centrifuged at 12 500 g for 20 min at 4°C. The supernatant was taken off and discarded without disturbing the (blue) pellet. The pellet was washed with 70% cold ethanol by adding 500 µl of 70% ethanol to the pellet and returning the tube to the freezer for 20 min. After the incubation the tube was centrifuged for 10 min at 4°C at 12 500 g and the supernatant discarded. The tube was spun again briefly to collect residual ethanol to the bottom of the tube and then as much liquid as possible was removed with gel loading tip. Pellet was air-dried at RT until it looked dry (about 5 min). Pellet was then resuspended in 100 µl of nuclease free water.

Equal amounts of DNA or ncRNA from each individuals sperm from 3–4 different individuals for the F1 and F2 generations and 4–6 different individuals for the F3 generation were pooled and three different pools generation for each F1, F2, and F3 generation control and vinclozolin lineage males. Therefore, each pool had different individuals and there were three pools for each group. A summary of the pools for the DNA and ncRNA pools is shown in Supplementary Table S14. Two analyses of the same pool were taken, one for DNA and one for ncRNA. Therefore, between 10 and 17 individuals were present in the three pools for the subsequent analysis.

RNA Isolation

The F1–F3 generation vinclozolin and control lineage male epididymal sperm were collected and processed as previously described and stored at −80°C until use [57]. The total RNA (messenger RNA, lncRNA, ribosomal RNA, sncRNA) was isolated using the mirVana miRNA Isolation Kit (Life Technologies) following the manufacturer's instructions with modifications at the lysis stage. In brief, after addition of lysis buffer, the sperm pellets were manually homogenized, followed by a 20-min incubation at 65°C. Samples were then placed on ice, and the default protocol was resumed. For quality control, RNA integrity numbers (RIN) were obtained by RNA 6000 Pico chips run on an Agilent 2100 Bioanalyzer (Agilent). A RIN of 2–4 indicates good sperm RNA quality. Concentration was determined using the Qubit RNA HS Assay Kit (ThermoFisher). Biological replicates of sperm were pooled by equal ncRNA content and were concentrated using Agencourt AMPure XP beads (Beckman Coulter). Some pools had underrepresented replicates due to low concentration. In this case, the maximum RNA content from the replicate was used in the pool and the pool was concentrated. The pools and samples that were underrepresented are as follows: F1 control pool 3, samples 1 and 2; F2 control pool 2, sample 3; and F2 vinclozolin pool 2, sample 3. Equal amounts of each pool were used in the final analysis.

Methylated DNA Immunoprecipitation

MeDIP with genomic DNA was performed as follows: rat sperm DNA pools were generated using the appropriate amount of genomic DNA from each individual for three pools each of control and vinclozolin lineage animals. Genomic DNA was sonicated using the Covaris M220 the following way: the pooled genomic DNA was diluted to 130 µl with TE buffer into the appropriate Covaris tube. Covaris was set to 300-bp program and the program was run for each tube in the experiment. Each sonicated DNA of 10 µl was run on 1.5% agarose gel to verify fragment size. The sonicated DNA was transferred from the Covaris tube to a 1.7-ml microfuge tube and the volume measured. The sonicated DNA was then diluted with TE buffer (10 mM Tris HCl, pH7.5; 1 mM EDTA) to 400 µl, heat-denatured for 10 min at 95°C, then immediately cooled on ice for 10 min. Then 100 µl of 5× IP buffer and 5 µg of antibody (monoclonal mouse anti-5-methyl cytidine; Diagenode #C15200006) were added to the denatured sonicated DNA. The DNA–antibody mixture was incubated overnight on a rotator at 4°C.

The following day magnetic beads (Dynabeads M-280 Sheep anti-Mouse IgG; 11201 D) were pre-washed as follows: the beads were resuspended in the vial, then the appropriate volume (50 µl per sample) was transferred to a microfuge tube. The same volume of Washing Buffer (at least 1 ml PBS with 0.1% BSA and 2 mM EDTA) was added and the bead sample was resuspended. Tube was then placed into a magnetic rack for 1–2 min and the supernatant was discarded. The tube was removed from the magnetic rack and the beads were washed once. The washed beads were resuspended in the same volume of 1× IP buffer (50 mM sodium phosphate ph7.0, 700 mM NaCl, 0.25% TritonX-100) as the initial volume of beads. Fifty microliters of beads was added to the 500 µl of DNA–antibody mixture from the overnight incubation, then incubated for 2 h on a rotator at 4°C.

After the incubation the bead–antibody–DNA complex was washed three times with 1× IP buffer as follows: the tube was placed into magnetic rack for 1–2 min and the supernatant discarded, then washed with 1× IP buffer three times. The washed bead–DNA solution is then resuspended in 250 µl digestion buffer with 3.5 µl Proteinase K (20 mg/ml). The sample was then incubated for 2–3 h on a rotator at 55°C and then 250 µl of buffered phenol–chloroform–isoamylalcohol solution was added to the supe and the tube vortexed for 30 s then centrifuged at 12 500 g for 5 min at room temperature. The aqueous supernatant was carefully removed and transferred to a fresh microfuge tube. Then 250 µl chloroform was added to the supernatant from the previous step, vortexed for 30 s and centrifuged at 12 500 g for 5 min at room temperature. The aqueous supernatant was removed and transferred to a fresh microfuge tube. To the supernatant 2 µl of glycoblue (20 mg/ml), 20 µl of 5 M NaCl and 500 µl ethanol were added and mixed well, then precipitated in −20°C freezer for 1 h to overnight.

Downloaded from https://academic.oup.com/eep/article/4/2/dvy010/4987173 by guest on 30 November 2022

The precipitate was centrifuged at 12 500 g for 20 min at 4°C and the supernatant removed, while not disturbing the pellet. The pellet was washed with 500 µl cold 70% ethanol in −20°C freezer for 15 min, then centrifuged again at 12 500 g for 5 min at 4°C and the supernatant was discarded. The tube was spun again briefly to collect residual ethanol to the bottom of the tube and as much liquid as possible was removed with gel loading tip. Pellet was air-dried at RT until it looked dry (about 5 min) then resuspended in 20 µl H_2O or TE. DNA concentration was measured in Qubit (Life Technologies) with ssDNA kit (Molecular Probes Q10212).

ncRNA Sequencing Analysis

LRNA and noncoding RNA were constructed using total RNA with the KAPA Stranded RNA-Seq Library Preparation kit with RiboErase, according to the manufacturer's instructions, with some modifications. The adaptor and barcodes used were from NEBNext Multiplex Oligos for Illumina. Prior to PCR amplification, libraries were incubated at 37°C for 15 min with the USER enzyme (NEB). PCR cycle number was determined using qPCR with the KAPA RealTime Library Amplification kit before final amplification. Size selection (300–700 bp) was performed using Agencourt AMPure XP beads (Beckman Coulter). Quality control was performed using Agilent DNA High Sensitivity chips (Agilent) and Qubit dsDNA high sensitivity assay (ThermoFisher). Libraries were pooled and loaded onto an Illumina NextSeq High Output v2 1x75 chip, and sequenced on an Illumina NextSeq 500 sequencer. Bioinformatics analysis was used to separate mRNA libraries from ncRNA libraries (see ncRNA Bioinformatics section).

Prior to sncRNA library preparation, total sperm RNA samples were enriched for sncRNAs using the miRNA enrichment protocol (Beckman Coulter), and libraries were constructed using the NEBNext Multiplex Small RNA Library Prep Set for Illumina, and barcoded with NEBNext Multiplex Oligos for Illumina. Size selection (135–170 bp) was performed using the Pippin Prep (Sage Science). Quality control was performed using Agilent DNA High Sensitivity chips (Agilent) and Qubit dsDNA high sensitivity assay (ThermoFisher). Libraries were pooled and loaded onto an Illumina NextSeq High Output v2 1x75 chip, and sequenced on an Illumina NextSeq 500 sequencer.

Histone Chromatin Immunoprecipitation ChIP-Seq

Histone chromatin immunoprecipitation with genomic DNA was performed as follows (adapted from [72]): rat sperm pools were generated using a total of 8 million sperm per pool for 3 pools of control and vinclozolin lineage animals. The control pools contained equal amounts of sperm for each of 3–4 individuals for a total of $n = 11$ rats and the vinclozolin pools contained equal amounts of sperm for each of 3 individuals for a total of $n = 9$ rats per exposure group. To remove any somatic cell contamination, sperm samples from each animal were sonicated 10 s using a Sonic Dismembrator Model 300 (Thermo Scientific Fisher, USA) then centrifuged 4000 g for 5 min at 4°C. The supernatant was discarded and the pellet was resuspended and counted individually on a Neubauer counting chamber (Propper Manufacturing Co., Inc., New York, USA) prior to pooling. The sperm pools were reconstituted up to 1 ml with 1× PBS. To reduce disulfide bonds, 50 µl of 1 M DTT was added to each pool and the pools were then incubated for 2 h at room temperature under constant rotation. To quench any residual DTT in the reaction, 120 µl of fresh 1 M NEM (*N*-ethylmaleimide, Thermo Scientific, Rockford, USA) was then added and the samples were incubated for 30 min at room temperature under constant rotation. The sperm cells were pelleted at 2000 g for 5 min at room temperature and the supernatant was discarded. Pellets were resuspended in 1× PBS and then spun again at 2000 g for 5 min at room temperature. The supernatant was discarded. The sperm cell DNA was divided into aliquots of 4 µg of DNA and was then suspended in "complete buffer" [final concentration: 15 mM Tris-HCl (pH 7.5), 5 mM $MgCl_2$, 0.1 mM EGTA; all filtered through a 0.22-µm filter and stored at room temperature; 0.5% tergitol (vol/vol) and 1% DOC (wt/vol), sodium deoxycholate]. A 130 µl of this complete buffer was added to each DNA aliquot. The samples were mixed and incubated for 20 min on ice. These aliquots were sonicated using the Covaris M220 the following way: 4 µg of genomic DNA was resuspended in 130 µl of complete buffer supplemented with tergitol 0.5% and DOC 1%. Covaris was set to a 10-min "Chromatin shearing" program and the program was run for each tube in the experiment.

For each sample 10 µl was run on a 1.5% agarose gel to verify fragment size. Aliquoted samples were pooled back together and centrifuged at 12 500 g for 10 min at room temperature. The supernatant was transferred to a fresh microfuge tube. Sixty-five microliters of protease inhibitor cocktail (1 tablet dissolved in 500 µl, 20× concentrated) (Roche, cat. no. 11 873 580 001) was added to each sample as well as 3 µl of antibody (monoclonal rabbit antihistone H3, Millipore 05-928). The DNA–antibody mixture was incubated overnight on a rotator at 4°C. The following day, magnetic beads (ChIP-Grade protein G magnetic beads, Cell Signaling 9006) were pre-washed as follows: the beads were resuspended in the vial, then 30 µl per sample was transferred to a microfuge tube. The same volume of Washing Buffer (at least 1 ml) was added and the bead sample was resuspended. Tube was then placed into a magnetic rack for 1–2 min and the supernatant was discarded. The tube was removed from the magnetic rack and the beads were washed once. The washed beads were resuspended in the same volume of 1× IP buffer as the initial volume of beads. Thirty microliters of beads was added to each DNA–antibody mixture from the overnight incubation, then incubated for 2 h on a rotator at 4°C. After the incubation, the bead–antibody–DNA complex was washed three times with 1× IP buffer as follows: the tube was placed into a magnetic rack for 1–2 min and the supernatant was discarded, then washed with 1× IP buffer 3 times. The washed bead–antibody–DNA solution was then resuspended in 300 µl of digestion buffer and 3 µl proteinase K (20 mg/ml). The sample was incubated for 3 h on a rotator at 56°C. After incubation the samples were extracted with phenol–chloroform–isoamylalcohol and precipitated with 2 µl of glycoblue (20 mg/ml), a one-tenth volume of 3 M sodium acetate and two volumes of ethanol overnight at −20°C.

The precipitate was centrifuged at 14 000 g for 30 min at 4°C and the supernatant was removed, while not disturbing the pellet. The pellet was washed with 500 µl cold 70% ethanol, then centrifuged again at 14 000 g for 10 min at 4°C and the supernatant was discarded. The tube was spun briefly to collect residual ethanol and as much liquid as possible was removed with a gel loading tip. Pellet was air-dried at RT until it looked dry (about 5 min) then resuspended in 20 µl H20. DNA concentration was measured in the Qubit (Life Technologies) with the BR dsDNA kit (Molecular Probes Q32853).

MeDIP-Seq Analysis

The MeDIP pools were used to create libraries for NGS using the NEBNext® Ultra™ RNA Library Prep Kit for Illumina® (NEB, San

Downloaded from https://academic.oup.com/eep/article/4/2/dvy010/4987173 by guest on 30 November 2022

Diego, CA) starting at step 1.4 of the manufacturer's protocol to generate double-stranded DNA. After this step the manufacturer's protocol was followed. Each pool received a separate index primer. NGS was performed at WSU Spokane Genomics Core using the Illumina HiSeq 2500 with a PE50 application, with a read size of ~50 bp and ~100 million reads per pool. Two to three libraries were run in one lane.

Histone ChIP-Seq Analysis

The ChIP pools were used to create libraries for NGS using the NEBNext® Ultra™ II DNA Library Prep Kit for Illumina® (NEB, San Diego, CA). The manufacturer's protocol was followed. Each pool received a separate index primer. NGS was performed at WSU Spokane Genomics Core using Ilumina HiSeq 2500 with a PE50 application, with a read size of ~50 bp and ~35 million reads per pool. Six libraries were run in one lane.

ncRNA Bioinformatics

The sncRNA-Seq data were annotated as follows: reads shorter than 15 nt were discarded by Cutadapt [73]. The remaining reads were matched to known rat sncRNA, consisting of mature miRNA (miRBase, release 21), tRNA (Genomic tRNA Database, rn5), piRNA (piRNABank), rRNA (ENSEMBL, release 76), and mitochondrial RNA (ENSEMBL, release 76) using AASRA pipeline with default parameters [74]. Read counts generated by AASRA were statistically normalized by DESeq2 [75].

The lncRNA data were annotated as follows: trimmomatic was used to remove adaptor sequences and the low-quality reads from the RNA sequencing data [76]. To identify all the transcripts, we used Tophat2 and Cufflinks to assemble the sequencing reads based on the Ensembl_Rnor_6.0 [77]. The differential expression analyses were performed by Cuffdiff. The coding and the noncoding genes were primarily annotated through rat CDS data ensembl_Rnor_6.0. The non-annotated genes were extracted through our in-house script, then analyzed by CPAT, indicating the true ncRNAs [78].

Statistics and Bioinformatics

For the DMR and DHR analyses, the basic read quality was verified using summaries produced by the FastQC program (http://www.bioinformatics.babraham.ac.uk/projects/fastqc/). The raw reads were trimmed and filtered using Trimmomatic. The reads for each MeDIP sample were mapped to the Rnor 6.0 rat genome using Bowtie2 [76] with default parameter options. The mapped read files were then converted to sorted BAM files using SAMtools [79]. To identify DMRs and DHRs, the reference genome was broken into 100-bp windows. The MEDIPS R package [80] was used to calculate differential coverage between control and exposure sample groups. The edgeR *P*-value [81] was used to determine the relative difference between the two groups for each genomic window. Windows with an edgeR *P*-value $<10^{-6}$ were considered DMRs or DHRs. The DMR or DHR edges were extended until no genomic window with a *P*-value <0.1 remained within 1000 bp of the DMR or DHR. CpG density and other information were then calculated for the DMR based on the reference genome.

DMRs, DHRs, and ncRNA were annotated using the biomaRt R package [82] to access the Ensembl database [83]. The genes that fell within 10 kb of the DMR, DHR, or ncRNA edges were then input into the KEGG pathway search [84, 85] to identify associated pathways. The associated genes were then sorted into functional groups by consulting information provided by the DAVID [86], Panther [87], and Uniprot databases incorporated into an internal curated database (www.skinner.wsu.edu under genomic data).

Acknowledgments

We acknowledge Ms Deepika Kubsad and Ms Jayleana Barton for technical assistance and Ms Heather Johnson for assistance in preparation of the manuscript. We thank the Genomics Core Laboratories at WSU and UNR. This study was supported by a John Templeton Foundation (50183) grant to M.K.S. and NIH (ES012974) grant to M.K.S. and NIH grants (HD085506 and GM110767) to W.Y.

Supplementary data

Supplementary data are available at *EnvEpig* online.

Conflict of interest statement. None declared.

References

1. Holliday R. The inheritance of epigenetic defects. *Science* 1987; **238**:163–70.
2. Cosgrove MS, Wolberger C. How does the histone code work? *Biochem Cell Biol* 2005; **83**:468–76.
3. Gray SG, Teh BT. Histone acetylation/deacetylation and cancer: an "open" and "shut" case? *Curr Mol Med* 2001; **1**:401–29.
4. Cao J. The functional role of long non-coding RNAs and epigenetics. *Biol Proced Online* 2014; **16**:11.
5. Yan W. Potential roles of noncoding RNAs in environmental epigenetic transgenerational inheritance. *Mol Cell Endocrinol* 2014; **398**:24–30.
6. Mohammad F, Mondal T, Kanduri C. Epigenetics of imprinted long noncoding RNAs. *Epigenetics* 2009; **4**:277–86.
7. Skinner Mk, Ben Maamar M, Sadler-Riggleman I, Beck D, Nilsson E, McBirney M, Klukovich R, Xie Y, Tang C, Yan W, et al. Alterations in sperm DNA methylation, non-coding RNA and histone retention associate with DDT induced epigenetic transgenerational inheritance of disease. *Epigenetics Chromatin* 2018; **11**:8.
8. Burdge GC, Lillycrop KA, Jackson AA. Nutrition in early life, and risk of cancer and metabolic disease: alternative endings in an epigenetic tale? *Br J Nutr* 2009; **101**:619–30.
9. Jirtle RL, Skinner MK. Environmental epigenomics and disease susceptibility. *Nat Rev Genet* 2007; **8**:253–62.
10. Tang WY, Ho SM. Epigenetic reprogramming and imprinting in origins of disease. *Rev Endocr Metab Disord* 2007; **8**:173–82.
11. Quadrana L, Colot V. Plant transgenerational epigenetics. *Annu Rev Genet* 2016; **50**:467–91.
12. Brookheart RT, Duncan JG. *Drosophila melanogaster*: an emerging model of transgenerational effects of maternal obesity. *Mol Cell Endocrinol* 2016;**435**:20–8.
13. Kelly WG. Transgenerational epigenetics in the germline cycle of *Caenorhabditis elegans*. *Epigenetics Chromatin* 2014;**7**:6.
14. Carvan MJ, Kalluvila TA, Klingler RH, Larson JK, Pickens M, Mora-Zamorano FX, Connaughton VP, Sadler-Riggleman I, Beck D, Skinner MK, et al. Mercury-induced epigenetic transgenerational inheritance of abnormal neurobehavior is correlated with sperm epimutations in zebrafish. *PLoS One* 2017; **12**:e0176155.
15. Leroux S, Gourichon D, Leterrier C, Labrune Y, Coustham V, Rivière S, Zerjal T, Coville J-L, Morisson M, Minvielle F, et al. Embryonic environment and transgenerational effects in quail. *Genet Sel Evol* 2017; **49**:14.

Downloaded from https://academic.oup.com/eep/article/4/2/dvy010/4987173 by guest on 30 November 2022

16. Anway MD, Cupp AS, Uzumcu M, Skinner MK. Epigenetic transgenerational actions of endocrine disruptors and male fertility. *Science* 2005; **308**:1466–9.
17. Padmanabhan N, Jia D, Geary-Joo C, Wu X, Ferguson-Smith AC, Fung E, Bieda MC, Snyder FF, Gravel RA, Cross JC, et al. Mutation in folate metabolism causes epigenetic instability and transgenerational effects on development. *Cell* 2013; **155**:81–93.
18. Rassoulzadegan M, Grandjean V, Gounon P, Vincent S, Gillot I, Cuzin F. RNA-mediated non-Mendelian inheritance of an epigenetic change in the mouse. *Nature* 2006; **441**:469–74.
19. Braunschweig M, Jagannathan V, Gutzwiller A, Bee G. Investigations on transgenerational epigenetic response down the male line in F2 pigs. *PLoS One* 2012; **7**:e30583.
20. Northstone K, Golding J, Davey Smith G, Miller LL, Pembrey M. Prepubertal start of father's smoking and increased body fat in his sons: further characterisation of paternal transgenerational responses. *Eur J Hum Genet* 2014; **22**:1382–6.
21. Skinner MK. Endocrine disruptor induction of epigenetic transgenerational inheritance of disease. *Mol Cell Endocrinol* 2014; **398**:4–12.
22. Manikkam M, Tracey R, Guerrero-Bosagna C, Skinner MK. Dioxin (TCDD) induces epigenetic transgenerational inheritance of adult onset disease and sperm epimutations. *PLoS One* 2012; **7**:e46249.
23. Manikkam M, Tracey R, Guerrero-Bosagna C, Skinner M. Pesticide and insect repellent mixture (permethrin and DEET) induces epigenetic transgenerational inheritance of disease and sperm epimutations. *Reprod Toxicol* 2012; **34**:708–19.
24. Tracey R, Manikkam M, Guerrero-Bosagna C, Skinner M. Hydrocarbons (jet fuel JP-8) induce epigenetic transgenerational inheritance of obesity, reproductive disease and sperm epimutations. *Reprod Toxicol* 2013; **36**:104–16.
25. Manikkam M, Tracey R, Guerrero-Bosagna C, Skinner M. Plastics derived endocrine disruptors (BPA, DEHP and DBP) induce epigenetic transgenerational inheritance of adult-onset disease and sperm epimutations. *PLoS One* 2013; **8**:e55387.
26. Skinner MK, Manikkam M, Tracey R, Guerrero-Bosagna C, Haque MM, Nilsson E. Ancestral dichlorodiphenyltrichloroethane (DDT) exposure promotes epigenetic transgenerational inheritance of obesity. *BMC Med* 2013; **11**:228.
27. Manikkam M, Haque MM, Guerrero-Bosagna C, Nilsson E, Skinner MK. Pesticide methoxychlor promotes the epigenetic transgenerational inheritance of adult onset disease through the female germline. *PLoS One* 2014; **9**:e102091.
28. McBirney M, King SE, Pappalardo M, Houser E, Unkefer M, Nilsson E, Sadler-Riggleman I, Beck D, Winchester P, Skinner MK, et al. Atrazine induced epigenetic transgenerational inheritance of disease, lean phenotype and sperm epimutation pathology biomarkers. *PLoS One* 2017; **12**:e0184306.
29. Bayley M, Larsen PF, Baekgaard H, Baatrup E. The effects of vinclozolin, an anti-androgenic fungicide, on male guppy secondary sex characters and reproductive success. *Biol Reprod* 2003; **69**:1951–6.
30. Uzumcu M, Suzuki H, Skinner MK. Effect of the anti-androgenic endocrine disruptor vinclozolin on embryonic testis cord formation and postnatal testis development and function. *Reprod Toxicol* 2004; **18**:765–74.
31. Buckley J, Willingham E, Agras K, Baskin LS. Embryonic exposure to the fungicide vinclozolin causes virilization of females and alteration of progesterone receptor expression in vivo: an experimental study in mice. *Environ Health* 2006; **5**:4.
32. Skinner M, Guerrero-Bosagna C, Haque MM, Nilsson E, Bhandari R, McCarrey J. Environmentally induced transgenerational epigenetic reprogramming of primordial germ cells and subsequent germline. *PLoS One* 2013; **8**:e66318.
33. Nilsson EE, Skinner MK. Environmentally induced epigenetic transgenerational inheritance of disease susceptibility. *Transl Res* 2015; **165**:12–7.
34. Anway MD, Memon MA, Uzumcu M, Skinner MK. Transgenerational effect of the endocrine disruptor vinclozolin on male spermatogenesis. *J Androl* 2006; **27**:868–79.
35. Anway MD, Rekow SS, Skinner MK. Transgenerational epigenetic programming of the embryonic testis transcriptome. *Genomics* 2008; **91**:30–40.
36. Nilsson EE, Anway MD, Stanfield J, Skinner MK. Transgenerational epigenetic effects of the endocrine disruptor vinclozolin on pregnancies and female adult onset disease. *Reproduction* 2008; **135**:713–21.
37. Skinner MK, Anway MD, Savenkova MI, Gore AC, Crews D. Transgenerational epigenetic programming of the brain transcriptome and anxiety behavior. *PLoS One* 2008; **3**:e3745.
38. Guerrero-Bosagna C, Savenkova M, Haque MM, Nilsson E, Skinner MK. Environmentally induced epigenetic transgenerational inheritance of altered Sertoli cell transcriptome and epigenome: molecular etiology of male infertility. *PLoS One* 2013; **8**:e59922.
39. Gapp K, Jawaid A, Sarkies P, Bohacek J, Pelczar P, Prados J, Farinelli L, Miska E, Mansuy IM. Implication of sperm RNAs in transgenerational inheritance of the effects of early trauma in mice. *Nat Neurosci* 2014; **17**:667–9.
40. Schuster A, Skinner MK, Yan W. Ancestral vinclozolin exposure alters the epigenetic transgenerational inheritance of sperm small noncoding RNAs. *Environ Epigenet* 2016; **2**:1–10.
41. Mancini-Dinardo D, Steele SJ, Levorse JM, Ingram RS, Tilghman SM. Elongation of the Kcnq1ot1 transcript is required for genomic imprinting of neighboring genes. *Genes Dev* 2006; **20**:1268–82.
42. Mohammad F, Mondal T, Guseva N, Pandey GK, Kanduri C. Kcnq1ot1 noncoding RNA mediates transcriptional gene silencing by interacting with Dnmt1. *Development* 2010; **137**:2493–9.
43. Zhao Y, Sun H, Wang H. Long noncoding RNAs in DNA methylation: new players stepping into the old game. *Cell Biosci* 2016; **6**:45.
44. Zhao J, Ohsumi TK, Kung JT, Ogawa Y, Grau DJ, Sarma K, Song JJ, Kingston RE, Borowsky M, Lee JT. Genome-wide identification of polycomb-associated RNAs by RIP-seq. *Mol Cell* 2010; **40**:939–53.
45. Cifuentes-Rojas C, Hernandez AJ, Sarma K, Lee JT. Regulatory interactions between RNA and polycomb repressive complex 2. *Mol Cell* 2014; **55**:171–85.
46. Khalil AM, Guttman M, Huarte M, Garber M, Raj A, Rivea Morales D, Thomas K, Presser A, Bernstein BE, van Oudenaarden A, et al. Many human large intergenic noncoding RNAs associate with chromatin-modifying complexes and affect gene expression. *Proc Natl Acad Sci USA* 2009; **106**:11667–72.
47. Rechavi O, Houri-Ze'evi L, Anava S, Goh WSS, Kerk SY, Hannon GJ, Hobert O. Starvation-induced transgenerational inheritance of small RNAs in *C. elegans*. *Cell* 2014;**158**:277–87.
48. Krawetz SA, Kruger A, Lalancette C, Tagett R, Anton E, Draghici S, Diamond MP. A survey of small RNAs in human sperm. *Hum Reprod* 2011; **26**:3401–12.
49. Zhang X, Gao F, Fu J, Zhang P, Wang Y, Zeng X. Systematic identification and characterization of long non-coding RNAs in mouse mature sperm. *PLoS One* 2017; **12**:e0173402.

Downloaded from https://academic.oup.com/eep/article/4/2/dvy010/4987173 by guest on 30 November 2022

50. Jodar M, Selvaraju S, Sendler E, Diamond MP, Krawetz SA. The presence, role and clinical use of spermatozoal RNAs. *Hum Reprod Update* 2013; **19**:604–24.
51. Chen Q, Yan W, Duan E. Epigenetic inheritance of acquired traits through sperm RNAs and sperm RNA modifications. *Nat Rev Genet* 2016; **17**:733–43.
52. Ben Maamar M, Sadler-Riggleman I, Beck D, Skinner MK. Epigenetic transgenerational inheritance of altered sperm histone retention sites. *Sci Rep* 2018; **8**:5308.
53. Hammoud SS, Nix DA, Hammoud AO, Gibson M, Cairns BR, Carrell DT. Genome-wide analysis identifies changes in histone retention and epigenetic modifications at developmental and imprinted gene loci in the sperm of infertile men. *Hum Reprod* 2011; **26**:2558–69.
54. Anway MD, Leathers C, Skinner MK. Endocrine disruptor vinclozolin induced epigenetic transgenerational adult-onset disease. *Endocrinology* 2006; **147**:5515–23.
55. Skinner MK, Guerrero-Bosagna C. Role of CpG deserts in the epigenetic transgenerational inheritance of differential DNA methylation regions. *BMC Genomics* 2014; **15**:692.
56. Anway MD, Skinner MK. Transgenerational effects of the endocrine disruptor vinclozolin on the prostate transcriptome and adult onset disease. *Prostate* 2008; **68**:517–29.
57. Guerrero-Bosagna C, Settles M, Lucker B, Skinner M. Epigenetic transgenerational actions of vinclozolin on promoter regions of the sperm epigenome. *PLoS One* 2010; **5**: e13100.
58. Beck D, Sadler-Riggleman I, Skinner MK. Generational comparisons (F1 versus F3) of vinclozolin induced epigenetic transgenerational inheritance of sperm differential DNA methylation regions (epimutations) using MeDIP-Seq. *Environ Epigenet* 2017; **3**:1–12.
59. Tang L, Liu Z, Zhang R, Su C, Yang W, Yao Y, Zhao S. Imprinting alterations in sperm may not significantly influence ART outcomes and imprinting patterns in the cord blood of offspring. *PLoS One* 2017; **12**:e0187869.
60. Dallaire A, Simard MJ. The implication of microRNAs and endo-siRNAs in animal germline and early development. *Dev Biol* 2016; **416**:18–25.
61. Ruden DM, Lu X. Hsp90 affecting chromatin remodeling might explain transgenerational epigenetic inheritance in *Drosophila*. *Curr Genomics* 2008;**9**:500–8.
62. Oliva R, Ballesca JL. Altered histone retention and epigenetic modifications in the sperm of infertile men. *Asian J Androl* 2012; **14**:239–40.
63. Balhorn R. The protamine family of sperm nuclear proteins. *Genome Biol* 2007; **8**:227.
64. Jenkins TG, Carrell DT. The paternal epigenome and embryogenesis: poising mechanisms for development. *Asian J Androl* 2011; **13**:76–80.
65. Hammoud SS, Nix DA, Zhang H, Purwar J, Carrell DT, Cairns BR. Distinctive chromatin in human sperm packages genes for embryo development. *Nature* 2009; **460**:473–8.
66. Hammoud SS, Purwar J, Pflueger C, Cairns BR, Carrell DT. Alterations in sperm DNA methylation patterns at imprinted loci in two classes of infertility. *Fertil Steril* 2010; **94**:1728–33.
67. Zhang X, San Gabriel M, Zini A. Sperm nuclear histone to protamine ratio in fertile and infertile men: evidence of heterogeneous subpopulations of spermatozoa in the ejaculate. *J Androl* 2006; **27**:414–20.
68. Joh RI, Palmieri CM, Hill IT, Motamedi M. Regulation of histone methylation by noncoding RNAs. *Biochim Biophys Acta* 2014; **1839**:1385–94.
69. Miyoshi N, Stel JM, Shioda K, Qu NA, Odahima J, Mitsunaga S, Zhang X, Nagano M, Hochedlinger K, Isselbacher KJ, et al. Erasure of DNA methylation, genomic imprints, and epimutations in a primordial germ-cell model derived from mouse pluripotent stem cells. *Proc Natl Acad Sci USA* 2016; **113**: 9545–50.
70. Manikkam M, Guerrero-Bosagna C, Tracey R, Haque MM, Skinner MK. Transgenerational actions of environmental compounds on reproductive disease and identification of epigenetic biomarkers of ancestral exposures. *PLoS One* 2012; **7**: e31901.
71. Skinner MK, Manikkam M, Guerrero-Bosagna C. Epigenetic transgenerational actions of environmental factors in disease etiology. *Trends Endocrinol Metab* 2010; **21**:214–22.
72. Hisano M, Erkek S, Dessus-Babus S, Ramos L, Stadler MB, Peters AH. Genome-wide chromatin analysis in mature mouse and human spermatozoa. *Nat Protoc* 2013; **8**:2449–70.
73. Martin M. Cutadapt removes adapter sequences from high-throughput sequencing reads. *EMBnet J* 2011; **17**:10–2.
74. Tang C, Xie Y, Yan W. AASRA: an anchor alignment-based small RNA annotation pipeline. bioRxiv. 2017: 132928. doi: https://doi.org/10.1101/132928.
75. Love MI, Huber W, Anders S. Moderated estimation of fold change and dispersion for RNA-seq data with DESeq2. *Genome Biol* 2014; **15**:550.
76. Bolger AM, Lohse M, Usadel B. Trimmomatic: a flexible trimmer for Illumina sequence data. *Bioinformatics* 2014; **30**: 2114–20.
77. Trapnell C, Roberts A, Goff L, Pertea G, Kim D, Kelley DR, Pimentel H, Salzberg SL, Rinn JL, Pachter L, et al. Differential gene and transcript expression analysis of RNA-seq experiments with TopHat and Cufflinks. *Nat Protoc* 2012; **7**:562–78.
78. Wang L, Park HJ, Dasari S, Wang S, Kocher JP, Li W. CPAT: Coding-Potential Assessment Tool using an alignment-free logistic regression model. *Nucleic Acids Res* 2013; **41**:e74.
79. Langmead B, Salzberg Sl. Fast gapped-read alignment with Bowtie 2. *Nat Methods* 2012; **9**:357–9.
80. Lienhard M, Grimm C, Morkel M, Herwig R, Chavez L. MEDIPS: genome-wide differential coverage analysis of sequencing data derived from DNA enrichment experiments. *Bioinformatics* 2014; **30**:284–6.
81. Robinson MD, McCarthy DJ, Smyth GK. edgeR: a Bioconductor package for differential expression analysis of digital gene expression data. *Bioinformatics* 2010; **26**:139–40.
82. Durinck S, Spellman PT, Birney E, Huber W. Mapping identifiers for the integration of genomic datasets with the R/Bioconductor package biomaRt. *Nat Protoc* 2009; **4**:1184–91.
83. Cunningham F, Amode MR, Barrell D, Beal K, Billis K, Brent S, Carvalho-Silva D, Clapham P, Coates G, Fitzgerald S, et al. Ensembl 2015. *Nucleic Acids Res* 2015; **43** (Database issue): D662–9.
84. Kanehisa M, Goto S. KEGG: kyoto encyclopedia of genes and genomes. *Nucleic Acids Res* 2000; **28**:27–30.
85. Kanehisa M, Goto S, Sato Y, Kawashima M, Furumichi M, Tanabe M. Data, information, knowledge and principle: back to metabolism in KEGG. *Nucl Acids Res* 2014; **42**:D199–205.
86. Huang da W, Sherman BT, Lempicki RA. Systematic and integrative analysis of large gene lists using DAVID bioinformatics resources. *Nat Protoc* 2009; **4**:44–57.
87. Mi H, Muruganujan A, Casagrande JT, Thomas PD. Large-scale gene function analysis with the PANTHER classification system. *Nat Protoc* 2013; **8**:1551–66.

Downloaded from https://academic.oup.com/eep/article/4/2/dvy010/4987173 by guest on 30 November 2022

Developmental Biology 445 (2019) 280–293

Contents lists available at ScienceDirect

Developmental Biology

journal homepage: www.elsevier.com/locate/developmentalbiology

Developmental origins of transgenerational sperm DNA methylation epimutations following ancestral DDT exposure

Millissia Ben Maamar[a], Eric Nilsson[a], Ingrid Sadler-Riggleman[a], Daniel Beck[a], John R. McCarrey[b], Michael K. Skinner[a,*]

[a] Center for Reproductive Biology, School of Biological Sciences, Washington State University, Pullman, WA 99164-4236, USA
[b] Department of Biology, University of Texas at San Antonio, San Antonio, TX 78249, USA

ARTICLE INFO

Keywords:
Epigenetic
Transgenerational
Primordial germ cells
Spermatogenesis
Sperm
Epimutation
DNA methylation
Testis

ABSTRACT

Epigenetic alterations in the germline can be triggered by a number of different environmental factors from diet to toxicants. These environmentally induced germline changes can promote the epigenetic transgenerational inheritance of disease and phenotypic variation. In previous studies, the pesticide DDT was shown to promote the transgenerational inheritance of sperm differential DNA methylation regions (DMRs), also called epimutations, which can in part mediate this epigenetic inheritance. In the current study, the developmental origins of the transgenerational DMRs during gametogenesis have been investigated. Male control and DDT lineage F3 generation rats were used to isolate embryonic day 16 (E16) prospermatogonia, postnatal day 10 (P10) spermatogonia, adult pachytene spermatocytes, round spermatids, caput epididymal spermatozoa, and caudal sperm. The DMRs between the control versus DDT lineage samples were determined at each developmental stage. The top 100 statistically significant DMRs at each stage were compared and the developmental origins of the caudal epididymal sperm DMRs were assessed. The chromosomal locations and genomic features of the different stage DMRs were analyzed. Although previous studies have demonstrated alterations in the DMRs of primordial germ cells (PGCs), the majority of the DMRs identified in the caudal sperm originated during the spermatogonia stages in the testis. Interestingly, a cascade of epigenetic alterations initiated in the PGCs is required to alter the epigenetic programming during spermatogenesis to obtain the sperm epigenetics involved in the epigenetic transgenerational inheritance phenomenon.

1. Introduction

Numerous environmental factors have been shown to promote the epigenetic transgenerational inheritance of disease such as the agricultural fungicide vinclozolin [1] and the pesticide DDT (dichlorodiphenyltrichloroethane) [2]. Caloric restriction, high fat diets, stress and a variety of different toxicants have also been linked to the transgenerational epigenetic inheritance phenomenon [3–5]. This non-genetic form of inheritance involves epigenetic modifications of the germline (sperm and egg) to pass an altered epigenome to the early embryo that can then impact the transcriptomes and epigenetics of all subsequently derived somatic cells [1,5]. Different epigenetic processes are involved in the transgenerational germline transmission where the environment can impact the health and evolution of species [3,4,6].

Epigenetics is defined as “molecular factors and processes around the DNA that regulate genome activity independent of DNA sequence and that are mitotically stable” [7]. Transgenerational epigenetic inheritance requires the germline transmission of epigenetic information. Different epigenetic processes have been shown to be involved in the transgenerational phenomenon such as DNA methylation [8–10], non-coding RNA [11,12], and histone modifications and retention [10,13,14]. Recently, concurrent alterations in all three of these processes have been observed in transgenerational sperm transmission after exposure to DDT and vinclozolin [15,16]. Most previous studies have been conducted in sperm due to the ability to isolate large numbers of cells and the inability to isolate large numbers of eggs, but experiments have shown that the female germline also has the capacity to transmit epigenetic inheritance [2,17]. The current study investigated the transgenerational sperm transmission of DNA methylation alterations after DDT exposure.

The primordial germ cells (PGCs), which give rise to spermatogenic (or oogenic) cells, develop and migrate down the genital ridge to colonize the indifferent gonad [18]. Upon sex determination and depending on the chromosomal sex, the PGCs differentiate into the

* Corresponding author.
E-mail address: skinner@wsu.edu (M.K. Skinner).

https://doi.org/10.1016/j.ydbio.2018.11.016
Received 5 September 2018; Received in revised form 1 November 2018; Accepted 26 November 2018
Available online 27 November 2018
0012-1606/ © 2018 The Authors. Published by Elsevier Inc. This is an open access article under the CC BY-NC-ND license (http://creativecommons.org/licenses/BY-NC-ND/4.0/).

male or female germline lineage [19]. In the rat gonad, the early developing testis germ cells will become prospermatogonia cells during the male gonadal sex determination period by embryonic day 16 (E16) [20,21]. By postnatal day 10 (P10) the germline develops into spermatogonia. Following the onset of puberty the initial wave of spermatogenesis begins in the testis where the spermatocytes, including the meiotic stage of pachytene spermatocytes, develop. After meiosis the round spermatid stage differentiates, then in the final spermatozoa stage the cells are released into the lumen of the seminiferous tubules [22], Fig. 1A. After entering the caput region of the epididymis the spermatozoa undergo further differentiation. During the transit in the epididymis the spermatozoa mature. When the spermatozoa reach the final caudal stage of the epididymis, the sperm have developed the capacity for motility and fertility [23,24]. Prior to ejaculation or degradation the mature caudal epididymal sperm will be stored in the vas deferens. In the current study we used several male germline developmental periods (E16 prospermatogonia, P10 spermatogonia, adult pachytene spermatocytes, round spermatids, caput epididymal spermatozoa, and caudal epididymal sperm), Fig. 1A, to investigate the developmental origins of the transgenerational sperm DMRs following DDT exposure in the F0 generation.

Epigenetic programming occurs during these male germline developmental periods. The migrating PGCs have an erasure of DNA methylation that then re-methylate during gonadal sex determination to create the male germline and prospermatogonia [25]. In the adult testis, during spermatogenesis some epigenetic programming events occur [26,27]. The first examples of this male germline epigenetic programming were observed with imprinted genes [28,29]. Imprinted genes can develop either early in the embryonic period or develop during spermatogenesis. Although previous studies have discussed the

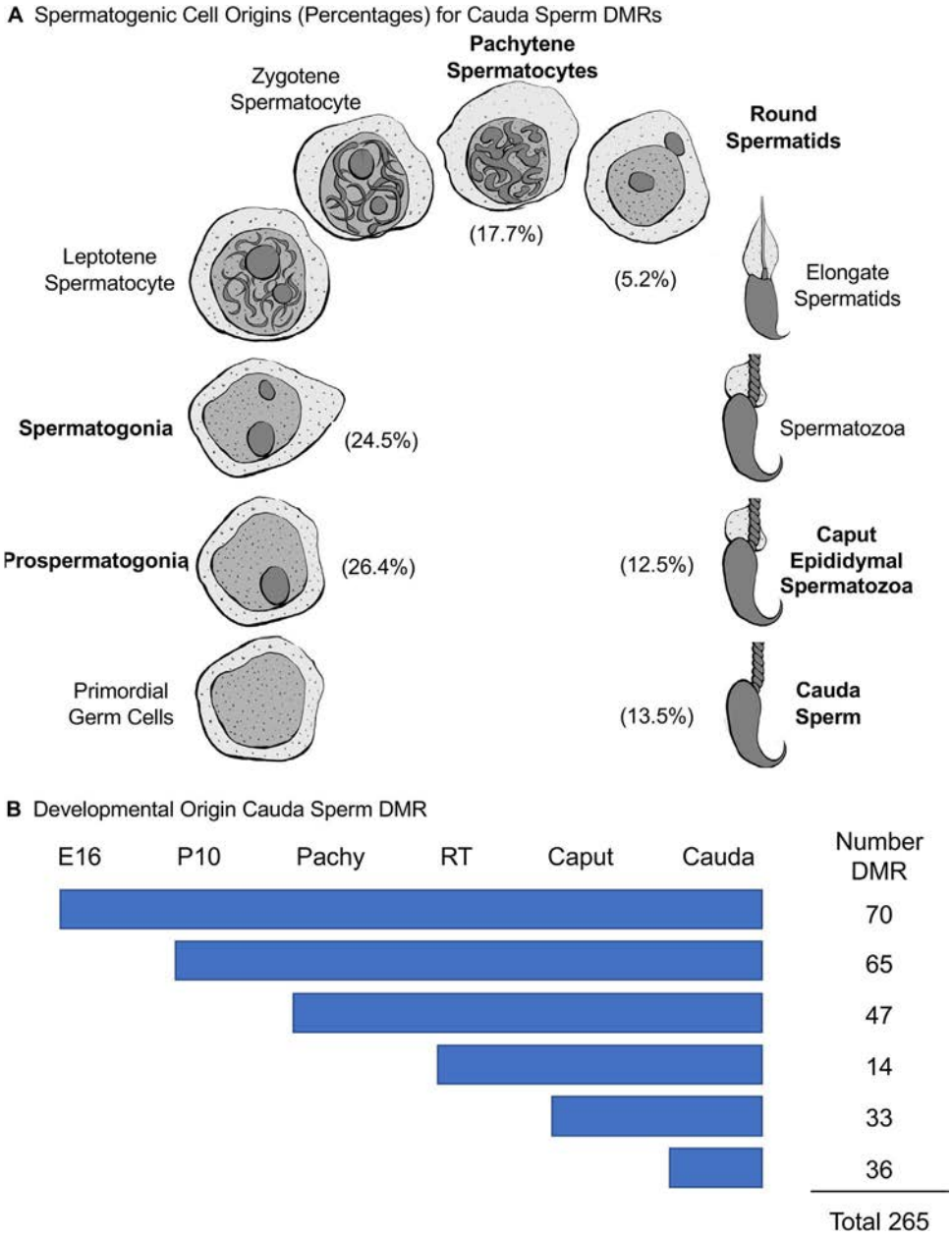

Fig. 1. Sperm DMR developmental origins. (A) Spermatogenic cell origin percentages for cauda sperm DMRs. The schematic of each developmental cell morphology listed during gametogenesis and spermatogenesis and epididymal maturation. The percentage DMR in brackets is presented for the developmental stages analyzed. (B) Developmental origins of cauda sperm DMRs for each stage of development with number DMRs at specific stages listed. The prospermatogonia (E16), spermatogonia (P10), pachytene spermatocytes (Pachy), round spermatids (RT), caput spermatozoa (Caput) and cauda sperm (Cauda) are presented.

germline developmental origins of epigenetic inheritance [5,30–34], none of these studies identified the developmental programming origins of the transgenerational epigenetic alterations observed in sperm.

The current study was designed to investigate the developmental origins of the DDT induced transgenerational sperm DMRs termed epimutations. The hypothesis tested is that a cascade of epigenetic changes occurs during development such that the majority of DMRs develop throughout gametogenesis and spermatogenic stages. It has been previously demonstrated that epigenetic alterations occur in the PGC [35]. However, due to this being the earliest stem cell stage of the germline, the PGCs DMRs were found to be different from the epimutations observed in sperm [35]. These observations suggest that the epimutations in sperm develop at later stages of epigenetic programming. The present study shows the majority of sperm DMRs originate during spermatogonia development and spermatogenesis, but some also do originate during epididymal maturation. This is one of the first genome-wide analyses of epigenetic programming during gametogenesis for transgenerational sperm epimutations [36].

2. Results

F3 generation control and DDT lineage male rats were used in this experimental design to isolate various germ cell stages for epigenetic analysis. The F0 generation gestating female rats at 90 days of age were transiently exposed to DDT or a vehicle control during gestational days 8–14. This stage of fetal development corresponds to when the PGCs migrate to colonize the indifferent gonad through the early stage of gonadal sex determination as previously described [18,25,35]. The F1 generation offspring were obtained and when they reached 90 days of age they were bred within the control and DDT lineages to generate the F2 generation (grand offspring) which were then bred at 90 days of age to obtain the transgenerational F3 generation for each control and DDT lineage. No cousin or sibling breedings were used to avoid any inbreeding artifacts. Only the F0 generation gestating females were exposed to DDT, which also directly exposed the F1 generation fetus and the germline within the F1 generation fetus that will generate the F2 generation. Therefore, the F3 generation is the first transgenerational generation not directly exposed [37] and was used to study the developmental origins of the transgenerational sperm epimutations. The F3 generation control and DDT lineage male rats were aged to the embryonic day 16 (E16) fetal stage for prospermatogonia cell isolation, to postnatal day 10 (P10) for spermatogonial cell isolation, and to 120 days of age for pachytene spermatocyte isolation, round spermatid isolation, caput spermatozoa isolation, and cauda epididymal sperm isolation. A gravity sedimentation StaPut protocol, as described in the Methods [38,39], was used to isolate the prospermatogonia, spermatogonia, pachytene spermatocytes and round spermatids cells. Three different pools each with different individual sets of animals from different litters were obtained with 5–6 males per pool for the E16 stage, 6–7 males per pool for the P10 stage, 3 adult males per pool for the adult stages. Therefore, 3–7 different males were used in the analysis within each of the three different pools analyzed for both the control and DDT lineages. Genomic DNA was isolated from each purified germ cell stage pool and from individual animals for epididymal caput spermatozoa and cauda sperm [8,13] and then three pools generated for subsequent epigenetic analysis.

The analysis of differential DNA methylation regions (DMRs) was performed with a methylated DNA immunoprecipitation (MeDIP) procedure followed by next generation sequencing for an MeDIP-Seq protocol described in the Methods [8]. The F3 generation control versus DDT lineage pools were compared to identify the DMRs at each developmental stage of the male germline. The DMRs at various p-value thresholds are presented at each developmental stage in Fig. 2. An EdgeR p-value of $p < 1e-05$ was selected at all stages for further analysis of the DMRs. This correlated with an FDR (false discovery rate) value of < 0.1 for all except the E16 prospermatogonia which was more variable. The All Windows is all DMRs with at least one 100 bp region (window) with statistical significance and the Multiple Windows being ≥2 significant 100 bp windows. The number of DMRs with multiple windows is also presented in Fig. 2. Most developmental stages showed approximately 100–300 DMRs. The epigenetic alterations were higher at the pachytene spermatocyte and round spermatid stages which showed more than 300 DMRs. The chromosomal locations of the DMRs at each developmental stage are presented in Fig. 3. The red arrowheads indicate the location of a DMR with the black boxes indicating clusters of DMRs. In most stages, all the chromosomes, except the Y and mitochondrial DNA (MT), were found to contain DMRs. The genomic features of the DMRs at each stage of development were investigated. The CpG density of the DMRs at all stages was 1–5 CpG per 100 bp with 1 CpG per 100 bp being predominant, Fig. 4. This is characteristic of a low density CpG desert [40] which has been observed with previous transgenerational DMRs. The length of the DMRs at all the developmental stages were between 1 and 4 kb with 1 kb length being predominant, Fig. 5. Therefore, the DMRs are generally 1 kb in size with around 10 CpGs as previously observed [40]. The overlap between the various developmental stage DMRs was investigated and is presented in Fig. 6A. The DMRs were found to be primarily stage specific with a very low number of DMRs overlapping between the stages with a $p < 1e-05$. The cauda sperm and the caput spermatozoa had the highest level of overlap with 88 DMRs, Fig. 6B and S7 Table, comprising over 45% of the caput epididymal spermatozoa DMRs. These observations suggest a cascade of epigenetic programming occurs throughout male germline development.

The DNA methylation alterations of the DMRs at each stage of development were investigated. For the developmental time-course the top 100 statistically significant DMRs at each stage of development were examined regarding the scaled mean read depth between the control versus DDT lineage DMR data. The scaled mean read depths at each DMR was separated into control greater than DDT data (i.e. decrease in DNA methylation) and DDT greater than control data (i.e. increase in DNA methylation) which is presented as a scaled mean read depth, Figs. 7 and 8. The E16 prospermatogonia DMRs had 28 DMR with a decrease in methylation and 72 DMR with an increase in methylation, Figs. 7A & 8A. For both data sets the DMR methylation alterations generally dropped by the P10 spermatogonia stage and became mixed with no distinct patterns in later stages. Although a few of both populations stayed elevated, the majority had an alteration in DNA methylation at later stages of development. The P10 spermatogonia DMRs had 38 DMRs with a decrease in methylation and 62 with an increase in methylation in regard to % mean read depth, Figs. 7B & 8B. A dramatic change in methylation between the prospermatogonia to spermatogonia stage and from the spermatogonia to later stages of development were observed. Therefore, the E16 prospermatogonia and P10 spermatogonia stage DMRs are for the most part unique at these stages of development. The pachytene spermatocyte DMRs had predominantly a decrease in methylation with 63 DMRs and 37 DMRs with an increase, Figs. 7C & 8C. Therefore, DNA methylation was primarily decreased in the pachytene spermatocyte DMRs. The round spermatid DMRs had a higher number of 72 DMR with an increase and 28 DMR with a decrease, Figs. 7D & 8D. The caput epididymal spermatozoa DMRs had 46 DMR with a decrease and 54 DMR with an increase in methylation, Figs. 7E & 8E. The cauda epididymal sperm DMRs had 49 DMR with a decrease and 51 DMR with an increase, Figs. 7F & 8F. The caput spermatozoa and cauda epididymal sperm have relatively consistent DNA methylation characteristics for both data sets. Therefore, the cauda sperm show more consistent DNA methylation profiles during spermatogenesis and epididymal sperm maturation, but are distinct in the spermatogonial stem cell stages.

Genes associated with the DMRs were identified and compared at each of the developmental stages. The DMRs that had a gene within 10 kb distance, so the promoter is considered, were identified and the

A Prospermatogonia (E16)

P-value	All Window	Multiple Window
0.001	4011	265
1e-04	522	25
1e-05	**94**	**11**
1e-06	27	5
1e-07	12	4

Number Windows	1	2	3	4	5
Number of DMR	83	7	2	1	1

B Spermatogonia (P10)

P-value	All Window	Multiple Window
0.001	4728	464
1e-04	722	107
1e-05	**195**	**47**
1e-06	86	32
1e-07	48	19

Number Windows	1	2	3	4	5	20
Number of DMR	148	35	4	5	2	1

C Pachytene Spermatocytes

P-value	All Window	Multiple Window
0.001	11776	891
1e-04	1917	78
1e-05	**340**	**13**
1e-06	71	5
1e-07	20	2

Number Windows	1	2	3
Number of DMR	327	9	4

D Round Spermatids

P-value	All Window	Multiple Window
0.001	11006	1276
1e-04	1816	131
1e-05	**323**	**17**
1e-06	60	0
1e-07	7	0

Number Windows	1	2
Number of DMR	306	17

E Caput Epididymal Spermatozoa

P-value	All Window	Multiple Window
0.001	6644	616
1e-04	1146	148
1e-05	**284**	**72**
1e-06	117	52
1e-07	74	38

Number Windows	1	2	3	4	≥5
Number of DMR	212	39	13	5	15

F Cauda Sperm

P-value	All Window	Multiple Window
0.001	4611	478
1e-04	809	143
1e-05	**265**	**82**
1e-06	140	55
1e-07	87	40

Number Windows	1	2	3	4	≥5
Number of DMR	183	39	20	10	13

Fig. 2. DMR identification and numbers. The number of DMRs found using different p-value cutoff thresholds. The All Window column shows all DMRs. The Multiple Window column shows the number of DMRs containing at least two significant windows (100 bp each). The number of DMRs with the number of significant windows (100 bp per window) at a p-value threshold of 1e-05 is presented. (A) E16 prospermatogoina. (B) P10 spermatogonia. (C) Pachytene spermatocytes. (D) Round Spermatids. (E) Caput Spermatozoa. (F) Cauda Sperm.

associated genes and gene functional categories determined, S1–S6 Tables. The DMRs with a p < 1e-05 were used in this analysis at all the developmental stages. The number of genes associated with specific gene functional categories is presented in Fig. 9A. Each of the developmental stages are presented to compare the major gene categories. The signaling, metabolism, transcription and receptor gene categories were the major categories present in the different developmental stages. Additional categories were cytoskeleton, development, transport and immune system, that were present in all the developmental stages, Fig. 9A. The DMR associated genes at each developmental stage were also used in a gene pathway analysis applying the KEGG pathway association as described in the Methods. The number of DMR associated genes involved with the major pathways is presented in Fig. 9B. The most predominant pathways present in at least two different developmental stages are shown. The E16 prospermatogonia, round spermatids, caput spermatozoa and cauda sperm had DMR associated genes in the metabolic pathways. The E16 prospermatogonia, P10 spermatogonia, pachytene spermatocytes had DMR associated genes in the pathways in cancer in common. Therefore, the only pathways that were present in nearly all the stages are metabolism and pathways in cancer. The caput epididymal spermatozoa and cauda sperm were more consistent than the others which were more distinct.

The final aspect of the study involved an investigation of the developmental origins of the cauda sperm DMRs, meaning when the differential DNA methylation alterations appeared within the developmental stages examined. In the cauda sperm there are 265 DMRs at p < 1e-05. For the analysis of developmental origins the 265 DMRs were examined individually with a reduced statistical stringency of p < 0.05 to see the first stage the DMR appears or originates. Fig. 1B demonstrates 70 DMRs were developed in the E16 prospermatogonia stage, 65 DMRs in the P10 spermatogonia stage, 47 DMRs in the spermatocyte stage, 14 DMRs in the round spermatid stage, 33 DMRs in the caput epididymal spermatozoa stage, and 36 DMRs in the cauda sperm stage, S8 Table. The cauda sperm had a total of 265 DMRs at p < 1e-05 with the majority of DMRs originating in the prospermatogonia and spermatogonia. Fewer were observed in the round spermatids and caput epididymal spermatozoa stages, Fig. 1B. The percentage of the total DMR origins and schematic of the different

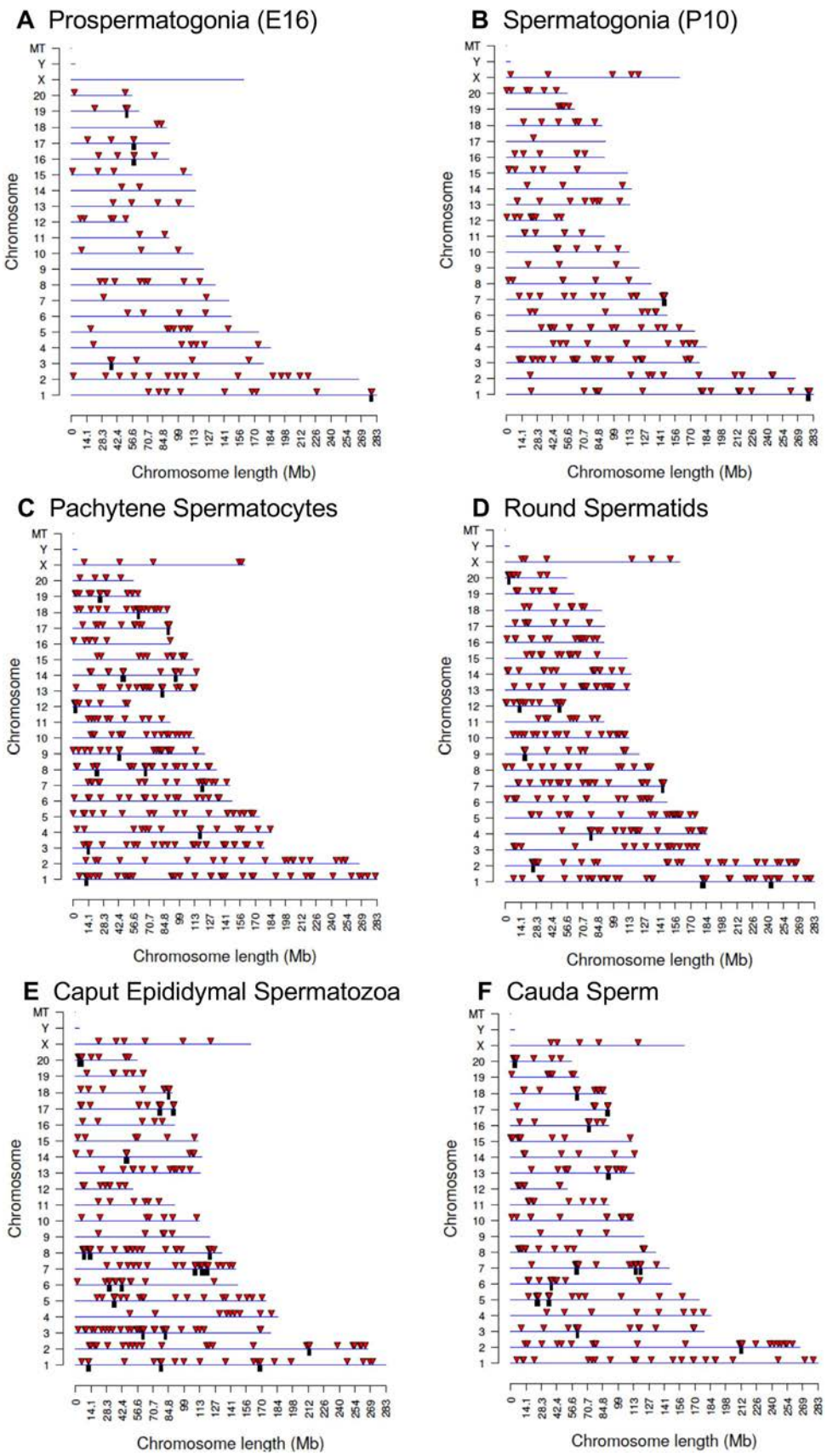

Fig. 3. DMR chromosomal locations. The DMR locations on the individual chromosomes is represented with an arrowhead and a cluster of DMRs with a black box. All DMRs containing at least one significant window at a p-value threshold of 1e-05 are shown. (A) E16 prospermatogoina. (B) P10 spermatogonia. (C) Pachytene spermatocytes. (D) Round Spermatids. (E) Caput Spermatozoa. (F) Cauda Sperm.

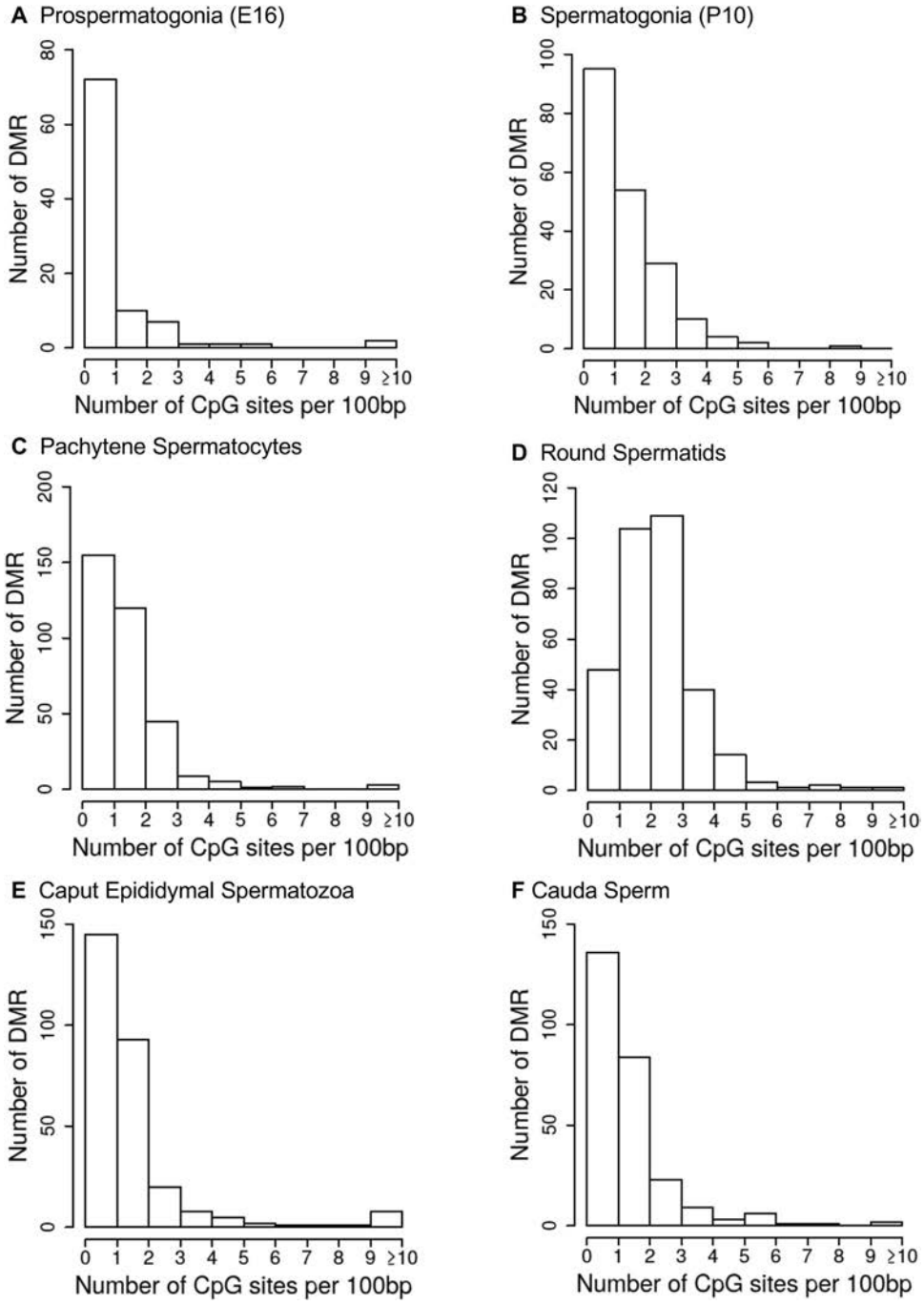

Fig. 4. DMR genomic features. The number of DMRs at different CpG densities. All DMRs at a p-value threshold of 1e-05 are shown. (A) E16 prospermatogoina. (B) P10 spermatogonia. (C) Pachytene spermatocytes. (D) Round Spermatids. (E) Caput Spermatozoa. (F) Cauda Sperm.

stage cells during development is presented in Fig. 1A. Therefore, the majority of the transgenerational sperm DMRs were developed during the prospermatogonia and spermatogonia stages with a small number developed in the epididymal maturation stages. This correlated to a cascade of epigenetic and transcriptome changes during these stages of male germline development to generate the transgenerational sperm epimutations, Fig. 1A.

3. Discussion

The aim of the current study was to identify the developmental origins of the cauda sperm transgenerational DMRs that transmit the epigenetic transgenerational inheritance of disease and phenotypic variation. During embryonic day 8–14 in the rat, when the primordial germ cells (PGCs) migrate to colonize the indifferent fetal gonad, the F0 generation gestating female exposure to DDT was performed [18,25,35]. Five different stages of male germ cell development were investigated: E16 prospermatogonia, P10 spermatogonia, and adult pachytene spermatocytes, round spermatids, caput epididymal spermatozoa and cauda sperm, Fig. 1A. The functional considerations of these cell populations involve the prospermatogonia precursor stem cell population, spermatogonia stem cell population in the testis, the meiotic pachytene spermatocyte cell population, the post-meiotic spermatid population and the spermatozoa present in the caput epididymis, and mature sperm in the cauda epididymis. The caput spermatozoa and cauda epididymal sperm were directly isolated as described in the Methods then sonicated and washed to remove any contaminating somatic cells, so are pure sperm cell preparations. For

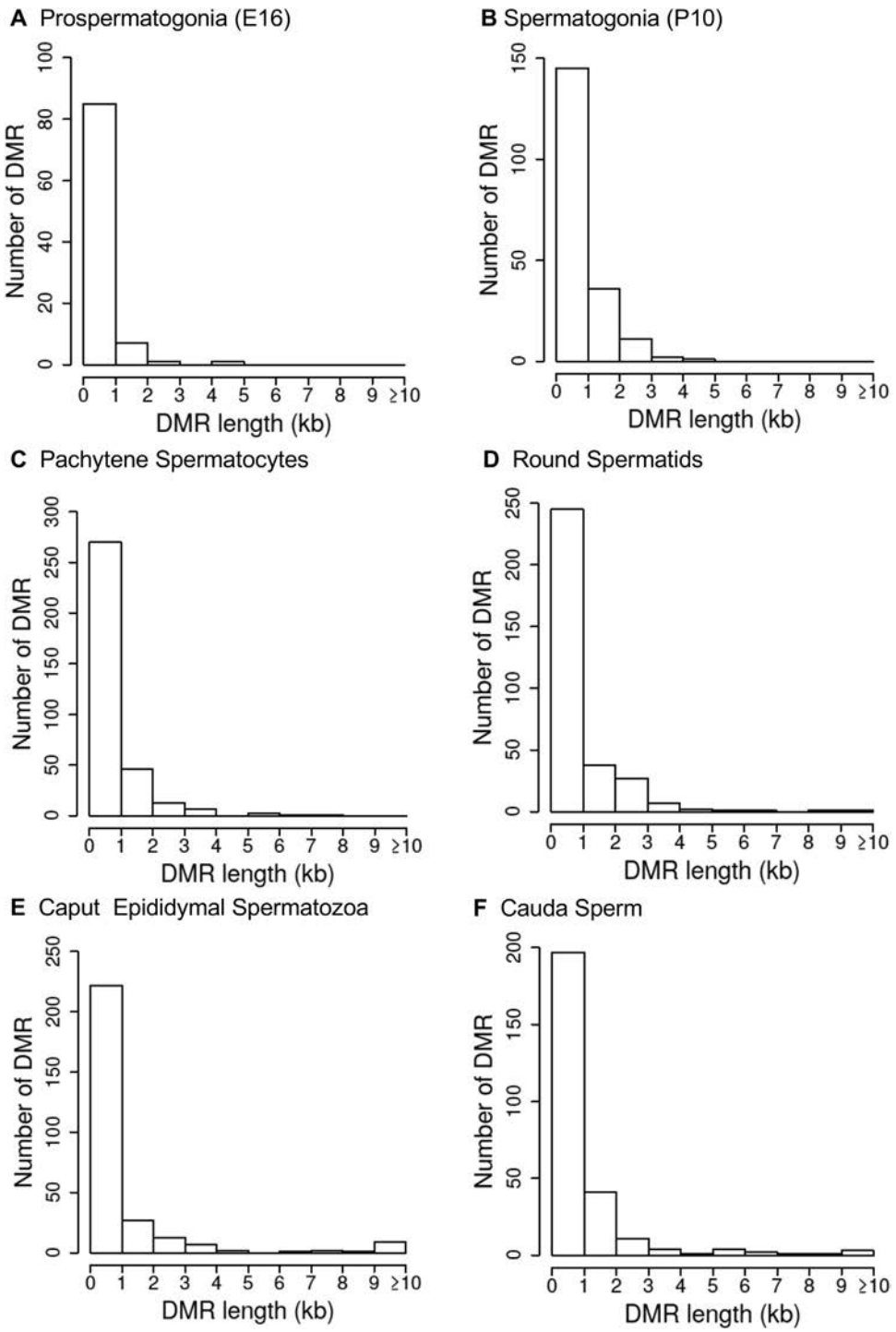

Fig. 5. DMR lengths. All DMRs at a p-value threshold of 1e-05 are shown. (A) E16 prospermatogoina. (B) P10 spermatogonia. (C) Pachytene spermatocytes. (D) Round Spermatids. (E) Caput Spermatozoa. (F) Cauda Sperm.

the other cell populations a gravity sedimentation on a StaPut apparatus procedure was used to isolate the specific cell populations as previously described [39,40]. The E16 prospermatogonia and P10 spermatogonia were found to have a greater than 85% purity. The pachytene spermatocytes were greater than 95% spermatocytes with two-thirds of these cells pachytene spermatocytes and one-third other spermatocyte stages. This is due to the longer developmental life span or developmental period of pachynema compared to the other stages of first meiotic prophase [41] and to the efficiency of the StaPut gradient protocol. For the isolated round spermatids 95% of them were spermatids with 90% of them being round spermatids and 10% being elongate spermatids and other spermatogenic cell stages [42]. Despite obtaining a high purity for these developmental stage male germline cell populations, cell purity needs to be considered in the data interpretations. The embryonic day 16 (E16) prospermatogonia were isolated from the fetal gonad, the postnatal day 10 (P10) from the early pubertal age, the pachytene spermatocytes, round spermatids, caput epididymal spermatozoa and cauda sperm were all isolated from postnatal day 120 (P120) age adult male rats. DDT has been previously shown to induce transgenerational inheritance of disease between 6 and 12 months of age [5]. Therefore, by choosing the postnatal day 120 or earlier with negligible disease present, no disease artifacts are

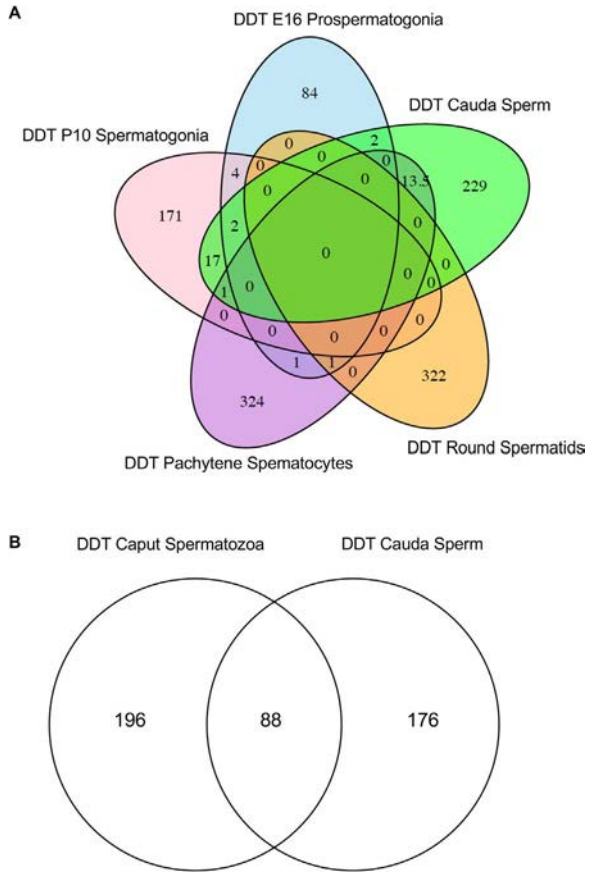

Fig. 6. Developmental stage DMR overlaps. (A) Different developmental stage DMRs overlap. (B) Epididymal caput spermatozoa and caudal sperm DMR overlap.

anticipated in the current study. This is consistent with the primary objective of the study to investigate the developmental origins of the sperm DMR, but future studies can now consider disease correlations.

The transgenerational F3 generation control and DDT lineage germline samples were compared at each of the developmental stages. The F1 and F2 generations have somatic cell and germline epigenetic alterations due to the F1 generation fetal direct exposure and F1 generation fetal germline direct exposure that will generate the F2 generation. Therefore, the F3 generation is the first transgenerational generation not having any direct exposures, so was the focus of the current study [37]. A comparison of the F1 generation direct exposure sperm DMR development with the transgenerational F3 generation observations will be an interesting future study to consider. All F3 generation developmental samples had differential DNA methylation regions (DMRs). Excluding the caput spermatozoa and cauda epididymal sperm with common DMRs, all the other stage DMRs were found to be primarily distinct from each other, Fig. 6. The majority of the epigenome was not altered (i.e. potentially millions of CpG regions) and the current study focused on the transgenerational alterations at each stage of development. The distinct DMRs at each stage indicate a cascade of epigenetic changes occur to program the sperm transgenerational epigenome.

A comparison of the different developmental stage germline populations was conducted in regard to DNA methylation alterations for the top 100 most statistically significant DMRs at each developmental stage separately. Analysis of these DNA methylation alterations for the different developmental stage DMRs revealed that the E16 prospermatogonia and P10 spermatogonia presented distinct patterns of DNA methylation compared to the other stages, Figs. 7 and 8. The statistically significant top 100 DMRs at both these developmental stages altered greatly with adjacent stages and often lost their statistical significance. In contrast, the pachytene spermatocytes, round spermatids, caput epididymal spermatozoa and caudal sperm were more consistent between each other regarding the DMRs maintaining similar DNA methylation alterations and statistical significance, Figs. 7 and 8. This suggests that the developing stem cells and spermatogonia have principally unique DNA methylation profiles associated with the cascade of epigenetic programming of the cells. When the spermatogonia initiate the spermatogenesis process there is a cascade of epigenetic programming and DNA methylation observed between the spermatogenic cell populations, as well as between spermatozoa undergoing epididymal maturation. Observations suggest a dynamic epigenetic programming of the male germline in the testis and epididymis. Epididymal maturation has been shown to promote structural and molecular alterations in the developing sperm, which also appear to be involved in the transgenerational sperm DMR programming [32].

Significant epigenetic reprogramming in the primordial germ cells (PGCs) has already been described. DNA methylation erasure during migration and colonization of the fetal gonad has been shown to occur [18]. This process enables the germline stem cell population to facilitate the generation of the male or female germ lines following gonadal sex determination [18,25]. A stable epigenetic cascade of events occurs to produce the spermatogonial stem cell population in the adult testis. Studies have shown that environmental toxicants have the ability to promote epigenetic DNA methylation alterations in the PGCs and prospermatogonia [35]. These transgenerational DMRs observed in the PGCs were found to be distinct from the caudal epididymal sperm DMRs [35]. The current study supports this observation and determines that sperm DMRs not only originate in the fetal period, but trigger a cascade of epigenetic alterations that eventually impact the mature sperm epigenome, Fig. 1B. Therefore, the developmental cascade of epigenetic programming initiated by fetal exposure induces a number of DMRs that are also maintained throughout development.

In the cauda sperm, the origins of the DMRs were identified. The majority of them originate throughout the development of prospermatogonia, spermatogonia and spermatocytes, Fig. 1B and S9 Table. A smaller number of DMRs also arose in the round spermatids and cauda epididymal sperm. The highest number of DMRs was observed in the prospermatogonia, the stage of development during which the initial F0 generation gestating female and F1 generation developing fetus were exposed. The DMRs in the cauda sperm originated in all the earlier developmental spermatogenic stages and through epididymal maturation. These observations correlated with the DNA methylation alteration data for DMRs between the different developmental stages shown in Figs. 7 and 8. Thus, the primary origin of the transgenerational sperm DMR epimutations/DMRs does not occur during early PGC development or in the embryonic stem cell population, but throughout development and spermatogenesis in the testis, as well as during epididymal maturation. Although the induction of a cascade of epigenetic programming in the PCGs is critical as previously suggested [7,35], there is a continual cascade of epigenetic alterations throughout spermatogenesis to give rise to the transgenerational sperm DMRs, Fig. 1A. Another recent study investigating vinclozolin induced sperm DMR origins found similar observations, but the highest level of DMRs were developed at the pachytene spermatocyte stage [36]. Therefore, an exposure specificity may exist in the developmental epigenetics observed.

The DMRs associated genes were identified for DMRs at $p < 1e\text{-}05$ at each stage of development. The analysis of associated gene functional categories identified signaling, transcription, metabolism and receptor as the major categories at all stages of development. The pathway analysis also identified a number of stage specific pathways with negligible overlap except in metabolism and pathways in cancer. Gene pathways more specific to testis development such as meiosis or the pyruvate pathway did not contain more than a few DMR associated

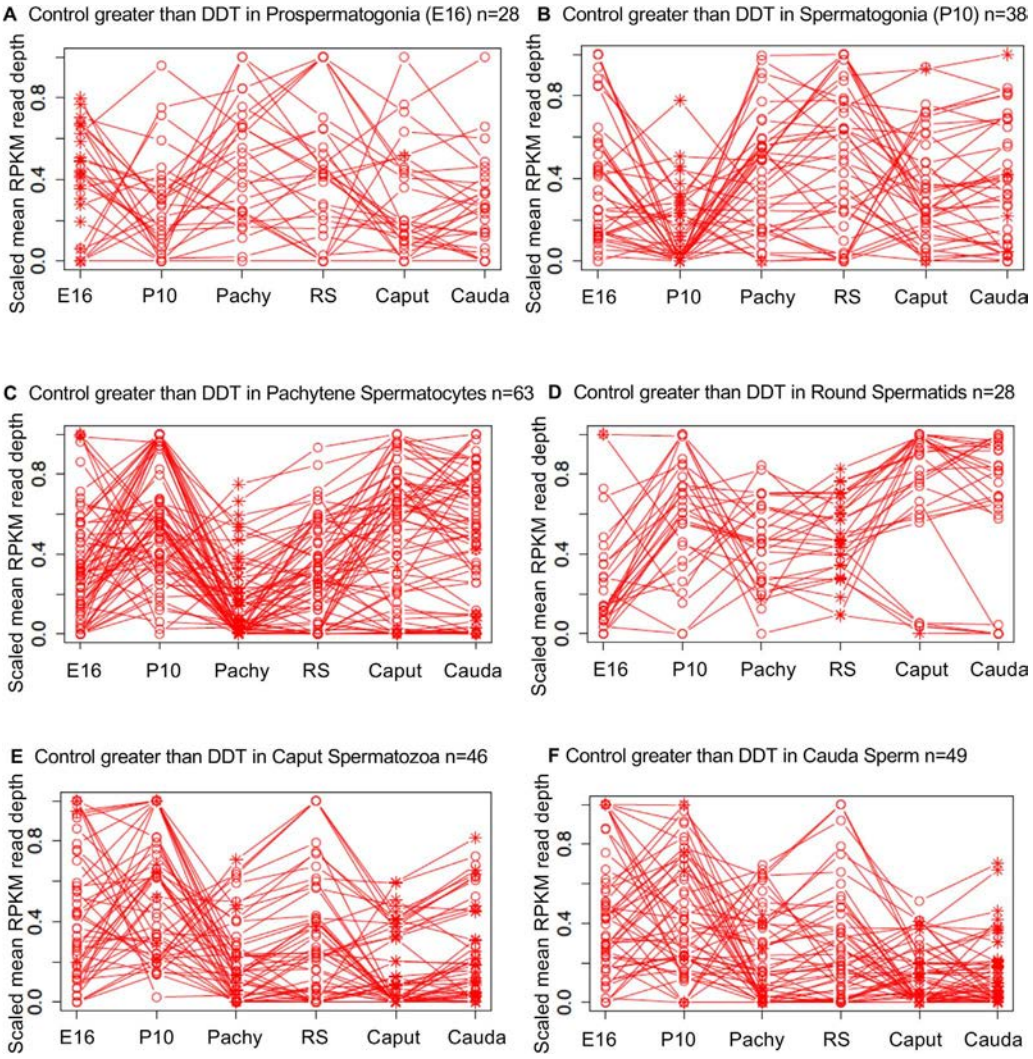

Fig. 7. Timeline DMR development. Top 100 statistically significant DMR developmental alterations for control greater than DDT in read depths (decrease in DNA methylation). Genomic windows with an edgeR p-value < 10^{-5} are indicated by astrisks and windows separated showing only those with an RPKM read depth elevated in the control. (A) E16 prospermatogoina. (B) P10 spermatogonia. (C) Pachytene spermatocytes. (D) Round spermatids. (E) Caput spermatozoa. (F) Cauda sperm.

genes. Therefore, for all the stages of development for the DMR-associated genes involved similar gene categories, but different pathways. Future studies are needed to correlate the DMRs with data identified from transcriptome and altered non-coding RNA expression to provide a better understanding as to how the DMRs may regulate genome activity.

The caput epididymal spermatozoa displayed unique DMRs and others that were in common with the cauda sperm. Interestingly, the cauda epididymal sperm did acquire DMRs that were not present in earlier stages of development. Even though the majority of the cauda epididymal sperm DMRs were obtained during prior developmental stages, 36 DMRs were acquired at the cauda epididymal sperm stage of maturation only, S7 and S8 Tables. Two studies have previously suggested that epididymal maturation (epididymosomes) may be involved with transgenerational sperm maturation regarding epigenetic alterations, but no direct data have been provided [43–45]. The current study supports a role for epididymal maturation altering sperm DMRs. However, the majority of DMRs originated during earlier developmental stages and spermatogenesis in the testis and not the epididymis, Fig. 1B. A combination of early development, spermatogenesis and epididymal mutation appears to be involved in the development of the transgenerational sperm epimutations. Further investigation is needed to elucidate the molecular mechanisms in the epididymis that alter sperm epigenetics.

4. Conclusions

The current study was designed to investigate the developmental origins of transgenerational sperm DMRs induced by the pesticide DDT. Results show that each stage of male germ cell development examined, including the E16 prospermatogonia, P10 spermatogonia, pachytene spermatocytes, round spermatids, caput epididymal spermatozoa and cauda sperm, has distinct and unique DMRs when the DDT lineage and control lineage F3 generation samples are compared. Both the prospermatogonia and spermatogonia display unique DNA methylation alterations in comparison with later stages that are more consistent. The origins of the cauda sperm DMRs developed throughout the earlier developmental stages with the highest number during prospermatogonia, spermatogonia and pachytene spermatocytes, and fewer originating during epididymal maturation. In conclusion, a developmental cascade of epigenetic programming occurs from the PGCs to the sperm with epimutations developing throughout the different stages of development, Fig. 1A. The initial speculation that the DMRs may develop in the PGCs is not the case, even though the developmental cascade initiated is important. Recently, sperm carrying transgenerational epimutations were found to have alterations in DNA methylation, ncRNAs and histone retention, such that all epigenetic factors are involved in the epigenetic transgenerational inheritance phenomenon [15,16]. Future studies will now need to investigate these

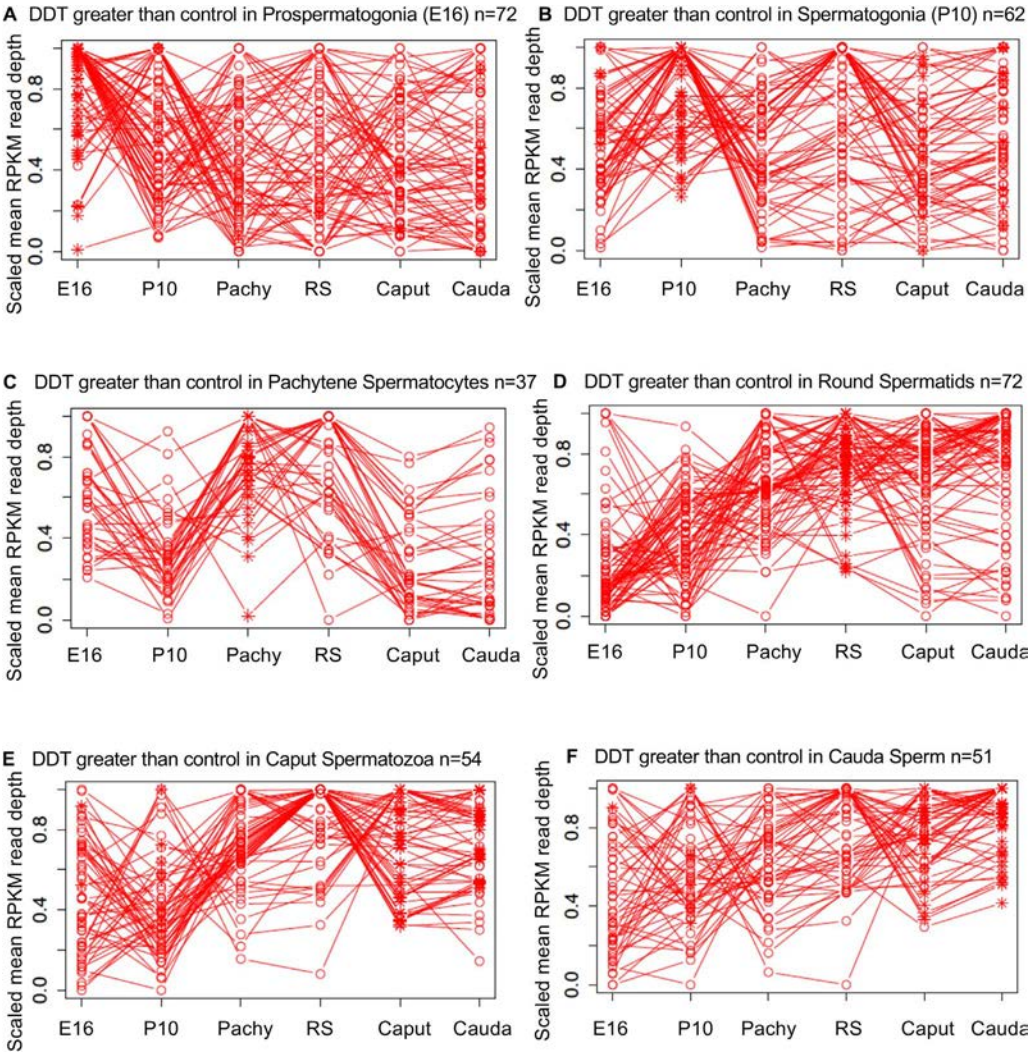

Fig. 8. Timeline DMR development. Top 100 statistically significant DMR developmental alterations for DDT greater than control in read depths (increase in DNA methylation). Genomic windows with an edgeR p-value < 10^{-5} are indicated by astrisks and windows separated showing only those with an RPKM read depth elevated in the DDT over control. (A) E16 prospermatogoina. (B) P10 spermatogonia. (C) Pachytene spermatocytes. (D) Round spermatids. (E) Caput spermatozoa. (F) Cauda sperm.

other epigenetic processes and correlated gene expression to develop a more systems biology assessment of the molecular mechanism involved.

5. Methods

5.1. Animal studies and breeding

Female and male rats of an outbred strain Hsd: Sprague Dawley®™SD®™ obtained from Harlan/Envigo (Indianapolis, IN) at about 70–100 days of age were maintained in ventilated (up to 50 air exchanges/hour) isolator cages (cages with dimensions of 10 ¾″ W×19 ¼″ D×10 ¾″ H, 143 square inch floor space, fitted in Micro-vent 36-cage rat racks; Allentown Inc., Allentown, NJ) containing Aspen Sani chips (pinewood shavings from Harlan) as bedding, and a 14 h light: 10 h dark regimen, at a temperature of 70 F and humidity of 25–35%. The mean light intensity in the animal rooms ranged from 22 to 26 ft-candles. Rats were fed ad lib with standard rat diet (8640 Teklad 22/5 Rodent Diet; Harlan) and ad lib tap water for drinking. To obtain time-pregnant females, the female rats in proestrus were pair-mated with male rats. The sperm-positive (i.e. sperm plug present) (day 0) rats were monitored for diestrus and body weight. On days 8 through 14 of gestation [46], the females received daily intraperitoneal injections of DDT (25 mg/kg body weight/day) or dimethyl sulfoxide (DMSO). The DDT (dichlorodiphenyltrichloroethane) was obtained from Chem Service Inc. (West Chester, PA) and reported to have a purity of 98.2%. DDT were dissolved and injected in DMSO vehicle as previously described [47]. Treatment lineages are designated 'control' or 'DDT' lineages. The treated gestating female rats were designated as the F0 generation. The offspring of the F0 generation rats were the F1 generation. Non-littermate females and males aged 70–90 days from the F1 generation of control or DDT lineages were bred to obtain F2 generation offspring. The F2 generation rats were bred to obtain F3 generation offspring. The F1–F3 generation offspring were not themselves treated directly with DDT. The control and DDT lineages were housed in the same room and racks with lighting, food and water as previously described [47–49]. All experimental protocols for the procedures with rats were pre-approved by the Washington State University Animal Care and Use Committee (IACUC approval # 6252).

5.2. Epididymal sperm collection and DNA isolation

Testis and epididymis were collected from 12 month old rats for germ cell collection. The epididymis was dissected free of connective tissue and divided into caput and cauda halves with a cut in the mid-corpus. A small cut made to the cauda and to the caput and each half was placed in 3 ml of PBS for up to 2 h at 4 °C. Caput and cauda epididymal tissue were each coarsely minced and the liquid with the

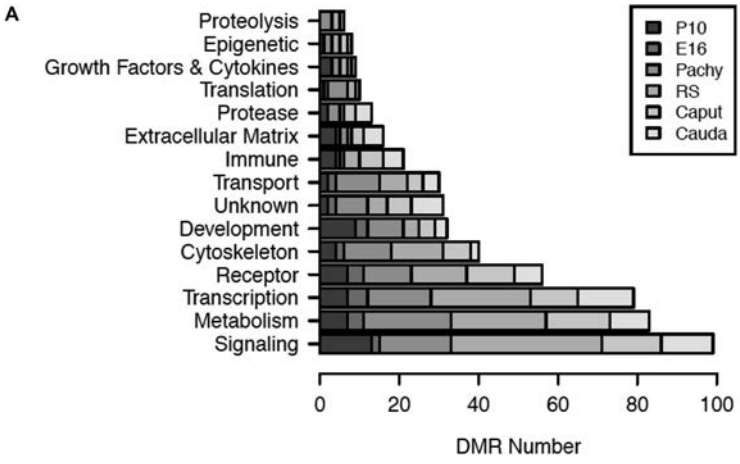

B DMR Gene Association Pathways

DDT Prospermatogonia E16
rno05160 Hepatitis C (2)
rno04913 Ovarian steroidogenesis (2)
rno04217 Necroptosis (2)
rno04976 Bile secretion (2)
rno01100 Metabolic pathways (2)

DDT Spermatogonia (P10)
rno05200 Pathways in cancer (6)
rno05224 Breast cancer (4)
rno05226 Gastric cancer (4)
rno04928 Parathyroid hormone synthesis, secretion and action (3)
rno04380 Osteoclast differentiation (3)

DDT Pachytene Spermatocytes
rno01100 Metabolic pathways (10)
rno04014 Ras signaling pathway (6)
rno05206 MicroRNAs in cancer (6)
rno05200 Pathways in cancer (6)
rno05165 Human papillomavirus infection (6)

DDT Round Spermatids
no01100 Metabolic pathways (11)
rno05200 Pathways in cancer (8)
rno04010 MAPK signaling pathway (7)
rno04360 Axon guidance (6)
rno04151 PI3K-Akt signaling pathway (6)
rno04144 Endocytosis (6)

DDT Caput Spermatozoa
rno05168 Herpes simplex infection (9)
rno04514 Cell adhesion molecules (CAMs) (9)
rno04612 Antigen processing and presentation (8)
rno05165 Human papillomavirus infection (8)
rno01100 Metabolic pathways (7)

DDT Cauda Sperm
rno01100 Metabolic pathways (5)
rno04514 Cell adhesion molecules (CAMs) (4)
rno04650 Natural killer cell mediated cytotoxicity (4)
rno04145 Phagosome (4)
rno04510 Focal adhesion (4)

Fig. 9. Sperm DMR associated gene categories and pathways. (A) DMR associated gene functional categories for each stage (color insert) versus DMR number. (B) DMR associated gene pathways for each stage of development with number of DMR associated genes in pathway in brackets. Bolded pathways show overlap in at least three developmental stages.

released sperm collected. For each sample the released sperm was centrifuged at 6000×*g*, then the supernatant removed, and the pellet resuspended in NIM buffer, to be stored at −80 °C until further use. One hundred µl of sperm suspension was sonicated to destroy somatic cells and tissue, spun down at 6000×*g*, the sperm pellet washed with 1x PBS once, and then combined with 820 µl DNA extraction buffer and 80 µl 0.1 M DTT. The sample was incubated at 65 °C for 15 min. Following this incubation 80 µl proteinase K (20 mg/ml) was added and the sample incubated at 55 °C for at least 2 h under constant rotation. Then 300 µl of protein precipitation solution (Promega, A7953) was added, the sample mixed thoroughly and incubated for 15 min on ice. The sample was centrifuged at 12,500×*g* for 30 min at 4 °C. One ml of the supernatant was transferred to a 2 ml tube and 2 µl of glycoblue and 1 ml of cold 100% isopropanol were added. The sample was mixed well by inverting the tube several times then left in −20 °C freezer for at least one hour. After precipitation the sample was centrifuged at 12,500×*g* for 20 min at 4 °C. The supernatant was taken off and discarded without disturbing the (blue) pellet. The pellet was washed with 70% cold ethanol by adding 500 µl of 70% ethanol to the pellet and returning the tube to the freezer for 20 min. After the incubation the tube was centrifuged for 10 min at 4 °C at 12,500×*g* and the supernatant discarded. The tube was spun again briefly to collect residual ethanol to bottom of tube and then as much liquid as possible was removed with gel loading tip. Pellet was air-dried at RT until it looked dry (about 5 min). Pellet was then resuspended in 100 µl of nuclease free water.

5.3. Developing germ cell stage isolation and DNA preparation

Harlan Sprague-Dawley rats (Harlan Inc., Indianapolis IN) were used for all experiments. The rats were kept in a temperature controlled environment and given food and water ad libitum. Estrous cycles of female rats were monitored by cellular morphology from vaginal smears. Rats in early estrus were paired with males overnight and mating confirmed by sperm-positive smears, denoted day 0 of pregnancy. Pregnant rats were euthanized at embryonic day 16 (E16) of gestation, and fetal gonads were collected for germ cell preparations. Sex was determined on the basis of gonadal morphology. Germ cells were isolated exclusively from males.

Purified populations of male PGCs type T1 prospermatogonia (at E16) were prepared using a mini StaPut gradient method as previously described [50,51]. Briefly, fetal testes were pooled and dissociated by incubation in 0.25% trypsin-EDTA (Sigma) with vigorous pipetting using a 1000 microliter pipette tip, and the resulting cell solution was filtered through 100 µm nylon mesh to yield a single cell suspension. This cell suspension was then loaded onto a 50 ml 2–4% bovine serum albumen (BSA) gradient prepared in KREBS buffer, and the cells were allowed to sediment at unit gravity at 4 °C for two hours as described [50,51]. The gradient was then fractionated and aliquots of the fractions were examined under phase optics to identify those enriched for the appropriate cell types on the basis of morphological characteristics. The enriched fractions were pooled to yield the final sample which was ≥85% pure for the desired male germ cell type in each case.

Three pools of prospermatogonia were prepared for each treatment group, with each pool derived from testes of 5–6 rats from different litters.

A similar mini StaPut gradient method [50,51] was used to isolate spermatogonia from testes of 10-day old rats, with the addition of incubation of the testes in 0.5 mg/ml collagenase (Sigma C1639) at 33 °C for 20 min with agitation to dissociate the seminiferous tubules. Three pools of spermatogonia from 10-day old rats were prepared for each treatment group, with each pool derived from testes of 6–7 rats from different litters.

To isolate pachytene spermatocytes and round spermatids, testes were collected from 12 month old rats suspended in F-12 culture medium (Gibco-Life Technologies, USA. Ref 11765-054) and shipped overnight on ice to Dr. John McCarrey. A StaPut gradient method was used to isolate the developing germ cell stages as previously described [50,51]. Three pools of cells of each cell type were prepared for each treatment group, with each pool derived from testes of three rats from different litters. DNA was isolated from prospermatogonia, spermatogonia, pachytene spermatocytes and round spermatids using the same procedure as was used for sperm, with the omission of sonication and DTT treatments.

5.4. Methylated DNA immunoprecipitation MeDIP

Methylated DNA Immunoprecipitation (MeDIP) with genomic DNA was performed as follows: rat DNA pools were generated using the appropriate amount of genomic DNA from each individual for 3 pools each of control and DDT lineage animals. Genomic DNA pools were sonicated using the Covaris M220 the following way: the pooled genomic DNA was diluted to 130 µl with TE buffer into the appropriate Covaris tube. Covaris was set to 300 bp program and the program was run for each tube in the experiment. 10 µl of each sonicated DNA was run on 1.5% agarose gel to verify fragment size. The sonicated DNA was transferred from the Covaris tube to a 1.7 ml microfuge tube and the volume measured. The sonicated DNA was then diluted with TE buffer (10 mM Tris HCl, pH7.5; 1 mM EDTA) to 400 µl, heat-denatured for 10 min at 95 °C, then immediately cooled on ice for 10 min. Then 100 µl of 5X IP buffer and 5 µg of antibody (monoclonal mouse anti 5-methyl cytidine; Diagenode #C15200006) were added to the denatured sonicated DNA. The DNA-antibody mixture was incubated overnight on a rotator at 4 °C.

The following day magnetic beads (Dynabeads M-280 Sheep anti-Mouse IgG; 11201D) were pre-washed as follows: The beads were resuspended in the vial, then the appropriate volume (50 µl per sample) was transferred to a microfuge tube. The same volume of Washing Buffer (at least 1 ml PBS with 0.1% BSA and 2 mM EDTA) was added and the bead sample was resuspended. Tube was then placed into a magnetic rack for 1–2 min and the supernatant discarded. The tube was removed from the magnetic rack and the beads washed once. The washed beads were resuspended in the same volume of IP buffer (50 mM sodium phosphate ph7.0, 700 mM NaCl, 0.25% TritonX-100) as the initial volume of beads. 50 µl of beads were added to the 500 µl of DNA-antibody mixture from the overnight incubation, then incubated for 2 h on a rotator at 4 °C.

After the incubation the bead-antibody-DNA complex was washed three times with IP buffer as follows: The tube was placed into magnetic rack for 1–2 min and the supernatant discarded, then washed with IP buffer 3 times. The washed bead-DNA solution is then resuspended in 250 µl digestion buffer with 3.5 µl Proteinase K (20 mg/ml). The sample was then incubated for 2–3 h on a rotator at 55 °C and then 250 µl of buffered Phenol-Chloroform-Isoamylalcohol solution was added to the supe and the tube vortexed for 30 s then centrifuged at 12,500×*g* for 5 min at room temperature. The aqueous supernatant was carefully removed and transferred to a fresh microfuge tube. Then 250 µl chloroform were added to the supernatant from the previous step, vortexed for 30 s and centrifuged at 12,500×*g* for 5 min at room temperature. The aqueous supernatant was removed and transferred to a fresh microfuge tube. To the supernatant 2 µl of glycoblue (20 mg/ml), 20 µl of 5 M NaCl and 500 µl ethanol were added and mixed well, then precipitated in −20 °C freezer for 1 h to overnight.

The precipitate was centrifuged at 12,500×*g* for 20 min at 4 °C and the supernatant removed, while not disturbing the pellet. The pellet was washed with 500 µl cold 70% ethanol in −20 °C freezer for 15 min then centrifuged again at 12,500×*g* for 5 min at 4 °C and the supernatant discarded. The tube was spun again briefly to collect residual ethanol to bottom of tube and as much liquid as possible was removed with gel loading tip. Pellet was air-dried at RT until it looked dry (about 5 min) then resuspended in 20 µl H2O or TE. DNA concentration was measured in Qubit (Life Technologies) with ssDNA kit (Molecular Probes Q10212).

5.5. MeDIP-Seq analysis

The MeDIP pools were used to create libraries for next generation sequencing (NGS) using the NEBNext® Ultra™ RNA Library Prep Kit for Illumina® (NEB, San Diego, CA) starting at step 1.4 of the manufacturer's protocol to generate double stranded DNA. After this step the manufacturer's protocol was followed. Each pool received a separate index primer. NGS was performed at WSU Spokane Genomics Core using the Illumina HiSeq. 2500 with a PE50 application, with a read size of approximately 50 bp and approximately 30 million reads per pool. Five to six libraries were run in one lane.

5.6. Statistics and bioinformatics

For the DMR analyses, the basic read quality was verified using summaries produced by the FastQC program http://www.bioinformatics.babraham.ac.uk/projects/fastqc/. The raw reads were trimmed and filtered using Trimmomatic. The reads for each MeDIP sample were mapped to the Rnor 6.0 rat genome using Bowtie2 [52] with default parameter options. The mapped read files were then converted to sorted BAM files using SAMtools [53]. To identify DMRs, the reference genome was broken into 100 bp windows. Genomic windows with no CpG or ambiguous base within 1000 bp were identified in the reference genome and used as control genes to perform RUVg normalization [54]. The MEDIPS [55] and edgeR [56] R packages were used to calculate differential coverage between control and exposure sample groups. The edgeR p-value was used to determine the relative difference between the two groups for each genomic window. Windows with an edgeR p-value less than 10–5 were considered DMRs. The FDR adjusted p-values were also calculated. The DMR edges were extended until no genomic window with an edgeR p-value < 0.1 remained within 1000 bp of the DMR. CpG density and other information was then calculated for the DMR based on the reference genome. DMRs were annotated using the biomaRt R package [57] to access the Ensembl database [58]. The genes that fell within 10kbp of the DMR edges were then input into the KEGG pathway search [59,60] to identify associated pathways. The associated genes were then sorted into functional groups by consulting information provided by the DAVID [61], Panther [62], and Uniprot databases incorporated into an internal curated database (www.skinner.wsu.edu under genomic data). All molecular data has been deposited into the public database at NCBI (GEO # GSE121585).

Acknowledgments

We acknowledge Ms. Margaux McBirney, Ms. Deepika Kubsad and Mr. Ryan Thompson for technical assistance and Ms. Heather Johnson for assistance in preparation of the manuscript. We thank Ms. Stephanie E. King for generating the germ cell schematics in Fig. 9. We thank the Genomics Core laboratory at WSU Spokane. This study was supported by a John Templeton Foundation, USA (50183)

(https://templeton.org/) grant to MKS and NIH, USA (ES012974) (https://www.nih.gov/) grant to MKS. The funders had no role in study design, data collection and analysis, decision to publish, or preparation of the manuscript

Declaration of interests

The authors declare no competing interests.

CRediT authorship contribution statement

Millissia Ben Maamar: Writing - original draft, Writing - review & editing, Formal analysis, Investigation, **Eric Nilsson:** Writing - review & editing, Formal analysis, Investigation, **Ingrid Sadler-Riggleman:** Writing - review & editing, Formal analysis, Investigation, Validation, **Daniel Beck:** Writing - review & editing, Data curation, Investigation, Validation, **John R. McCarrey:** Writing - review & editing, Investigation, Supervision, **Michael K. Skinner:** Writing - original draft, Writing - review & editing, Conceptualization, Funding acquisition, Investigation, Project administration, Supervision

Appendix A. Supporting information

Supplementary data associated with this article can be found in the online version at doi:10.1016/j.ydbio.2018.11.016.

References

Anway, M.D., Cupp, A.S., Uzumcu, M., Skinner, M.K., 2005]. Epigenetic transgenerational actions of endocrine disruptors and male fertility. Science 308 (5727), 1466–1469.

Skinner, M.K., Manikkam, M., Tracey, R., Guerrero-Bosagna, C., Haque, M.M., Nilsson, E., 2013]. Ancestral dichlorodiphenyltrichloroethane (DDT) exposure promotes epigenetic transgenerational inheritance of obesity. BMC Med. 11 (1–16), 228.

Soubry, A., 2015]. Epigenetic inheritance and evolution: a paternal perspective on dietary influences. Prog. Biophys. Mol. Biol. 118 (1–2), 79–85.

Vaiserman, A.M., Koliada, A.K., Jirtle, R.L., 2017]. Non-genomic transmission of longevity between generations: potential mechanisms and evidence across species. Epigenetics Chromatin 10 (1), 38.

Nilsson, E., Sadler-Riggleman, I., Skinner, M.K., 2018]. Environmentally induced epigenetic transgenerational inheritance of disease. Environ. Epigenetics 4 (2), 1–13, (dvy016).

Skinner, M.K., 2015]. Environmental epigenetics and a unified theory of the molecular aspects of evolution: a Neo-Lamarckian concept that facilitates Neo-Darwinian evolution. Genome Biol. Evol. 7 (5), 1296–1302.

Skinner, M.K., 2011]. Environmental epigenetic transgenerational inheritance and somatic epigenetic mitotic stability. Epigenetics 6 (7), 838–842.

Beck, D., Sadler-Riggleman, I., Skinner, M.K., 2017]. Generational comparisons (F1 versus F3) of vinclozolin induced epigenetic transgenerational inheritance of sperm differential DNA methylation regions (epimutations) using MeDIP-seq. Environ. Epigenetics 3 (3), 1–12, (dvx016).

Quadrana, L., Colot, V., 2016]. Plant transgenerational epigenetics. Annu. Rev. Genet. 50, 467–491.

Sharma, U., Rando, O.J., 2017]. Metabolic inputs into the epigenome. Cell Metab. 25 (3), 544–558.

Gapp, K., Jawaid, A., Sarkies, P., Bohacek, J., Pelczar, P., Prados, J., Farinelli, L., Miska, E., Mansuy, I.M., 2014]. Implication of sperm RNAs in transgenerational inheritance of the effects of early trauma in mice. Nat. Neurosci. 17 (5), 667–669.

Yan, W., 2014]. Potential roles of noncoding RNAs in environmental epigenetic transgenerational inheritance. Mol. Cell Endocrinol. 398 (1–2), 24–30.

Ben Maamar, M., Sadler-Riggleman, I., Beck, D., Skinner, M.K., 2018]. Epigenetic transgenerational inheritance of altered sperm histone retention sites. Sci. Rep. 8, 5308, (1-10).

Furuhashi, H., Kelly, W.G., 2010]. The epigenetics of germ-line immortality: lessons from an elegant model system. Dev. Growth Differ. 52 (6), 527–532.

Skinner, M.K., Ben Maamar, M., Sadler-Riggleman, I., Beck, D., Nilsson, E., McBirney, M., Klukovich, R., Xie, Y., Tang, C., Yan, W., 2018]. Alterations in sperm DNA methylation, non-coding RNA and histone retention associate with DDT-induced epigenetic transgenerational inheritance of disease. Epigenetics Chromatin 11 (1), 1–24, (8).

Ben Maamar, M., Sadler-Riggleman, I., Beck, D., McBirney, M., Nilsson, E., Klukovich, R., Xie, Y., Tang, C., Yan, W., Skinner, M.K., 2018]. Alterations in sperm DNA methylation, non-coding RNA expression, and histone retention mediate Vinclozolin induced epigenetic transgenerational inheritance of disease. Environ. Epigenetics 4 (2), 1–19, (dvy010).

Manikkam, M., Haque, M.M., Guerrero-Bosagna, C., Nilsson, E., Skinner, M.K., 2014]. Pesticide methoxychlor promotes the epigenetic transgenerational inheritance of adult onset disease through the female germline. PLoS One 9 (7), 1–19, (e102091).

Seisenberger, S., Andrews, S., Krueger, F., Arand, J., Walter, J., Santos, F., Popp, C., Thienpont, B., Dean, W., Reik, W., 2012]. The dynamics of genome-wide DNA methylation reprogramming in mouse primordial germ cells. Mol. Cell 48 (6), 849–862.

Jost, A., Vigier, B., Prepin, J., Perchellet, J.P., 1973]. Studies on sex differentiation in mammals. Recent Prog. Horm. Res. 29, 1–41.

McCarrey, J.R., 2013]. Toward a more precise and informative nomenclature describing fetal and neonatal male germ cells in rodents. Biol. Reprod. 89 (2), 47.

McCarrey, J.R., 2012]. The epigenome as a target for heritable environmental disruptions of cellular function. Mol. Cell Endocrinol. 354 (1–2), 9–15.

Dym, M., Fawcett, D.W., 1971]. Further observations on the numbers of spermatogonia, spermatocytes, and spermatids connected by intercellular bridges in the mammalian testis. Biol. Reprod. 4 (2), 195–215.

Orgebin-Crist, M.C., Danzo, B.J., Cooper, T.G., 1976]. Re-examination of the dependence of epididymal sperm viability on the epididymal environment. J. Reprod. Fertil. Suppl. 24 suppl, 115–128.

Cornwall, G.A., 2009]. New insights into epididymal biology and function. Hum. Reprod. Update 15 (2), 213–227.

Tang, W.W., Kobayashi, T., Irie, N., Dietmann, S., Surani, M.A., 2016]. Specification and epigenetic programming of the human germ line. Nat. Rev. Genet. 17 (10), 585–600.

Ku, H.Y., Gangaraju, V.K., Qi, H., Liu, N., Lin, H., 2016]. Tudor-SN interacts with Piwi antagonistically in regulating spermatogenesis but synergistically in silencing transposons in drosophila. PLoS Genet. 12 (1), e1005813.

La Salle, S., Oakes, C.C., Neaga, O.R., Bourc'his, D., Bestor, T.H., Trasler, J.M., 2007]. Loss of spermatogonia and wide-spread DNA methylation defects in newborn male mice deficient in DNMT3L. BMC Dev. Biol. 7, 104.

Mann, J.R., 2001]. Imprinting in the germ line. Stem Cells 19 (4), 287–294.

Barlow, D.P., Bartolomei, M.S., 2014]. Genomic imprinting in mammals. Cold Spring Harb. Perspect. Biol. 6 (2), 1–21.

Hanson, M.A., Skinner, M.K., 2016]. Developmental origins of epigenetic transgenerational inheritance. Environ. Epigenetics 2 (1), 1–9, (dvw002).

Soubry, A., Hoyo, C., Jirtle, R.L., Murphy, S.K., 2014]. A paternal environmental legacy: evidence for epigenetic inheritance through the male germ line. Bioessays 36 (4), 359–371.

Boskovic, A., Rando, O.J., 2018]. Transgenerational epigenetic inheritance. Annu. Rev. Genet. 52, (p. Epub ahead of print).

Soubry, A., Hoyo, C., Butt, C.M., Fieuws, S., Price, T.M., Murphy, S.K., Stapleton, H.M., 2017]. Human exposure to flame-retardants is associated with aberrant DNA methylation at imprinted genes in sperm. Environ. Epigenetics 3 (1), dvx003.

del Mazo, J., Prantera, G., Torres, M., Ferraro, M., 1994]. DNA methylation changes during mouse spermatogenesis. Chromosome Res. 2 (2), 147–152.

Skinner, M., Guerrero-Bosagna, C., Haque, M.M., Nilsson, E., Bhandari, R., McCarrey, J., 2013]. Environmentally induced transgenerational epigenetic reprogramming of primordial germ cells and subsequent germline. PLoS One 8 (7), 1–15, (e66318).

Skinner, M.K., Nilsson, E., Sadler-Riggleman, I., Beck, D., McCarrey, J.R., 2018]. Developmental origins of transgenerational sperm DNA methylation epimutations Following ancestral vinclozolin exposure. Pending.

Skinner, M.K., 2008]. What is an epigenetic transgenerational phenotype? F3 or F2. Reprod. Toxicol. 25 (1), 2–6.

Ariel, M., McCarrey, J., Cedar, H., 1991]. Methylation patterns of testis-specific genes. Proc. Natl. Acad. Sci. USA 88 (6), 2317–2321.

Hermann, B.P., Mutoji, K.N., Velte, E.K., Ko, D., Oatley, J.M., Geyer, C.B., McCarrey, J.R., 2015]. Transcriptional and translational heterogeneity among neonatal mouse spermatogonia. Biol. Reprod. 92 (2), 54.

Skinner, M.K., Guerrero-Bosagna, C., 2014]. Role of CpG deserts in the epigenetic transgenerational inheritance of differential DNA methylation regions. BMC Genom. 15 (1), 692.

Ventela, S., Ohta, H., Parvinen, M., Nishimune, Y., 2002]. Development of the stages of the cycle in mouse seminiferous epithelium after transplantation of green fluorescent protein-labeled spermatogonial stem cells. Biol. Reprod. 66 (5), 1422–1429.

Suresh, R., Aravindan, G.R., Moudgal, N.R., 1992]. Quantitation of spermatogenesis by DNA flow cytometry: comparative study among six species of mammals. J. Biosci. 17 (4), 413–419.

Sharma, U., Conine, C.C., Shea, J.M., Boskovic, A., Derr, A.G., Bing, X.Y., Belleannee, C., Kucukural, A., Serra, R.W., Sun, F., Song, L., Carone, B.R., Ricci, E.P., Li, X.Z., Fauquier, L., Moore, M.J., Sullivan, R., Mello, C.C., Garber, M., Rando, O.J., 2016]. Biogenesis and function of tRNA fragments during sperm maturation and fertilization in mammals. Science 351 (6271), 391–396.

Rompala, G.R., Mounier, A., Wolfe, C.M., Lin, Q., Lefterov, I., Homanics, G.E., 2018]. Heavy chronic intermittent ethanol exposure alters small noncoding RNAs in mouse sperm and epididymosomes. Front. Genet. 9, 32.

Ariel, M., Cedar, H., McCarrey, J., 1994]. Developmental changes in methylation of spermatogenesis-specific genes include reprogramming in the epididymis. Nat. Genet. 7 (1), 59–63.

Nilsson, E.E., Anway, M.D., Stanfield, J., Skinner, M.K., 2008]. Transgenerational epigenetic effects of the endocrine disruptor vinclozolin on pregnancies and female adult onset disease. Reproduction 135 (5), 713–721.

Manikkam, M., Guerrero-Bosagna, C., Tracey, R., Haque, M.M., Skinner, M.K., 2012]. Transgenerational actions of environmental compounds on reproductive disease and identification of epigenetic biomarkers of ancestral exposures. PLoS One 7 (2), 1–12, (e31901).

Skinner, M.K., Manikkam, M., Guerrero-Bosagna, C., 2010]. Epigenetic transgenerational actions of environmental factors in disease etiology. Trends Endocrinol. Metab. 21 (4), 214–222.

Anway, M.D., Leathers, C., Skinner, M.K., 2006]. Endocrine disruptor vinclozolin

induced epigenetic transgenerational adult-onset disease. Endocrinology 147 (12), 5515–5523.
McCarrey, J.R., Berg, W.M., Paragioudakis, S.J., Zhang, P.L., Dilworth, D.D., Arnold, B.L., Rossi, J.J., 1992]. Differential transcription of Pgk genes during spermatogenesis in the mouse. Dev. Biol. 154 (1), 160–168.
Kafri, T., Ariel, M., Brandeis, M., Shemer, R., Urven, L., McCarrey, J., Cedar, H., Razin, A., 1992]. Developmental pattern of gene-specific DNA methylation in the mouse embryo and germ line. Genes Dev. 6 (5), 705–714.
Bolger, A.M., Lohse, M., Usadel, B., 2014]. Trimmomatic: a flexible trimmer for Illumina sequence data. Bioinformatics 30 (15), 2114–2120.
Langmead, B., Salzberg, S.L., 2012]. Fast gapped-read alignment with Bowtie 2. Nat. Methods 9 (4), 357–359.
Risso, D., Ngai, J., Speed, T.P., Dudoit, S., 2014]. Normalization of RNA-seq data using factor analysis of control genes or samples. Nat. Biotechnol. 32 (9), 896–902.
Lienhard, M., Grimm, C., Morkel, M., Herwig, R., Chavez, L., 2014]. MEDIPS: genome-wide differential coverage analysis of sequencing data derived from DNA enrichment experiments. Bioinformatics 30 (2), 284–286.
Robinson, M.D., McCarthy, D.J., Smyth, G.K., 2010]. edgeR: a Bioconductor package for differential expression analysis of digital gene expression data. Bioinformatics 26 (1), 139–140.
Durinck, S., Spellman, P.T., Birney, E., Huber, W., 2009]. Mapping identifiers for the integration of genomic datasets with the R/Bioconductor package biomaRt. Nat. Protoc. 4 (8), 1184–1191.
Cunningham, F., Amode, M.R., Barrell, D., Beal, K., Billis, K., Brent, S., Carvalho-Silva, D., Clapham, P., Coates, G., Fitzgerald, S., Gil, L., Giron, C.G., Gordon, L., Hourlier, T., Hunt, S.E., Janacek, S.H., Johnson, N., Juettemann, T., Kahari, A.K., Keenan, S., Martin, F.J., Maurel, T., McLaren, W., Murphy, D.N., Nag, R., Overduin, B., Parker, A., Patricio, M., Perry, E., Pignatelli, M., Riat, H.S., Sheppard, D., Taylor, K., Thormann, A., Vullo, A., Wilder, S.P., Zadissa, A., Aken, B.L., Birney, E., Harrow, J., Kinsella, R., Muffato, M., Ruffier, M., Searle, S.M., Spudich, G., Trevanion, S.J., Yates, A., Zerbino, D.R., Flicek, P., 2015]. Ensembl 2015. Nucleic Acids Res. 43, D662–D669.
Kanehisa, M., Goto, S., 2000]. KEGG: kyoto encyclopedia of genes and genomes. Nucleic Acids Res. 28 (1), 27–30.
Kanehisa, M., Goto, S., Sato, Y., Kawashima, M., Furumichi, M., Tanabe, M., 2014]. Data, information, knowledge and principle: back to metabolism in KEGG. Nucleic Acids Res. 42, D199–D205.
Huang da, W., Sherman, B.T., Lempicki, R.A., 2009]. Systematic and integrative analysis of large gene lists using DAVID bioinformatics resources. Nat. Protoc. 4 (1), 44–57.
Mi, H., Muruganujan, A., Casagrande, J.T., Thomas, P.D., 2013]. Large-scale gene function analysis with the PANTHER classification system. Nat. Protoc. 8 (8), 1551–1566.

Circulation

ORIGINAL RESEARCH ARTICLE

Prenatal Lipopolysaccharides Exposure Induces Transgenerational Inheritance of Hypertension

Nian Cao, MD, PhD*; Cong Lan, MD, PhD*; Caiyu Chen, BS*; Zaicheng Xu, MD, PhD*; Hao Luo, MS; Shuo Zheng, BS; Xue Gong, MD, PhD; Hongmei Ren, BS; Zhuxin Li, BS; Shuang Qu, MS; Cheng Yu, MD, PhD; Jining Yang, PhD; Pedro A. Jose, MD, PhD; Yundai Chen, MD, PhD; Gengze Wu, MD, PhD; Cuimei Hu, PhD; Junyi Yu, MD, PhD; Chunyu Zeng, MD, PhD

BACKGROUND: Adverse environmental exposure during the prenatal period can lead to diseases in the offspring, including hypertension. Whether or not the hypertensive phenotype can be transgenerationally transmitted is not known.

METHODS: Pregnant Sprague Dawley rats were intraperitoneally injected with lipopolysaccharide (LPS) on gestation days 6, 8, 10, and 12 to generate the prenatal LPS exposure model. Blood pressure was monitored by both telemetry and tail-cuff method. RNA sequencing was performed to analyze transcriptome alteration in the kidney of the third generation. Tempol and spironolactone were used to test the potential preventative and therapeutic effect of targeting reactive oxygen species and mineralocorticoid receptor signaling, respectively. Molecular biological experiments were performed to illustrate the mechanism of epigenetic and transcription regulation.

RESULTS: Prenatal LPS exposure can impair the ability to excrete a salt load and induce hypertension from the first to the third generations, with the fourth and fifth generations, inducing salt-sensitive hypertension. Compared with control pups, the transcriptome in the kidney of the hypertensive third-generation prenatal LPS–exposed offspring have upregulation of the Ras-related C3 botulinum toxin substrate 1 (*Rac1*) gene and activation of mineralocorticoid receptor signaling. Furthermore, we found that LPS exposure during pregnancy triggered oxidative stress that upregulated KDM3B (histone lysine demethylase 3B) in the oocytes of first-generation female rats, leading to an inheritable low level of H3K9me2 (histone H3 lysine 9 dimethylation), resulting in the transgenerational upregulation of *Rac1*. Based on these findings, we treated the LPS-exposed pregnant rats with the reactive oxygen species scavenger, tempol, which successfully prevented hypertension in the first-generation offspring and the transgenerational inheritance of hypertension.

CONCLUSIONS: These findings show that adverse prenatal exposure induces transgenerational hypertension through an epigenetic-regulated mechanism and identify potentially preventive and therapeutic strategies for hypertension.

Key Words: epigenetics ■ hypertension ■ lipopolysaccharides ■ reactive oxygen species ■ receptors, mineralocorticoid

Editorial, see p 1096

Hypertension is one of the leading risk factors for cardiovascular disease and one of the largest contributors to morbidity and mortality worldwide.[1] The cause of hypertension is multifactorial in nature, with environmental, genetic, and social determinants having the potential to contribute to its development.[2] The understanding of the interplay among these determinants remains poor.

Besides the traditional environmental factors (eg, obesity, physical inactivity, excessive sodium intake, chronic stress)

Correspondence to: Chunyu Zeng, MD, PhD, Department of Cardiology, Daping Hospital, 10th Changjiang Rd, Yuzhong District, Chongqing, China 400042; Junyi Yu, MD, PhD, Department of Cardiology, Daping Hospital, 10th Changjiang Rd, Yuzhong District, Chongqing, China 400042; Cuimei Hu, PhD, Department of Cardiology, Daping Hospital, 10th Changjiang Rd, Yuzhong District, Chongqing, China 400042; or Gengze Wu, MD, PhD, Department of Cardiology, Daping Hospital, 10th Changjiang Rd, Yuzhong District, Chongqing, China 400042. Email chunyuzeng01@163.com, yujunyi@tmmu.edu.cn, hucuimeiuse@126.com, or wugengze@163.com

*N. Cao, C. Lan, C. Chen, and Z. Xu contributed equally.

Supplemental Material is available at https://www.ahajournals.org/doi/suppl/10.1161/CIRCULATIONAHA.122.059891.

For Sources of Funding and Disclosures, see page 1094.

© 2022 American Heart Association, Inc.

Circulation is available at www.ahajournals.org/journal/circ

Clinical Perspective

What Is New?

- Prenatal lipopolysaccharide exposure can induce transgenerationally transmitted hypertension and impairment of urinary sodium excretion.
- Renal Rac1-mineralocorticoid receptor axis is necessary for the development of transgenerationally transmitted hypertension and impaired natriuresis.
- Prenatal lipopolysaccharide exposure induces oxidative stress in F0, which increases the expression of histone demethylase KDM3B (histone lysine demethylase 3B) in the oocytes of F1 female rats and decreases the expression of H3K9me2 (histone H3 lysine 9 dimethylation) in the kidney of F2 offspring, leading to the activation of the RAC1-mineralocorticoid receptor axis, resulting in impaired urinary sodium excretion and hypertension.

What Are the Clinical Implications?

- Our analyses of transgenerational hypertension phenotypes in a prenatal lipopolysaccharide rat model suggested a strong maliferous effect of adverse stimulation during gestation.
- Reactive oxygen species antagonist treatment in F0 pregnant mother can prevent Prenatal lipopolysaccharide-induced transgenerational hypertension, whereas RAC1-mineralocorticoid receptor signaling can be a potential therapeutic target for transmitted hypertension in each subsequent generation.

Nonstandard Abbreviations and Acronyms

ENaCs	epithelial sodium channel
H3K9me2	histone H3 lysine 9 dimethylation
H3K4me1	histone H3 lysine 4 monomethylation
H3K27me3	histone H3 lysine 27 trimethylation
HS	high salt
KDMs	lysine demethylases
LPS	lipopolysaccharide
MR	mineralocorticoid receptor
PLPS	prenatal lipopolysaccharide
Rac1	Ras-related C3 botulinum toxin substrate 1
ROS	reactive oxygen species

and complex genetic background, parental life experiences and environmental exposures influence physical health across generations.[3] Studies from animal models have established the existence of a nongenetic mode of inheritance, which involves transmission of the effects of parental exposure to the offspring through epigenetic changes in the germline.[4,5] Adverse prenatal exposure, particularly in utero, is regarded as one of the causes of hypertension.[6] Maternal infection is a common event during pregnancy, and it is now clear that maternal infection is closely related to adverse pregnancy outcomes, including hypertension.[7,8] Our previous studies, using an animal model, showed that the intraperitoneal injection to dams of lipopolysaccharides (LPS), a toxic component of cell walls of gram-negative bacteria, was sufficient to induce hypertension in the offspring caused by renal and vascular dysfunctions.[8,9] However, whether prenatal LPS (PLPS) exposure can induce transgenerational hypertension is unclear.

METHODS

The data, analytic methods, and study materials will be made available to other researchers for purposes of reproducing the results or replicating the procedure. The RNA-sequencing datasets are deposited into Sequence Read Archive with accession number PRJNA825173. All experimental approaches are detailed in the Supplemental Methods.

Animal Studies

All animal procedures conformed to National Institutes of Health guidelines for the care and use of laboratory animals and were approved by The Third Military Medical University (Army Medical University) Animal Care and Use Committee.

Statistical Analysis

Data are shown as mean±SEM. All experiments were repeated at least 3 times. The data were analyzed with Prism 9.0 (GraphPad Inc). Comparison of means between 2 samples was performed using 2-tailed unpaired Student *t* tests and 1-way or 2-way ANOVA with Tukey post hoc analysis for ≥3 samples. $P<0.05$ is defined as statistically significant.

RESULTS

PLPS Exposure Induces Transgenerational Transmission of an Impaired Ability to Increase Urinary Sodium Excretion and Hypertension Across F1 to F3 Generations in Rats

Given the heritability of hypertension in the first generation (F1) of gestating rats prenatally exposed to LPS (F0),[8] we sought to test whether gestating rats prenatally exposed to LPS (F0) could transgenerationally transfer the hypertensive phenotype to the offspring. Pregnant Sprague Dawley rats were intraperitoneally injected with saline (0.2 mL) or LPS (0.79 mg/kg) on gestation days 6, 8, 10, and 12 (Figure 1A), to generate F1 control pups (dams injected with saline, control group) and F1 pups from LPS-exposed F0 mother (dams injected with LPS, PLPS group, Figure 1B). Female control F1 or hypertensive PLPS F1 offspring were then mated with wild-type male Sprague Dawley rats to generate control F2 and PLPS F2. In the same way, female control F2 or hypertensive PLPS F2 offspring were mated with wild-type male Sprague Dawley rats to generate F3 offspring, and

ORIGINAL RESEARCH ARTICLE

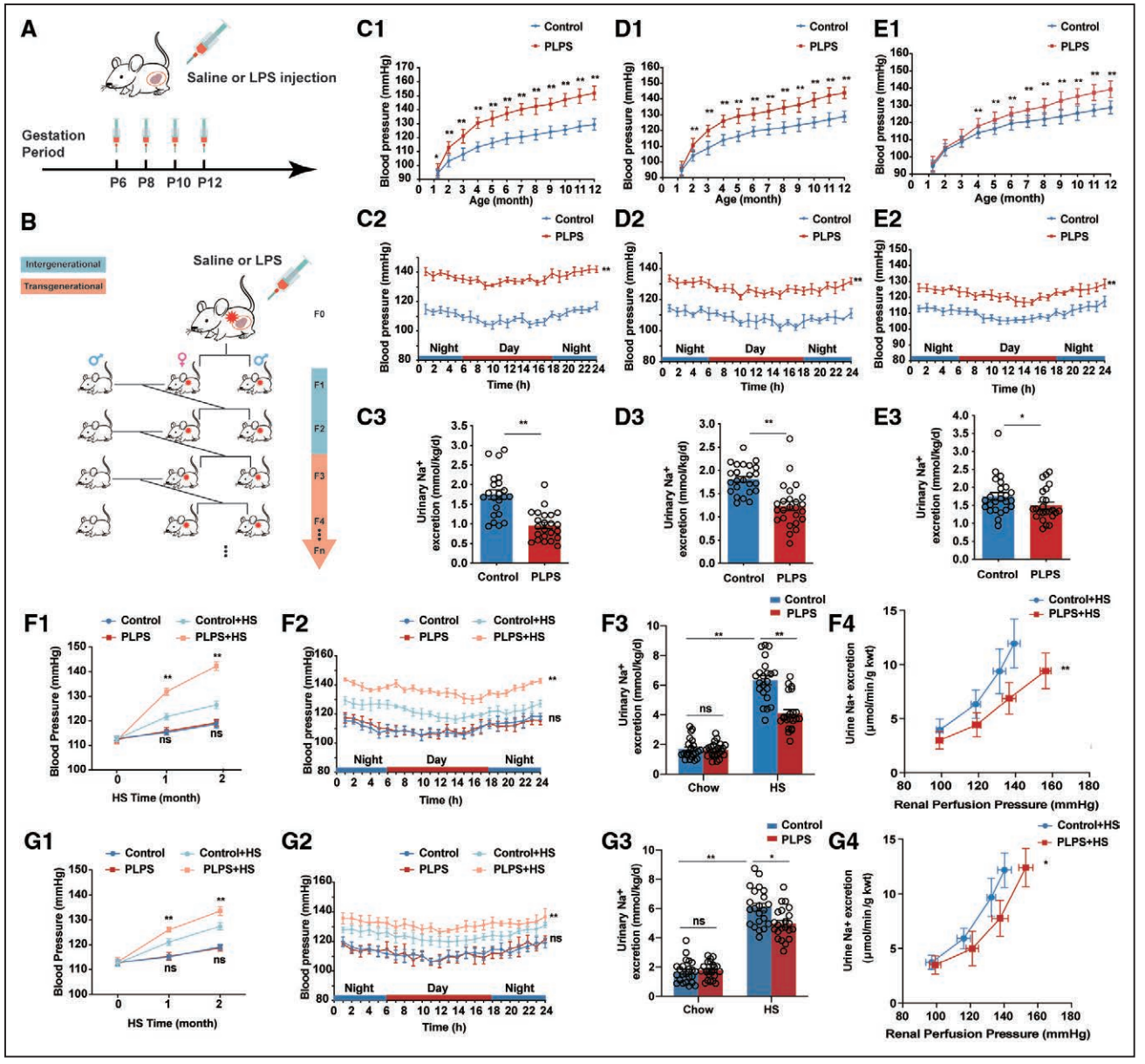

Figure 1. PLPS exposure induces transgenerational transmission of hypertension and impaired natriuresis.
A, Schematic illustration of PLPS exposure. **B**, Schematic illustration of the experimental design to generate intergenerational and transgenerational offspring of control or PLPS dams. **C** through **E**, Tail-cuff systolic blood pressure, 24-hour ambulatory systolic blood pressure, and 24-hour urinary Na^+ in F1 to F3 rats. **C1**, **D1**, **E1**, Systolic blood pressure measured monthly by tail-cuff method from 5-week-old to 1-year-old offspring (**C1**, F1 generation; **D1**, F2 generation; **E1**, F3 generation; n=20–40 rats/group). *P<0.05, **P<0.01, vs control, 2-way ANOVA followed by Bonferroni correction and within-test multiple corrections using Tukey multiple analysis. **C2**, **D2**, **E2**, 24-hour ambulatory systolic blood pressure measured by telemetry from 5-month-old offspring (**C2**, F1 generation; **D2**, F2 generation; **E2**, F3 generation; n=6). **P<0.01, vs control, 2-way ANOVA followed by Bonferroni correction and within-test multiple corrections using Tukey multiple analysis. **C3**, **D3**, **E3**, 24-hour urinary Na^+ of 5-month-old F1 control and PLPS offspring (**C3**, F1 generation; **D3**, F2 generation; **E3**, F3 generation; n=20–30 rats/group). *P<0.05, **P<0.01, vs control 2-tailed Student t test. **F** and **G**, Tail-cuff systolic blood pressure, 24-hour ambulatory systolic blood pressure, 24-hour urinary Na^+ measurement, and pressure-natriuresis curve in F4 and F5 rats fed with HS diet. **F1**, **G1**, Systolic blood pressure was measured monthly for 2 months by tail-cuff method from 4-month-old control and PLPS offspring fed HS (8% NaCl) diet for 2 months (**F1**, F4 generation; **G1**, F5 generation; n=20–40 rats/group). ns: not significant, vs Control, **P<0.01, vs Control+HS, 2-way ANOVA followed by Bonferroni correction and within-test multiple corrections using Tukey multiple analysis. **F2**, **G2**, 24-hour ambulatory systolic blood pressure was measured by telemetry from 6-month-old control and PLPS offspring fed HS (8% NaCl) diet for 2 months (**F2**, F4 generation; **G2**, F5 generation; n=6). ns: not significant, vs Control; **P<0.01, vs Control+HS, 2-way ANOVA followed by Bonferroni correction and within-test multiple corrections using Tukey multiple analysis. **F3**, **G3**, The first 24-hour urinary Na^+ of 4-month-old control and PLPS offspring fed with HS (8% NaCl) diet (**F3**, F4 generation; **G3**, F5 generation; n=20–40 rats/group). ns: not significant, *P<0.05, **P<0.01, 2-way ANOVA. **F4**, **G4**, Pressure-natriuresis curve illustrating the relationship between renal perfusion pressure and urinary sodium excretion in 6-month-old control and PLPS offspring fed HS (8% NaCl) diet for 2 months (**F4**, F4 generation; **G4**, F5 generation; n=6). *P<0.05, **P<0.01, vs Control+HS, 2-way ANOVA followed by Bonferroni correction and within-test multiple corrections using Tukey multiple analysis. F0 indicates gestating female; F1, first generation; F2, second generation; F3, third generation; F4, fourth generation; Fn, the "n" th generation; HS, high salt; LPS, lipopolysaccharide; P6, gestation day 6; P8, gestation day 8; P10, gestation day 10; P12, gestation day 12; and PLPS, prenatal lipopolysaccharide.

so on (Figure 1B). For each generation, blood pressure was monitored monthly by the tail-cuff method, starting from 5 weeks of age until 1 year of age. Blood pressure was also monitored by telemetry in conscious rats at 5 months of age.

After the first dose of LPS, the body temperature of F0 dams increased significantly, but the increase was less with subsequent exposures, such that the body temperature did not increase with the fourth injection (Figure S1A), indicating the successful induction of inflammation. The frequency of adverse maternal events in the F0 dams, including premature delivery, abortion, dystocia, and death, was significantly higher (Figure S1B) in PLPS F0 than control F0. The percentage of low birth weights (<7.0 g) of F1 surviving offspring was greater in the PLPS than in the control offspring (Figure S1C), indicating the adverse influence of PLPS exposure on embryonic development. However, the body weights of adult F1 PLPS rats were slightly higher than control offspring (Figure S1D), suggesting that postnatal influence can overcome the adverse effect on body weight of PLPS exposure.[8]

In agreement with our reported studies,[8,9] PLPS exposure led to an increase in blood pressure, especially systolic blood pressure, in the F1 PLPS offspring, as early as 5 weeks of age, which persisted up to 12 months of age (Figure 1C1). Twenty-four hour ambulatory systolic blood pressure monitored by telemetry was also higher (nighttime and daytime) in conscious F1 PLPS than F1 control offspring at 5 months of age (Figure 1C2). Urinary sodium excretion, a key process in the long-term regulation of blood pressure,[10] was markedly reduced in F1 PLPS, relative to F1 control offspring (Figure 1C3). We then assessed whether the hypertensive phenotype can be transmitted to F2 and F3 PLPS offspring. It is intriguing that significantly higher systolic blood pressure, and the decrease in urinary sodium excretion, as well, were transmitted to the second filial generation (F2, Figure 1D1–1D3) and the third filial generation (F3, Figure 1E1–1E3). However, other parameters, such as kidney weight, heart rate, plasma glucose, renal function (determined by serum creatinine, blood urea nitrogen, and urinary protein), serum dopamine, serum norepinephrine, and serum epinephrine in F1 to F3 generation offspring were not different between control and PLPS offspring (Table S1).

The blood pressure–monitoring data showed that the blood pressures of individual pups varied within the same group. To determine the frequency of hypertension in each generation, we labeled the blood pressure as normal when it was lower than the mean+1 SD of the control group and hypertensive when it was higher than the mean+1 SD of the control group at the first time a significant difference of blood pressure was observed between control and PLPS group. According to this classification, the frequency of hypertension is 86.8% in PLPS F1 generation, 76.1% in PLPS F2 generation, and 60.6% in PLPS F3 generation (Figure S1E). The frequency of hypertension is sex independent (Figure S1E).

PLPS Exposure Increases Salt Sensitivity of Blood Pressure in F4 and F5 Generations

Although the transgenerational hypertensive phenotype was observed in the F3 offspring, there was no difference in systolic blood pressure (Figure S2A1 and S2A2) or urinary sodium excretion (Figure S2A3) between the F4 control and PLPS offspring fed a normal NaCl diet. Salt-sensitive hypertension is one of the hypertension subtypes, which is also a risk factor of cardiovascular diseases.[11] We, therefore, fed the F4 to F6 generation control and PLPS offspring high salt (HS, 8% NaCl) diet to determine if the pups develop salt-sensitive hypertension. After a 2-month treatment with HS diet,[12] the PLPS offspring had a significantly higher elevation in systolic blood pressure in F4 (Figure 1F1 and F2) and F5 (Figure 1G1 and G2) offspring, whereas there was no significant difference between control and PLPS group treated with HS diet in the F6 generation (Figure S2B1 and S2B2). When fed with HS diet, the PLPS offspring had an impaired urinary sodium excretion compared with the control group in F4 (Figure 1F3) and F5 (Figure 1G3) generations but recovered in F6 generation (Figure S2B3). To depict further the relationship between blood pressure and sodium excretion, we plotted the pressure-natriuresis curve in F4 to F6 control and PLPS rats fed with 2 months of HS diet. The pressure-natriuresis curve flattened and shifted to the right in F4 (Figure 1F4) and F5 (Figure 1G4) in PLPS rats compared with control rats on a HS diet, indicating that pressure-related natriuresis was impaired in PLPS F4 and F5 generations. By contrast, the right-shifted pressure-natriuresis curve was not observed in the F6 PLPS rats, reflecting the recovery of renal sodium excretion in PLPS F6 rats when fed a HS diet (Figure S2B4).

PLPS Treatment Results in Altered Renal Transcriptome in the Offspring With Transgenerational Hypertension

To dissect the molecular mechanisms and the affected gene pathways underlying the transgenerationally inherited hypertension, and the impaired natriuresis induced by PLPS exposure, we performed RNA-sequencing (RNA-seq) analysis in the kidneys from F3 control and PLPS offspring (Figure 2A). There were 8162 differentially expressed genes in the kidney from F3 control and PLPS offspring. Using the Gene Set Enrichment Analysis to gain functional insight into the transcriptome, we found that some of the gene signatures altered in the renal transcriptome of F3 PLPS offspring, relative to F3

ORIGINAL RESEARCH ARTICLE

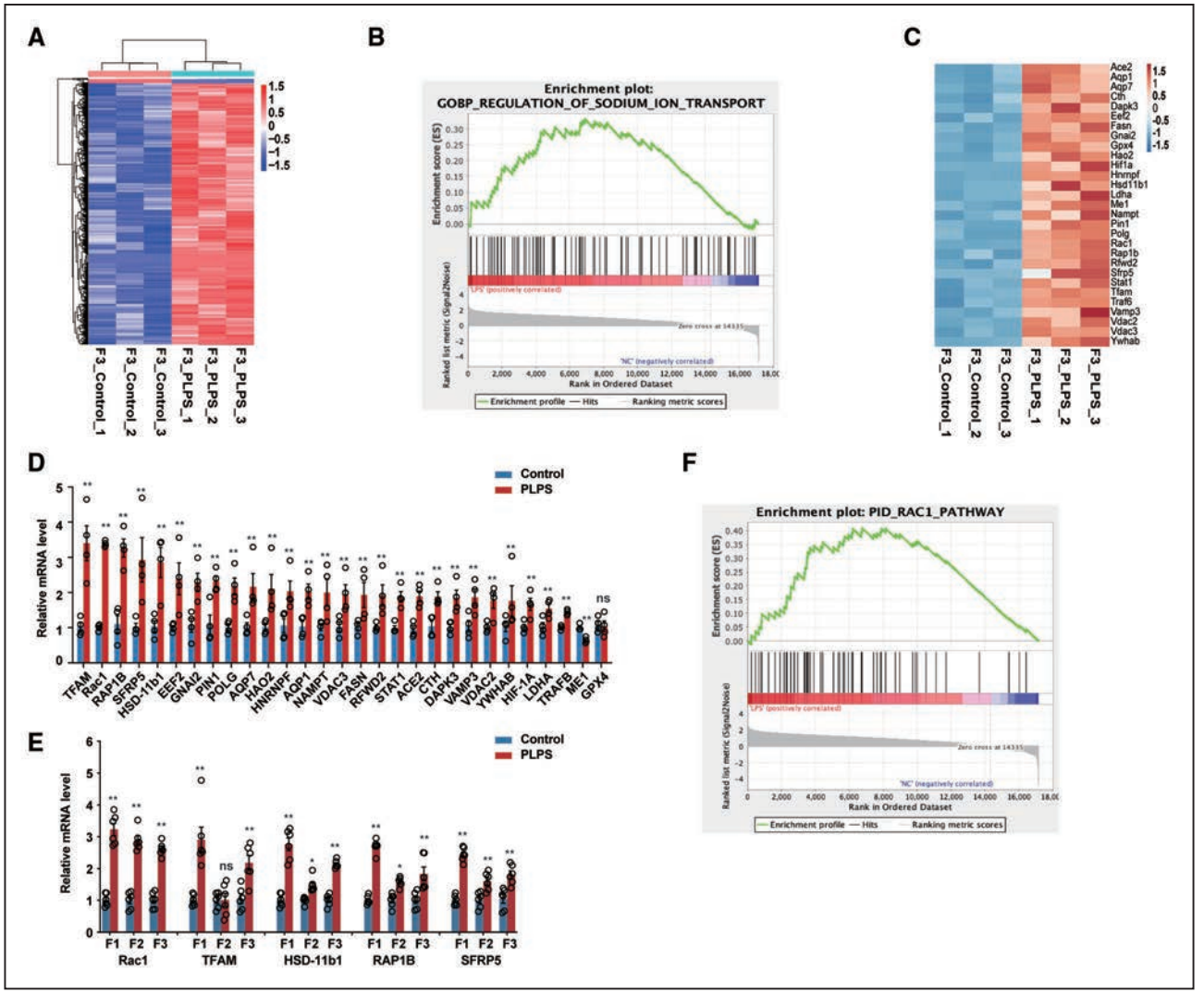

Figure 2. RNA-sequencing analysis of kidney in F3 control and PLPS offspring indicates altered expression of genes related to sodium transport and RAC1 signaling.

A, Heatmap illustrating differentially expressed genes in the kidney of F3 control and PLPS offspring (n=3). **B**, Gene enrichment plot illustrating regulation of sodium ion transport pathway activated in kidney of F3 PLPS offspring compared with F3 control offspring, analyzed by Gene Set Enrichment Analysis using RNA-sequencing data (normalized enrichment score>1, false discovery rate<0.25). **C**, Heatmap of 29 selected upregulated genes, from the RNA-sequencing data with known effect on blood pressure regulation and sodium-water metabolism in kidney of F3 control and PLPS offspring (n=3). **D**, Quantitative real-time polymerase chain reaction validation of the 29 selected genes in kidney of F3 control and PLPS offspring (n=4). $^{**}P<0.01$, ns: not significant, vs control, 2-tailed Student *t* test. **E**, Quantitative real-time polymerase chain reaction of the 5 most upregulated genes in kidney of F1 to F3 control and PLPS offspring (n=4). $^{*}P<0.05$, $^{**}P<0.01$, vs control, 2-tailed Student *t* test. **F**, Gene enrichment plot of RAC1 pathway activated in kidney of F3 PLPS offspring analyzed by Gene Set Enrichment Analysis by using the RNA-sequencing data (normalized enrichment score >1, false discovery rate<0.25). F1 indicates first generation; F2, second generation; F3, third generation; GOBP, Gene Ontology Biological Process; PID, the Pathway Interaction Database; and PLPS, prenatal lipopolysaccharide.

control offspring, participated in sodium ion transport (Figure 2B). The increase in renal tubular sodium and water reabsorption is a core process in the development of hypertension,[2] consistent with the phenotype found in the F3 PLPS offspring. We then selected 29 upregulated genes involved in the regulation of blood pressure and sodium-water metabolism[13–15] from the differentially expressed genes as candidates for further study (Figure 2C). Using quantitative real-time polymerase chain reaction, we validated the expression of these 29 genes in the kidney from F3 control and PLPS offspring (Figure 2D). Moreover, we measured the top 5 upregulated genes of the 29 blood pressure regulation and sodium-water metabolism–related genes in the kidneys of F1, F2, and F3 offspring, and found that the Ras-related C3 botulinum toxin substrate 1 (*Rac1*) gene is the most consistently upregulated gene across the F1 to F3 generations (Figure 2E). From the Gene Set Enrichment Analysis of the RNA-seq data, we noticed a significant activation of RAC1 signaling in the kidney of F3 PLPS, relative to F3 control offspring (Figure 2F), further indicating a potential functional role of *Rac1* gene in the

PLPS exposure–induced transgenerationally transmitted hypertension and impaired urinary sodium excretion.

RAC1 Is Responsible for the Transgenerational Impaired Urinary Sodium Excretion and Hypertension by Inducing Nuclear Accumulation of Mineralocorticoid Receptor

RAC1, also known as Rac Family Small GTPase 1, is involved in the development of hypertension,[16] including salt-sensitive[17] and obesity-related hypertension,[18] through activation of mineralocorticoid receptor (MR) signaling.[11,16] To determine whether the impaired urinary sodium excretion and hypertension in PLPS offspring were attributable to a high mineralocorticoid level, we measured plasma renin and serum aldosterone levels in 5-month-old rats. PLPS offspring had decreased plasma renin and serum aldosterone levels in F1 to F3 PLPS rats compared with control rats (Figure S3A and S3B), indicating that the hypertension in PLPS offspring is caused by a renin-aldosterone–independent mechanism. Considering that the transcriptome alteration in the kidney of F3 PLPS rats involved RAC1 signaling activation, we hypothesized that RAC1-MR signaling was the central pathway responsible for the transgenerational transmission of impaired sodium excretion and hypertension induced by PLPS. Using Western blotting, we compared the protein expression of RAC1 in the kidney from F1 to F3 generations of control and PLPS offspring and found that RAC1 in the kidney was upregulated across all 3 generations (Figure 3A1 and 3A2).

To test the critical role of RAC1 in the transgenerationally inherited natriuresis dysfunction and hypertension phenotype, a highly selective inhibitor of RAC1, NSC23766 (10 $mg{\cdot}kg^{-1}{\cdot}d^{-1}$),[16,19] was subcutaneously injected in both F1 and F3 offspring. Blood pressure monitoring showed that NSC23766 lowered the ambulatory systolic blood pressure and reached normal values at day 7 after injection in F1 (Figure 3B1) and at day 4 after injection in F3 (Figure 3C1) offspring. Consistent with the normalization of systolic blood pressure, NSC23766 also normalized the impaired natriuresis in F1 and F3 PLPS offspring without affecting the sodium excretion in the control offspring (Figure 3B2 and 3C2). These data suggested the essential role of RAC1 in the PLPS-induced transgenerational transmission of natriuresis dysfunction and hypertension.

RAC1 upregulation and activation are implicated in the pathogenesis of hypertension through MR activation, which is characterized by localization of MR in the nucleus.[11] Using GTP pulldown assay followed by Western blotting, we validated the successful inhibition of RAC1 activation (GTP-Rac1/total RAC1) in kidneys from F1 PLPS rats (Figure 3D1 and 3D2) and F3 PLPS rats (Figure 3E1 and 3E2) by NSC23766 treatment. Using Western blotting, we studied the subcellular distribution of MR, and the downstream target epithelial sodium channel (ENaC) genes αENaC, βENaC, δENaC, and γENaC, as well.[19,20] Nuclear MR and the target genes were significantly upregulated in the kidneys from F1 and F3 PLPS offspring, relative to F1 and F3 control offspring (Figure 3D1, 3D2, 3E1, and 3E2). NSC23766 treatment decreased these elevated expressions in PLPS offspring to the levels observed in vehicle-treated control offspring; NSC23766 treatment did not affect the levels in the control offspring (Figure 3D1, 3D2, 3E1, and 3E2). These data suggested that PLPS exposure induced the transgenerational activation of RAC1-MR axis in the kidney that is responsible for the development of hypertension in each generation.

We also studied the expression of active RAC1 (GTP-RAC1), total RAC1, nuclear MR, and MR downstream targets in the kidneys of F4 control and PLPS rats. Under basal conditions, there were no differences in RAC1-MR signaling between F4 control and PLPS rats (Figure S3C1–S3C3). However, after 2 months of HS diet, total RAC1 was unchanged, but RAC1 activity (GTP-Rac1/total RAC1) was upregulated in the kidney of F4 PLPS rats (Figure S3C1 and S3C2), along with the increase of nuclear MR and its downstream targets compared with F4 control rats (Figure S3C1 and S3C3). Consistent with effect in F1 to F3 generations, the subcutaneous injection of NSC23766 also significantly attenuated the HS diet–induced hypertension (Figure S3D) and impairment in urinary sodium excretion (Figure S3E) in F4 PLPS rats. These data indicated that RAC1-MR signaling is necessary for the development of salt-sensitive hypertension in the F4 generation of PLPS-treated rats.

We also explored a therapeutic approach targeting transgenerationally inherited hypertension with spironolactone (80 mg·kg-1·d-1), an antagonist of MR,[21] in F1 and F3 PLPS offspring. The intragastric administration by oral gavage of spironolactone significantly ameliorated the hypertension and increased the urinary sodium excretion in both F1 (Figure 3F1–3F3) and F3 PLPS offspring (Figure 3G1–3G3). Moreover, in the F4 generation, the intragastric administration of spironolactone could also partially reverse the hypertension and impaired sodium excretion in HS diet–fed rats (Figure S3F and S3G). These data suggested that inhibition of MR signaling could treat the PLPS-induced transgenerational impairment of urinary sodium excretion and hypertension in each generation.

Histone Demethylase KDM3B Reduces H3K9me2 Modification Leading to Transgenerational Upregulation of *Rac1* Gene in PLPS Offspring

To investigate further the mechanism of the transgenerationally transmitted upregulation of the *Rac1* gene, we first performed Sanger sequencing of polymerase chain reaction products targeting *Rac1* full exons, using

ORIGINAL RESEARCH ARTICLE

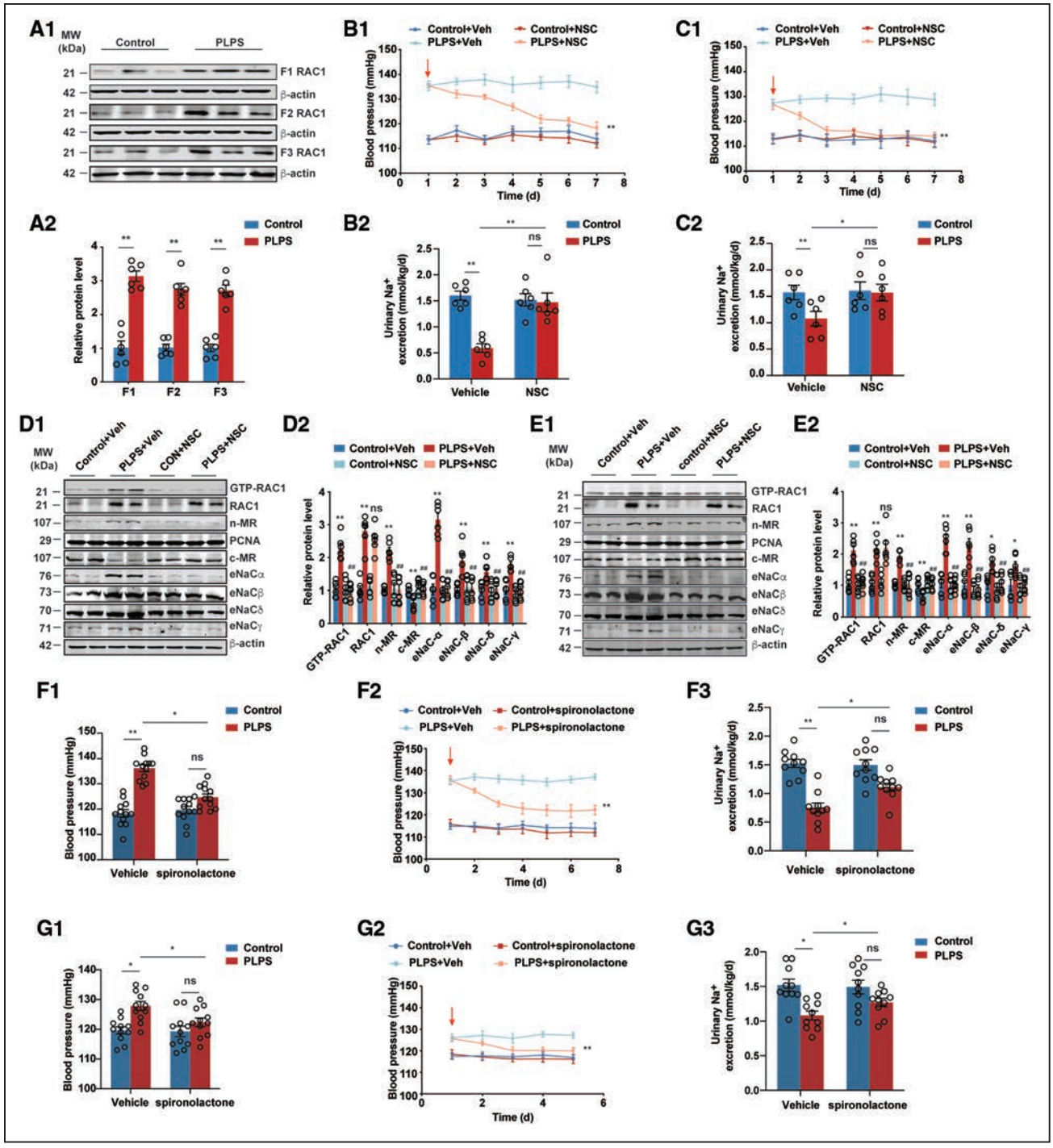

Figure 3. RAC1 is responsible for the transgenerational impairment in urinary sodium excretion and hypertension by inducing nuclear accumulation of MR.

A, Representative Western blots (WBs) of RAC1 expression in kidney of F1 to F3 generation control and PLPS offspring (**A1**). Quantification of WB, normalized to β-actin (**A2**, n=6). $^{**}P<0.01$, 2-tailed Student *t* test. **B**, Ambulatory systolic blood pressure, and 24-hour urinary Na^+ of F1 control and PLPS offspring treated with or without RAC1 inhibitor NSC23766 (NSC). **B1**, Ambulatory systolic blood pressure of 5-month-old F1 control and PLPS offspring monitored by telemetry, daily monitored from 9 AM to 10 AM, for 7 consecutive days after subcutaneous injection of the RAC1 inhibitor NSC or vehicle (Veh; n=6). Arrow points to the time of NSC or Veh injection. $^{**}P<0.01$, vs PLPS+Veh, 2-way ANOVA followed by Bonferroni correction and within-test multiple corrections using Tukey multiple analysis. **B2**, 24-hour urinary Na^+ was measured in 5-month-old F1 control and PLPS offspring with or without NSC treatment (n=6). $^{**}P<0.01$, ns: not significant, 2-tailed Student *t* test. **C**, Ambulatory systolic blood pressure and 24-hour urinary Na^+ of F3 control and PLPS offspring treated with or without RAC1 inhibitor NSC23766. **C1**, Ambulatory systolic blood pressure of 5-month-old F3 control and PLPS offspring monitored by telemetry, daily monitored from 9 AM to 10 AM, for 7 consecutive days after the subcutaneous injection of NSC or Veh (n=6). Arrow points to the time of NSC or Veh injection. $^{**}P<0.01$, vs PLPS+Veh, 2-way ANOVA followed by Bonferroni correction and within-test multiple corrections using Tukey multiple analysis. **C2**, 24-hour urinary Na^+ was measured in 5-month-old F3 control and PLPS offspring with or without NSC treatment (n=6). $^{*}P<0.05$, $^{**}P<0.01$, ns: not significant, 2-tailed Student *t* test. (*Continued*)

Figure 3 Continued. D, Representative WB of the expression of GTP pulldown RAC1 (GTP-RAC1), total-RAC1, nuclear MR (n-MR), cytoplasmic MR (c-MR), and downstream target genes of n-MR in kidney of F1 control and PLPS offspring with or without NSC treatment. PCNA was the internal control for nuclear protein, and β-actin was the internal control for cytoplasmic and total protein (**D1**). Quantification of WB (**D2**, n=6), normalized to PCNA or β-actin. ***P*<0.01, vs Control+Veh; ##*P*<0.01, ns: not significant, vs PLPS+Veh, 2-way ANOVA. **E**, Representative WB of the expression of GTP-RAC1, total-RAC1, n-MR, c-MR, and downstream target genes of n-MR in kidney of F3 control and PLPS offspring with or without NSC treatment. PCNA was the internal control for nuclear protein, and β-actin was the internal control for cytoplasmic and total protein. Quantification of WB (**E2**, n=6), normalized to PCNA or β-actin. **P*<0.05, ***P*<0.01, vs Control+Veh; ##*P*<0.01, ns: not significant, vs PLPS+Veh, 2-way ANOVA. **F**, Tail-cuff systolic blood pressure, ambulatory systolic blood pressure, and 24-hour urinary Na^+ of 5-month-old F1 control and PLPS offspring with or without spironolactone (MR antagonist) treatment. **F1**, Systolic blood pressure measured by tail-cuff method in 5-month-old F1 control and PLPS offspring with or without intragastric spironolactone treatment (n=12). **P*<0.05, ***P*<0.01, ns: not significant, 2-way ANOVA. **F2**, Ambulatory systolic blood pressure was monitored by telemetry, daily monitored from 9 AM to 10 AM, for 7 consecutive days after vehicle or intragastric spironolactone treatment (n=6), ***P*<0.01, vs PLPS+Veh, 2-way ANOVA followed by Bonferroni correction and within-test multiple corrections using Tukey multiple analysis. **F3**, 24-hour urinary Na^+ of 5-month-old F1 control and PLPS offspring with or without spironolactone treatment (n=10) **P*<0.05, ***P*<0.01, ns: not significant, 2-way ANOVA. **G**, Tail-cuff systolic blood pressure, ambulatory systolic blood pressure, and 24-hour urinary Na^+ of 5-month-old F3 control and PLPS offspring with or without spironolactone treatment. **G1**, Systolic blood pressure measured by tail-cuff method in 5-month-old F3 control and PLPS offspring with or without intragastric spironolactone treatment (n=11). **P*<0.05, ns: not significant, 2-way ANOVA. **G2**, Ambulatory systolic blood pressure was monitored by telemetry, daily monitored from 9 AM to 10 AM for 5 consecutive days after vehicle or intragastric spironolactone (n=6). ***P*<0.01, vs PLPS+Veh, 2-way ANOVA followed by Bonferroni correction and within-test multiple corrections using Tukey multiple analysis. **G3**, 24-hour urinary Na^+ of 5-month-old F3 control or PLPS offspring rats with or without spironolactone treatment (n=10). **P*<0.05. ns: not significant, 2-way ANOVA. F1 indicates first generation; F2, second generation; F3, third generation; MR, mineralocorticoid receptor; MW, molecular weight; PCNA, proliferating cell nuclear antigen; and PLPS, prenatal lipopolysaccharide.

genomic DNA extracted from kidneys of F1 control and PLPS offspring as template. We found that PLPS exposure did not induce DNA mutation in the exons of the *Rac1* gene (see Supplemental Material for Rac1 DNA sequencing data). Epigenomic modification has been reported to regulate transgenerational heritage of pathophysiological phenotypes.[4] Therefore, we investigated epigenomic modifications that may drive the transcriptional activation of the *Rac1* gene. Bisulfite sequencing did not show any change in the methylation level of the *Rac1* gene promoter (Figure S4A and S4B) in the kidney of F1 offspring, indicating that DNA methylation was not involved in the transgenerational inheritance. Histone modification is another major epigenetic modification that determines the loose and dense state of chromatin, thus regulating the accessibility of genes, leading to inheritable change of the transcription of target genes.[22] We investigated multiple major histone modifications in the kidneys from F1 offspring and found that H3K9me2 (histone H3 lysine 9 dimethylation) and H3K4me1 (histone H3 lysine 4 monomethylation) were downregulated, whereas H3K27me3 (histone H3 lysine 27 trimethylation) was upregulated in the PLPS offspring (Figure 4A1 and 4A2). Because H3K4me1 is associated with transcriptional activation,[23] whereas H3K27me3 is associated with gene repression,[24] and *Rac1* was upregulated in PLPS offspring, we focused on studying H3K9me2. H3K9me2 is strongly associated with transcriptional repression, and it was reported that the persistent suppression of *Rac1* expression is mediated by enhanced H3K9me2.[25] We then compared the H3K9me2 expression in the kidneys from F1 to F3 offspring and found that H3K9me2 was persistently repressed (Figure 4B1 and 4B2) in the PLPS offspring, relative to the control offspring. Using H3K9me2 chromatin immunoprecipitation followed by quantitative real-time polymerase chain reaction, we found that the H3K9me2 occupancy on *Rac1* promoter was decreased in the kidney tissue from F1 to F3 PLPS offspring (Figure 4C). These results suggested that the decreased deposition of H3K9me2 on *Rac1* gene promoter prevented its gene-repressive effect and contributed to the persistent upregulation of RAC1 in PLPS offspring.

Because H3K9me2 is regulated by many methylases and demethylases,[26] and considering that the repression of H3K9me2 may have originated from and transmitted through oocytes of PLPS-exposed female rats, we investigated the expression levels of several methylases and demethylases in the ovary of F1 offspring female rats with or without PLPS exposure. We found 2 lysine demethylases (KDMs), KDM3B and KDM5B, that were significantly upregulated (Figure 4D) in PLPS-exposed female rats. KDM5B is a major regulator of H3K4 methylation,[27] and several studies have shown that KDM3B demethylates the H3K9me2 in many tissues.[28,29] We therefore focused on KDM3B. The increase in KDM3B level and repression of H3K9me2 level was also observed in oocyte nuclei in vivo through immunofluorescence in ovaries of ovulation-induced F1 female offspring[30] (Figure 4E). The increased expression of KDM3B was only observed in the ovarian tissue of F1 but not in F2 or F3 female offspring (Figure 4F1 and 4F2), indicating that H3K9me2 is initially repressed but subsequently inherited.

PLPS-Induced Oxidative Stress Decreases H3K9me2 in Oocytes Leading to Transgenerational Activation of RAC1-MR Signaling

Our previous study showed that LPS exposure during pregnancy leads to impaired renal sodium excretion and hypertension in the offspring attributable to oxidative stress,

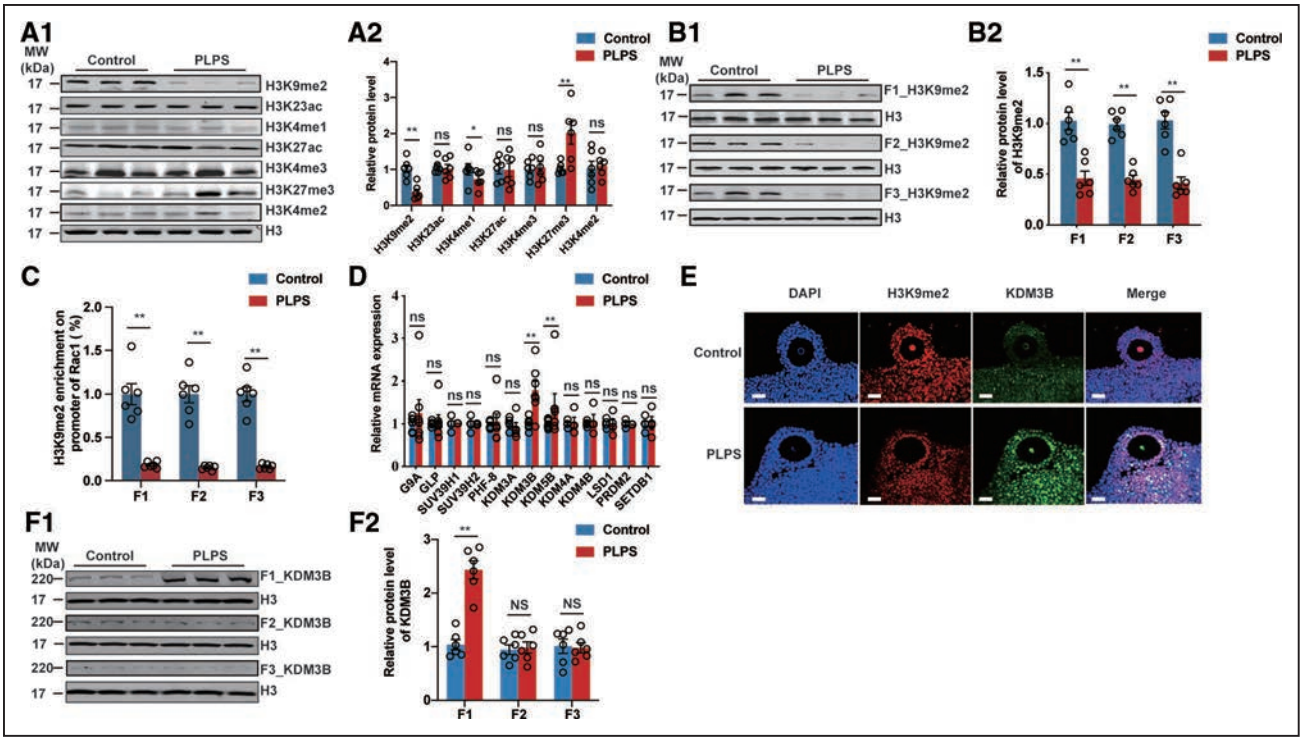

Figure 4. Histone demethylase KDM3B reduces H3K9me2 modification leading to transgenerational upregulation of *Rac1* gene in PLPS offspring.

A, Representative Western blots (WB) showing multiple histone modifications in kidney of F1 control and PLPS offspring (**A1**). Quantification of WB, normalized to total histone H3 (**A2**, n=6). **P*<0.05, ***P*<0.01, ns: not significant, 2-tailed Student *t* test. **B,** Representative WB of H3K9me2 expression in kidney of F1 to F3 control and PLPS offspring (**B1**). Quantification of WB, normalized to total histone H3 (**B2**, n=6). ***P*<0.01, 2-tailed Student *t* test. **C**, Chromatin immunoprecipitation–quantitative real-time polymerase chain reaction detecting H3K9me2 binding to the promoter region of *Rac1* gene in kidney tissue of F1 to F3 control and PLPS offspring (n=6). Normalized to Input, ***P*<0.01. 2-tailed Student *t* test. **D**, Quantitative real-time polymerase chain reaction of mRNA, normalized to GAPDH, of several methylases and demethylases in ovary of F1 control and PLPS female offspring (n=6). ***P*<0.01, ns: not significant, 2-tailed Student *t* test. **E,** Representative immunofluorescent staining of KDM3B (green) and H3K9me2 (red) in ovary of F1 control and PLPS female offspring induced by ovulation. Nuclei are labeled by DAPI (blue). Scale bar, 40 µm. **F**, Representative WB of KDM3B expression, normalized to total histone H3, in ovary of F1 to F3 control and PLPS female offspring (**F1**). Quantification of WB (**F2**, n=6). ***P*<0.01, ns: not significant, 2-tailed Student *t* test. DAPI indicates 4′,6-diamidino-2-phenylindole; H3K9me2, histone H3 lysine 9 dimethylation; KDM3B, histone lysine demethylase 3B; MW, molecular weight; and PLPS, prenatal lipopolysaccharide.

caused by decreased antioxidant capacity, resulting in the accumulation of reactive oxygen species (ROS) in the kidney.[8] To determine the oxidative stress level in the rats with transgenerational inherited hypertension induced by PLPS exposure, we measured the serum levels of malondialdehyde, a lipid peroxidation product used as an indicator of oxidative stress in the whole body,[31] in F0 to F3 control and PLPS offspring. The serum malondialdehyde levels, measured by ELISA, were significantly increased in F0 and F1 PLPS offspring compared with control rats but decreased to control levels in the F2 and F3 offspring (Figure 5A1). We also measured by ELISA the serum superoxide dismutase level, which indicates antioxidant capacity, in F0 to F3 control and PLPS offspring and found that serum superoxide dismutase levels were significantly decreased in F0 and F1 PLPS offspring but recovered to control levels in the F2 and F3 offspring (Figure 5A2). The serum malondialdehyde and superoxide dismutase data showed that oxidative stress was a direct result of PLPS exposure that influenced both F0 maternal rats and F1 offspring in utero.

To test further whether oxidative stress is a causal factor of the transgenerationally inherited hypertension induced by PLPS exposure through KDM3B-mediated H3K9me2, we treated control and PLPS F0 maternal rats with tempol, an ROS scavenger (superoxide dismutase mimetic), added to the drinking water at a concentration of 1.0 mmol/L on gestation days 5 to 13,[8] along with intraperitoneal injection of LPS (0.79 mg/kg) or saline (0.2 mL) on gestation days 6, 8, 10, and 12 (Figure 5B). Prenatal tempol treatment was sufficient to normalize the systolic blood pressure and urinary sodium excretion of F1 PLPS offspring (Figure S5A–S5C), consistent with our published results.[8,9] We also found that tempol treatment of F0 maternal rats significantly decreased the systolic blood pressure in F2 PLPS offspring to F2 control offspring level (Figure 5C), indicating a transgenerational effect. Moreover, tempol treatment of F0 female rats prevented the upregulation of KDM3B in the ovarian tissue from F1 PLPS female offspring (Figure 5D1 and 5D2), along with recovery of the downregulation of H3K9me2

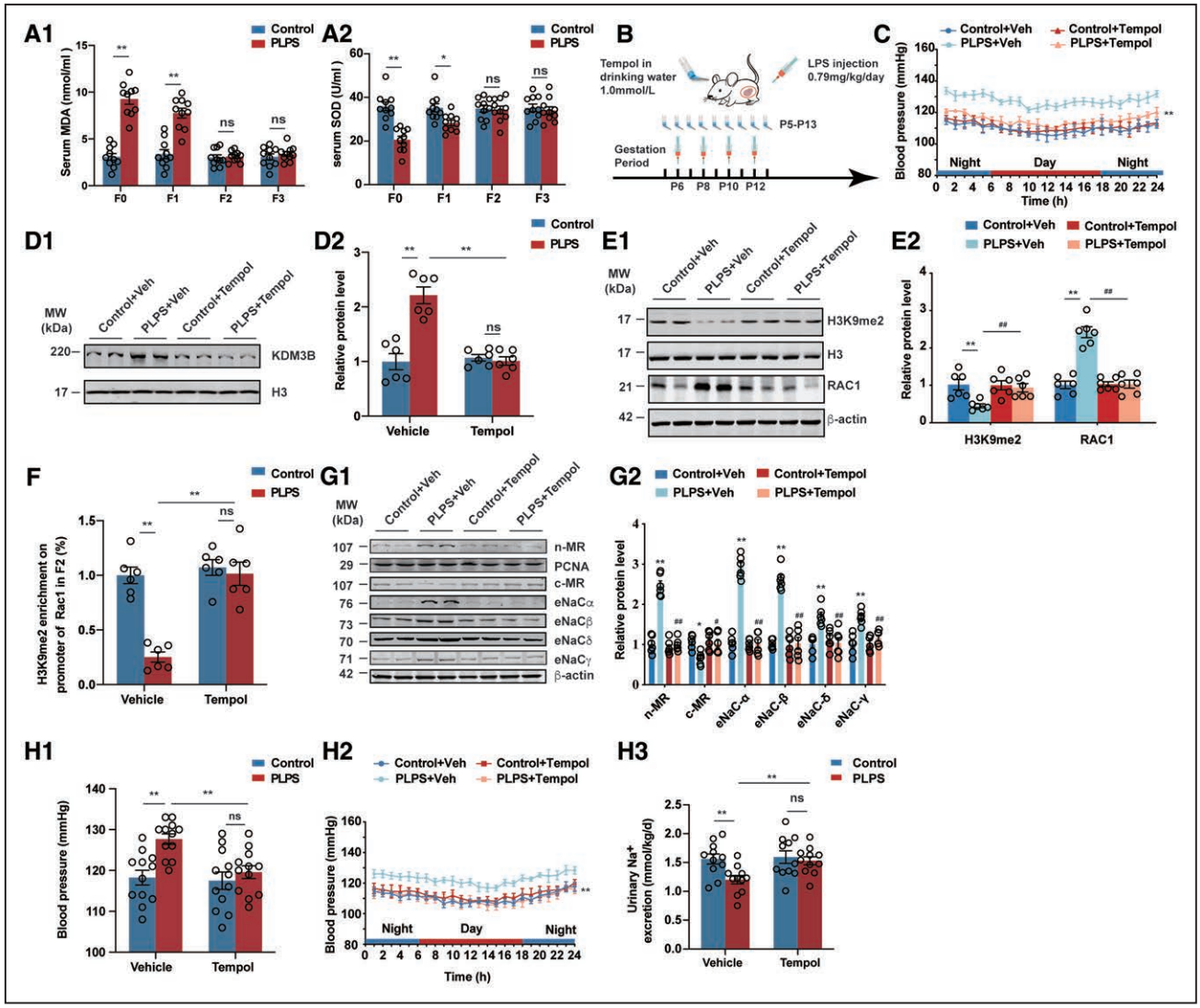

Figure 5. PLPS-induced oxidative stress decreases H3K9me2 in oocytes leading to transgenerational activation of RAC1-MR signaling.

A, Serum malondialdehyde (MDA, **A1**) and superoxide dismutase (SOD, **A2**) levels in F0 to F3 control and PLPS rats quantified by ELISA (n=10). **P*<0.05, ***P*<0.01, ns: not significant, 2-tailed Student *t* test. **B**, Schematic illustration showing pretreatment with the antioxidant (superoxide dismutase mimetic), tempol, added to drinking water before LPS injection. **C**, 24-hour ambulatory systolic blood pressure of conscious 5-month-old F2 control and PLPS offspring monitored by telemetry (n=6). ***P*<0.01, vs PLPS+Veh, 2-way ANOVA followed by Bonferroni correction and within-test multiple corrections using Tukey multiple analysis. **D**, Representative Western blot (WB) showing the expression of KDM3B in the ovary tissue from F1 control and PLPS female offspring with or without tempol treatment in F0 (**D1**). Quantification of WB (**D2**, n=6). Normalized to total histone H3. ***P*<0.01, ns: not significant, 2-way ANOVA. **E**, Representative WB showing the expression of H3K9me2 and RAC1 in kidney from F2 control and PLPS offspring with or without tempol added to the drinking water in F0 rats (**E1**). Quantification of WB (**E2**, n=6). H3K9me2 was normalized to total histone H3. RAC1 was normalized to β-actin. ***P*<0.01, vs Control+Veh; ##vs PLPS+Veh, 2-way ANOVA. **F,** Chromatin immunoprecipitation–quantitative real-time polymerase chain reaction detecting H3K9me2 binding to the promoter region of RAC1 gene in kidney tissue of F2 control and PLPS offspring with or without tempol treatment in F0 (n=6). Normalized to Input. ***P*<0.01, ns: not significant, 2-way ANOVA. **G**, Representative WB of the expression of n-MR, c-MR, and downstream target genes of MR in kidney of F2 control and PLPS offspring with or without tempol treatment in F0. Proliferating cell nuclear antigen is the internal control for nuclear protein and β-actin is the internal control for cytoplasmic and total protein (**G1**). Quantification of WB in **G1** (**G2**, n=6). **P*<0.05, ***P*<0.01, vs Control+Veh; #*P*<0.05, ##*P*<0.01, vs PLPS+Veh, 2-way ANOVA. **H**, Tail-cuff systolic blood pressure, 24-hour ambulatory systolic blood pressure, and 24-hour urinary Na^+ of 5-month-old F3 control or PLPS offspring from F0 control or PLPS rats with or without tempol treatment. **H1**, Systolic blood pressure, measured by tail-cuff method, of 5-month-old F3 control and PLPS offspring born from F0 control or PLPS female rats with or without tempol treatment (n=12). ***P*<0.01, ns: not significant, 2-way ANOVA. **H2**, 24-hour ambulatory systolic blood pressure was monitored by telemetry in 5-month-old F3 control and PLPS offspring born from F0 control or PLPS female rats with or without tempol treatment (n=6). ***P*<0.01, PLPS+tempol vs PLPS+Veh, 2-way ANOVA followed by Bonferroni correction and within-test multiple corrections using Tukey multiple analysis. **H3**, 24-hour urinary Na^+ excretion of 5-month-old F3 control or PLPS offspring from F0 control or PLPS rats with or without tempol treatment (n=11). ***P*<0.01, ns: not significant, 2-way ANOVA. c-MR indicates cytoplasmic MR; H3K9me2, histone H3 lysine 9 dimethylation; KDM3B, histone lysine demethylase 3B; MR, mineralocorticoid receptor; MW, molecular weight; n-MR, nuclear MR; PLPS, prenatal lipopolysaccharide; and Veh, vehicle.

and upregulation of RAC1 expressions in the kidneys of F2 PLPS offspring (Figure 5E). Tempol treatment in F0 also recovered the decreased binding of H3K9me2 to the promoter region of RAC1 gene in the renal tissue of F2 PLPS offspring (Figure 5F). In addition, the activation of MR signaling in F2 kidneys was alleviated by tempol treatment in F0 PLPS rats (Figure 5G1 and 5G2). Prenatal tempol treatment also alleviated PLPS-induced transgenerational hypertension and impaired urinary sodium excretion in F3 offspring (Figure 5H1 to 5H3), and in F4 offspring fed a HS diet, as well (Figure S5D–S5F), indicating a preventive effect of transgenerational hypertension using anti-ROS strategy. Taken together, these data demonstrated that PLPS exposure induced oxidative stress in F0, which was necessary to increase the expression of KDM3B in the oocytes of F1 female rats and decrease the expression of H3K9me2 in the kidney of F2 offspring, leading to the activation of the RAC1-MR axis, resulting in transgenerational impaired urinary sodium excretion and hypertension.

DISCUSSION

Clinical and preclinical studies indicate that hypertension is highly heritable.[6] However, numerous large-scale genetic studies, expecting to find the predisposing loci of hypertension, have found that genetic variants accounted for only a small proportion of variation in blood pressure levels,[1] suggesting that nongenomic mechanisms may be taking part in the heritability of hypertension. Parental exposure could have an important influence on the development and health of their offspring across generations.[22] Prenatal or in utero exposure is a major type of parental exposure that leads to adverse events, including premature delivery, abortion, and dystocia.[32,33] Our study provides the first evidence of transgenerational transmission of hypertension induced by PLPS exposure, a classic animal model in studies related to maternal infection.[34] Although there was no difference in systolic blood pressure between F4 PLPS and control offspring at the basal state, an HS diet for 2 months increased the systolic blood pressure of F4 PLPS rats, associated with impaired urinary sodium excretion, to a greater extent than the F4 control offspring. These phenotypes in F4 PLPS offspring were also observed in the F5 PLPS offspring, implying that the increased susceptibility to hypertension was transmitted to F4 and F5 offspring. The impairment in urinary sodium excretion with HS diet in F4 and F5 PLPS offspring suggests that the kidney could be the target organ taking part in the transgenerational phenotype of hypertension.

We used RNA-seq analysis to detect the alteration of the transcriptome in the kidney of F3 PLPS offspring, searching for candidate genes and pathways responsible for the transgenerational hypertension. Our RNA-seq analysis of F3 PLPS offspring kidneys revealed a significant enrichment in the "regulation of sodium ion transport," which is a major participant in the regulation of renal tubular sodium reabsorption.[10] Quantitative real-time polymerase chain reaction validation of several top candidate genes regulating renal sodium reabsorption showed a sustained upregulation of RAC1, a member of the Rho family of small GTPases, throughout the different generations. RAC1 has been shown to play a crucial role in the pathogenesis of salt-sensitive hypertension through the MR signaling pathway.[16,17,19] In our PLPS-exposed offspring, the delivery of the RAC1 highly selective inhibitor NSC23766 normalized their impaired urinary sodium excretion and elevated systolic blood pressure. RAC1 inhibition with NSC23766 also decreased in the F1 and F3 generations the renal expression of RAC1-MR axis target genes, αENaC, βENaC, δENaC, and γENaC, which are important in renal tubular sodium reabsorption, especially the distal nephron.[16–21] Moreover, treatment with the MR antagonist spironolactone in the F1 and F3 PLPS offspring significantly ameliorated the impaired sodium excretion and hypertension, indicating an essential role of RAC1-MR axis in the transgenerational hypertension induced by PLPS exposure.

Epigenetic modifications are implicated in the transgenerational inheritance of prenatally programmed diseases,[3,22] and epigenetic factors have gained considerable attention in the pathogenesis of hypertension.[6] To determine which epigenetic modification caused the transgenerational upregulation of *Rac1* gene, we first evaluated the DNA methylation level, which is a strong inheritable epigenetic factor inhibiting the expression of certain genes.[22,35] It is surprising, however, that there was no difference in DNA methylation level in the promoter region of the *Rac1* gene. Histone modification is another long-lasting epigenetic modification in both the positive and negative regulation of gene expression.[36–38] After screening, we focused on a downregulated histone modification, H3K9me2, because its gene-repressive action was found consistently decreased in each generation. Because H3K9me2 is a negative regulator of the expression of *Rac1*, we used chromatin immunoprecipitation–quantitative real-time polymerase chain reaction to validate the causal role of the low H3K9me2 occupancy in the transgenerational upregulation of the *Rac1* gene. Furthermore, we identified KDM3B, the histone demethylase of H3K9me2, serving as the histone marker "eraser," decreasing the H3K9me2 in the oocytes of F1 offspring, which was transmitted in the kidney through generations. These data added new evidence to the concept that heredity involves transmission of the effects of parental exposure to the offspring through epigenetic changes in the germline.[22,37]

Our previous study showed that PLPS exposure can induce global oxidative stress in the offspring, with decreased antioxidant capacity and accumulation of ROS in the kidney.[8,9] Oxidative stress was detected

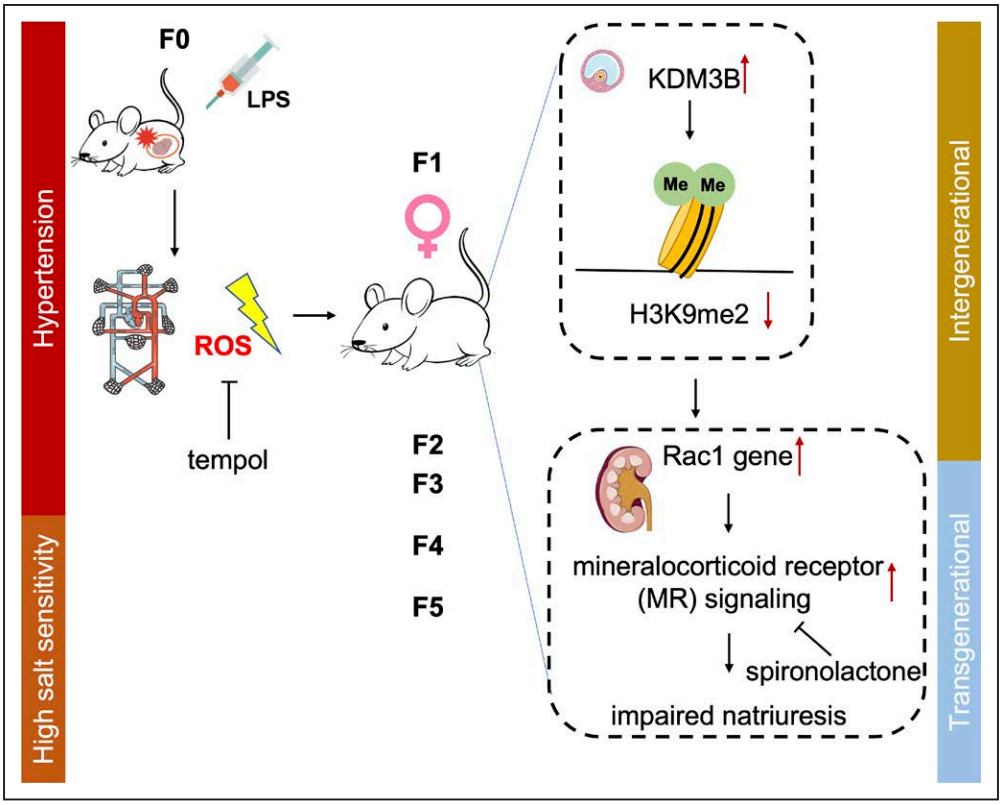

Figure 6. Schema of the working model of this study.
F0 indicates gestating female; F1, first generation; F2, second generation; F3, third generation; F4, fourth generation; F5, fifth generation; H3K9me2, histone H3 lysine 9 dimethylation; KDM3B, histone lysine demethylase 3B; LPS, lipopolysaccharide; and ROS, reactive oxygen species.

in F0 to F3 generations, but ROS level was only significantly increased in F0 and F1 PLPS rats, compared with control rats, indicating that the oxidative stress is a direct result of PLPS exposure. Treatment with an ROS scavenger, tempol, successfully rescued the transgenerational hypertension and impaired renal sodium excretion, with recovery of the upregulation of KDM3B in the ovaries from F1 PLPS female rats and amelioration of the decreased H3K9me2 level and overactivated RAC1 expression in the kidneys of F2 PLPS offspring. The phenomenon that ROS was only significantly increased in F0 and F1 suggests that PLPS exposure–induced oxidative stress may serve as the trigger that drives the KDM3B-regulated H3K9me2. Once H3M9me2 is written, the epigenetic cascade gets transmitted across generations. The reversible nature of epigenetic modifications makes them more druggable than approaches that target or correct defects in gene expression, per se. Therefore, we tried the commercially available reagent tempol to target upstream ROS in a preclinical investigation. Our investigation showed that treatment of F0 PLPS rats with the ROS scavenger tempol prevented the transgenerational natriuresis dysfunction and hypertension in F1 through F4 generations, indicating a potential preventive strategy for PLPS exposure–induced transgenerational hypertension.

This study has several limitations. First, although we demonstrated that the RAC1-MR axis in the kidney was essential for the development of transgenerationally transmitted hypertension, there are probably other pathways, together with the RAC1-MR axis, that affect the blood pressure level which need to be determined in the future. Moreover, we did not perform RNA-seq studies in other blood pressure–regulating organs, such as the central nervous system, autonomic nervous system, and resistance vessels. Thus, there may be other mechanisms, together with renal mechanism, responsible for the susceptibility of hypertension across generations. Second, to illustrate the mechanism of transgenerational alteration of RAC1 gene, we screened out and validated the role of KDM3B-H3K9me2 epigenomic modification. Considering that KDM3B regulates not only H3K9me2, but also other histone modifications, and H3K9me2 may influence multiple gene loci, we do not know how those other genes regulated by KDM3B-H3K9me2 participate in the regulation of blood pressure. Last, although we identified that the RAC1-MR signaling is essential for the development of salt-sensitive hypertension in F4 generation, we did not fully assess how the activation of RAC1 was increased by HS diet treatment. Further studies are necessary to explore more fully the mechanisms for the transgenerationally transmitted hypertension.

Taken together, this study showed that PLPS exposure can induce the transgenerational transmission of natriuresis dysfunction and hypertension, and that the underlying mechanism is related to an altered landscape of histone modification and transcriptome expression (Figure 6). This work could potentially uncover preventive and therapeutic approaches to the prenatal LPS exposure–induced transgenerational natriuresis dysfunction and hypertension.

ARTICLE INFORMATION

Received March 3, 2022; accepted July 26, 2022.

Affiliations

Department of Cardiology, Daping Hospital (N.C., C.L., C.C., Z.X., H.L., S.Z., X.G., H.R., Z.L., S.Q., C.Y., G.W., C.H., J.Yu, C.Z.), State Key Laboratory of Trauma, Burns and Combined Injury, Daping Hospital (C.Z.), Research Center for Nutrition and Food Safety, Chongqing Key Laboratory of Nutrition and Food Safety, Institute of Military Preventive Medicine (J. Yang), The Third Military Medical University (Army Medical University), P.R. China. Chongqing Key Laboratory for Hypertension Research, Chongqing Cardiovascular Clinical Research Center, Chongqing Institute of Cardiology, Chongqing, P. R. China (N.C., C.L., C.C., Z.X., H.L., S.Z., X.G., H.R., Z.L., S.Q., C.Y., G.W., C.H., J. Yu, C.Z.). Department of Cardiology, the Sixth Medical Centre, Chinese PLA General Hospital, Beijing, P.R. China (N.C., X.G., Y.C.). Division of Renal Diseases and Hypertension, The George Washington University School of Medicine and Health Sciences, Washington, DC (P.A.J.). Heart Center of Fujian Province, Union Hospital, Fujian Medical University, Fuzhou, P.R. China (C.Z.). Department of Cardiology, Chongqing General Hospital, P. R. China (C.Z.). Cardiovascular Research Center of Chongqing College, Chinese Academy of Sciences, University of Chinese Academy of Sciences, P. R. China (C.Z.).

Acknowledgments

Drs Cao, Lan, Chen, and Xu performed most of the experiments with the assistance from H. Lao, S. Zheng, Dr Gong, H. Ren, S. Qu, Dr Hu, Z. Li, and Dr Yu. Drs Wu, Hu, J. Yu, and Zeng conceived and supervised the study. Drs Cao, J. Yu, and Wu designed the study and analyzed the data. Drs Cao, J. Yang, and J. Yu prepared the figures. Drs Cao, J. Yu., Zeng, Y. Chen, and Jose wrote the manuscript with input from all the authors.

Sources of Funding

This work was supported in part by grants from the National Natural Science Foundation of China (31730043, 82100453), National Key R&D Program of China (2018YFC1312700), Program of Innovative Research Team by National Natural Science Foundation (81721001), and the National Institutes of Health (5R01DK039308-31, 5R01DK119652-02, and 5P01HL074940-11).

Disclosures

None.

Supplemental Material

Supplemental Methods

Figures S1–S5

Tables S1 and S2

Rac1 DNA sequencing data

REFERENCES

1. Brouwers S, Sudano I, Kokubo Y, Sulaica EM. Arterial hypertension. *Lancet*. 2021;398:249–261. doi: 10.1016/S0140-6736(21)00221-X
2. Zhou B, Perel P, Mensah GA, Ezzati M. Global epidemiology, health burden and effective interventions for elevated blood pressure and hypertension. *Nat Rev Cardiol*. 2021;18:785–802. doi: 10.1038/s41569-021-00559-8
3. Perez MF, Lehner B. Intergenerational and transgenerational epigenetic inheritance in animals. *Nat Cell Biol*. 2019;21:143–151. doi: 10.1038/s41556-018-0242-9
4. Skvortsova K, Iovino N, Bogdanovic O. Functions and mechanisms of epigenetic inheritance in animals. *Nat Rev Mol Cell Biol*. 2018;19:774–790. doi: 10.1038/s41580-018-0074-2
5. Szyf M. Nongenetic inheritance and transgenerational epigenetics. *Trends Mol Med*. 2015;21:134–144. doi: 10.1016/j.molmed.2014.12.004
6. Morton JS, Cooke, C, Davidge ST. In utero origins of hypertension: mechanisms and targets for therapy. *Physiol Rev*. 2016;96:549–603. doi: 10.1152/physrev.00015.2015
7. Lim AI, McFadden T, Link VM, Han SJ, Karlsson RM, Stacy A, Farley TK, Lima-Junior DS, Harrison OJ, Desai JV, et al. Prenatal maternal infection promotes tissue-specific immunity and inflammation in offspring. *Science* 2021;373:eabf3002. doi: 10.1126/science.abf3002
8. Wang X, Luo H, Chen C, Chen K, Wang J, Cai Y, Zheng S, Yang X, Zhou L, Jose PA, et al. Prenatal lipopolysaccharide exposure results in dysfunction of the renal dopamine D1 receptor in offspring. *Free Radic Biol Med*. 2014;76:242–250. doi: 10.1016/j.freeradbiomed.2014.08.010
9. Wang X, Wang J, Luo H, Chen C, Pei F, Cai Y, Yang X, Wang N, Fu J, Xu Z, et al. Prenatal lipopolysaccharide exposure causes mesenteric vascular dysfunction through the nitric oxide and cyclic guanosine monophosphate pathway in offspring. *Free Radic Biol Med*. 2015;86:322–330. doi: 10.1016/j.freeradbiomed.2015.05.040
10. Kalantar-Zadeh K, Jafar TH, Nitsch D, Neuen BL, Perkovic V. Chronic kidney disease. *Lancet*. 2021;398:786–802. doi: 10.1016/S0140-6736(21)00519-5
11. Kawarazaki W, Fujita T. Kidney and epigenetic mechanisms of salt-sensitive hypertension. *Nat Rev Nephrol*. 2021;17:350–363. doi: 10.1038/s41581-021-00399-2
12. Cho JH, Zhang R, Kilfoil PJ, Gallet R, de Couto G, Bresee C, Goldhaber JI, Marbán E, Cingolani E. Delayed repolarization underlies ventricular arrhythmias in rats with heart failure and preserved ejection fraction. *Circulation* 2017;136:2037–2050. doi: 10.1161/CIRCULATIONAHA.117.028202
13. Lakshmikanthan S, Zieba BJ, Ge ZD, Momotani K, Zheng X, Lund H, Artamonov MV, Maas JE, Szabo A, Zhang DX, et al. Rap1b in smooth muscle and endothelium is required for maintenance of vascular tone and normal blood pressure. *Arterioscler Thromb Vasc Biol*. 2014;34:1486–1494. doi: 10.1161/ATVBAHA.114.303678
14. Chung KW, Dhillon P, Huang S, Sheng X, Shrestha R, Qiu C, Kaufman BA, Park J, Pei L, Baur J, et al. Mitochondrial damage and activation of the STING pathway lead to renal inflammation and fibrosis. *Cell Metab*. 2019;30:784–799.e5. doi: 10.1016/j.cmet.2019.08.003
15. Chao Z, Liuyang T, Nan L, Qi C, Zhongqi C, Yang L, Yuqi L. Mitochondrial tRNA mutation with high-salt stimulation on cardiac damage: underlying mechanism associated with change of Bax and VDAC. *Am J Physiol Heart Circ Physiol*. 2016;311:H1248–H1257. doi: 10.1152/ajpheart.00874.2015
16. Shibata S, Mu S, Kawarazaki H, Muraoka K, Ishizawa K, Yoshida S, Kawarazaki W, Takeuchi M, Ayuzawa N, Miyoshi J, et al. Rac1 GTPase in rodent kidneys is essential for salt-sensitive hypertension via a mineralocorticoid receptor-dependent pathway. *J Clin Invest*. 2011;121:3233–3243. doi: 10.1172/JCI43124
17. Hirohama D, Nishimoto M, Ayuzawa N, Kawarazaki W, Fujii W, Oba S, Shibata S, Marumo T, Fujita T. Activation of Rac1-mineralocorticoid receptor pathway contributes to renal injury in salt-loaded db/db mice. *Hypertension*. 2021;78:82–93. doi: 10.1161/HYPERTENSIONAHA.121.17263
18. Fujita T. Mineralocorticoid receptors, salt-sensitive hypertension, and metabolic syndrome. *Hypertension*. 2010;55:813–818. doi: 10.1161/HYPERTENSIONAHA.109.149062
19. Shibata S, Nagase M, Yoshida S, Kawarazaki W, Kurihara H, Tanaka H, Miyoshi J, Takai Y, Fujita T. Modification of mineralocorticoid receptor function by Rac1 GTPase: implication in proteinuric kidney disease. *Nat Med*. 2008;14:1370–1376. doi: 10.1038/nm.1879
20. Bhalla V, Hallows KR. Mechanisms of ENaC regulation and clinical implications. *J Am Soc Nephrol*. 2008;19:1845–1854. doi: 10.1681/ASN.2008020225
21. Barrera-Chimal J, Lima-Posada I, Bakris GL, Jaisser F. Mineralocorticoid receptor antagonists in diabetic kidney disease: mechanistic and therapeutic effects. *Nat Rev Nephrol*. 2022;18:56–70. doi: 10.1038/s41581-021-00490-8
22. Fitz-James MH, Cavalli G. Molecular mechanisms of transgenerational epigenetic inheritance. *Nat Rev Genet*. 2022;23:325–341. doi: 10.1038/s41576-021-00438-5
23. Catarino RR, Stark A. Assessing sufficiency and necessity of enhancer activities for gene expression and the mechanisms of transcription activation. *Genes Dev*. 2018;32:202–223. doi: 10.1101/gad.310367.117
24. Zhang X, Liu L, Yuan X, Wei Y, Wei X. JMJD3 in the regulation of human diseases. *Protein Cell*. 2019;10:864–882. doi: 10.1007/s13238-019-0653-9
25. Joshi V, Subbanna S, Shivakumar M, Basavarajappa BS. CB1R regulates CDK5 signaling and epigenetically controls Rac1 expression contributing to neurobehavioral abnormalities in mice postnatally exposed to

ethanol. *Neuropsychopharmacology.* 2019;44:514–525. doi: 10.1038/s41386-018-0181-y
26. Yoo J, Jeon YH, Cho HY, Lee SW, Kim GW, Lee DH, Kwon SH. Advances in histone demethylase KDM3A as a cancer therapeutic target. *Cancers (Basel).* 2020;12:1098. doi: 10.3390/cancers12051098
27. Zhang SM, Cai WL, Liu X, Thakral D, Luo J, Chan LH, McGeary MK, Song E, Blenman KRM, Micevic G, et al. KDM5B promotes immune evasion by recruiting SETDB1 to silence retroelements. *Nature* 2021;598:682–687. doi: 10.1038/s41586-021-03994-2
28. Li Y, Xia L, Tan K, Ye X, Zuo Z, Li M, Xiao R, Wang Z, Liu X, Deng M, et al. N^6-Methyladenosine co-transcriptionally directs the demethylation of histone H3K9me2. *Nat Genet.* 2020;52:870–877. doi: 10.1038/s41588-020-0677-3
29. Tran KA, Dillingham CM, Sridharan R. Coordinated removal of repressive epigenetic modifications during induced reversal of cell identity. *EMBO J.* 2019;38:e101681. doi: 10.15252/embj.2019101681
30. Chen W, Chen J, Xu M, Zhong Z, Zhang Q, Yang W, Huang G. Electroacupuncture facilitates implantation by enhancing endometrial angiogenesis in a rat model of ovarian hyperstimulation. *Biol Reprod.* 2019;100:268–280. doi: 10.1093/biolre/ioy176
31. Luo H, Chen C, Guo L, Xu Z, Peng X, Wang X, Wang J, Wang N, Li C, Luo X, et al. Exposure to maternal diabetes mellitus causes renal dopamine D1 receptor dysfunction and hypertension in adult rat offspring. *Hypertension.* 2018;72:962–970. doi: 10.1161/HYPERTENSIONAHA.118.10908
32. Sun W, von Meyenn F, Peleg-Raibstein D, Wolfrum C. Environmental and nutritional effects regulating adipose tissue function and metabolism across generations. *Adv Sci (Weinh).* 2019;6:1900275. doi: 10.1002/advs.201900275
33. Jawaid A, Jehle KL, Mansuy IM. Impact of parental exposure on offspring health in humans. *Trends Genet.* 2021;37:373–388. doi: 10.1016/j.tig.2020.10.006
34. Parisi F, Milazzo R, Savasi VM, Cetin I. Maternal low-grade chronic inflammation and intrauterine programming of health and disease. *Int J Mol Sci .* 2021;22 doi: 10.3390/ijms22041732
35. Mimouni NEH, Paiva I, Barbotin AL, Timzoura FE, Plassard D, Le Gras S, Ternier G, Pigny P, Catteau-Jonard S, Simon V, et al. Polycystic ovary syndrome is transmitted via a transgenerational epigenetic process. *Cell Metab.* 2021;33:513–530.e8. doi: 10.1016/j.cmet.2021.01.004
36. Lismer A, Siklenka K, Lafleur C, Dumeaux V, Kimmins S. Sperm histone H3 lysine 4 trimethylation is altered in a genetic mouse model of transgenerational epigenetic inheritance. *Nucleic Acids Res.* 2020;48:11380–11393. doi: 10.1093/nar/gkaa712
37. Siklenka K, Erkek S, Godmann M, Lambrot R, McGraw S, Lafleur C, Cohen T, Xia J, Suderman M, Hallett M, et al. Disruption of histone methylation in developing sperm impairs offspring health transgenerationally. *Science.* 2015;350:aab2006. doi: 10.1126/science.aab2006
38. Zenk F, Loeser E, Schiavo R, Kilpert F, Bogdanovic O, Iovino N. Germ line-inherited H3K27me3 restricts enhancer function during maternal-to-zygotic transition. *Science.* 2017;357:212–216. doi: 10.1126/science.aam5339